Summer 8-15-2015

Screening Protein Ligand Interactions Using Microelectrode Arrays

Sakshi Uppal
Washington University in St. Louis

WASHINGTON UNIVERSITY IN ST. LOUIS

Department of Chemistry

Dissertation Examination Committee:
Kevin D. Moeller, Chair
Kendall J. Blumer
Garland R. Marshall
Liviu M. Mirica
John-Stephen A. Taylor

Screening Protein Ligand Interactions Using Microelectrode Arrays

by

Sakshi Uppal

A dissertation presented to the
Graduate School of Arts & Sciences
of Washington University in
partial fulfillment of the
requirements for the degree
of Doctor of Philosophy

August 2015
St. Louis, Missouri

TABLE OF CONTENTS

LIST OF FIGURES

Chapter 1

Chapter 2

Chapter 3

Chapter 4

Chapter 5

LIST OF SCHEMES

Chapter 4

LIST OF TABLES

Chapter 1

Chapter 5

LIST OF ABBREVIATIONS

AGS3	Activator of G protein signaling 3
BSA	Bovine serum albumin
CHAPS	3-[(3-cholamidopropyl)dimethylammonio]-1-propanesulfonate
cAMP	Cyclic adenosine monophosphate
cGMP	Cyclic guanosine monophosphate
Ci	Curie
cpm	Counts per minute
CV	Cyclic voltammetry
ddH_2O	Distilled deionized water
DAG	Diacylglycerol
DMSO	Dimethyl sulfoxide
DNase I	Deoxyribonuclease I
DTT	Dithiothreitol
E.coli	*Escherichia coli*
EDTA	Ethylenediaminetetraacetic acid
FCA	Ferrocene carboxylic acid
GAP	GTPase activating protein
GDI	Guanine nucleotide dissociation inhibitor
GDP	Guanosine diphosphate
GEF	Guanine nucleotide exchange factor
GIRK	G protein-coupled inwardly-rectifying potassium channels

GRK2	G protein-coupled receptor kinase 2
GTP	Guanosine triphosphate
GTPγS	Guanosine 5'-(gamma-thio) triphosphate
HEPES	4-(2-hydroxyethyl)-1-piperazineethanesulfonic acid
IP_3	Inositol trisphosphate
IPTG	Isopropyl-beta-D-thiogalactopyranoside
$MgCl_2$	Magnesium chloride
NaCl	Sodium chloride
Ni-NTA	Nickel-nitrilotriacetic acid
PCEMA-b-pBSt	Polycinnamoyloxy ethyl methacrylate-b-poly-4-pinacolatoborylstyrene
PDB	Protein databank
SDS	Sodium dodecyl sulfate
SDS-PAGE	Sodium dodecyl sulfate polyacrylamide gel electrophoresis
Tris-HCl	Tris(hydroxymethyl)aminomethane hydrochloride
TSH	Thyroid stimulating hormone
UBO-QIC	University of Bonn-$G\alpha_q$ inhibiting component

ACKNOWLEDGEMENTS

First and foremost, I would like to thank my advisor, **Dr. Kevin Moeller**. He has been extremely kind and supportive throughout my graduate school journey. I am extremely grateful to him for allowing me to join his research group. He struck a perfect balance between giving me the liberty to follow my heart whilst reining in my imagination sporadically and averting me from taking wrong turns. I don't think I could have done it without you and I cannot thank you enough for always being there. I am extremely grateful to **Dr. Kendall Blumer** for allowing a 'stranger' into his lab. He has been my mentor and not just a collaborator to me. All my G protein 'knowledge' is credited to him. He patiently transformed this chemist into a biochemist. I will surely miss our intellectual discussions.

I am thankful to **Drs. John-Stephen Taylor** and **Liviu Mirica** for their helpful suggestions and discussions throughout my advisory committee meetings. In addition, I would like to thank **Dr. Garland Marshall** for agreeing to serve on my dissertation committee and for his constructive feedback on my dissertation.

I would also like to thank Moeller group members (past and current) for making these past five years a memorable experience (specially Jen, Bo Bi, Libo, John, Derek, Bichlien, Jake, Rob, Matt, New Matt, Fang and Luis). I am especially grateful to my 'other' lab, Blumer lab (Kevin, Michi, Mo, Stephanie, Lixia and Matthew) for their generous support. All these guys were extremely kind, generous and more than just lab members to me. Especially Kevin, he was always there to help me.

I am grateful to both Dr. Zhongsheng You and Peter Harris for their insights on insect cell culture. In addition, this acknowledgement section will not be complete without the mention

of Drs. John Tesmer, Valerie Tesmer and Angeline Lyon at University of Michigan, Ann Arbor. Their valuable insights on the nucleotide exchange assays were extremely helpful.

Furthermore, I would like to acknowledge the administrative staff of Chemistry department (especially Rachel Dunn, Maria Guzman, Jessica Owens, Angela Potter, Angela Stevens, and Barbara Tessmer) for their help. I would also like to acknowledge my friends in the department, Manmilan Singh, Phyllis and Greg Noelken.

I am so grateful for my Northwest girls (Tiffany, Liz and Christine thank you for always keeping me sane). I am thankful to God for giving me such loving parents who always supported me and made me who I am today. A big thanks to my little brother for always being there. I would also like to thank my American parents (Lois and Earl Beaver) for their unconditional love and support. And a special appreciation to Zifan Li for always having my back. I can't express how much you mean to me! This graduate school journey would be incomplete with you and Wash U will always hold a special place in my heart because it gave me Zifan!

This dissertation is dedicated to my dearest parents, my loving brother, my American parents (Lois & Earl Beaver) and Zifan Li.

ABSTRACT OF THE DISSERTATION

Screening Protein Ligand Interactions Using Microelectrode Arrays

by

Sakshi Uppal

Doctor of Philosophy in Chemistry

Washington University in St. Louis, 2015

Professor Kevin D. Moeller, Chair

G proteins comprising of α subunit and βγ dimer are signaling proteins that play essential roles in various pathological conditions. Direct modulation of these G proteins (specifically Gα subunit) using small chemical probes to elucidate their acute function is of great value. YM-254890 is a small molecule which is the first selective inhibitor of a class of G proteins, $G\alpha_q$. However, despite its biological importance, this molecule is not available to researchers. In addition, the complex core structure of this cyclic depsipeptide has thwarted efforts to obtain a series of analogs by total synthesis. Moeller lab sought to overcome this obstacle by synthesizing simplified YM analogs that retain the ability to specifically inhibit $G\alpha_q$. Thereby, this effort requires not only the synthesis of the YM analogs, but also the availability of both the purified G proteins and a rapid, cost effective method for screening newly synthesized analogs in real-time for their potential activity toward G proteins. This dissertation focuses on the 1) isolation and characterization of G proteins necessary to test the potency of simplified analogs and 2) development of a rapid screening method by utilizing the power of microelectrode arrays.

In **Chapter 1** of this dissertation we discuss the potential utility of directly targeting G proteins and why it is essential to develop G protein modulators. In **Chapter 2**, we provide details on how three different G proteins ($G\alpha_q$ (wild type and mutant), $G\alpha_{i1}$ and $G\alpha_o$) were isolated. While expression of recombinant proteins from insect cells is widely used, we applied the Titerless Infected-cells Preservation and Scale up method to express $G\alpha_q$. A number of approaches were explored to optimize the biochemical assay that exhibits the activity of $G\alpha_q$. Eventually a receptor-assisted nucleotide exchange assay was developed that could test the activity of purified $G\alpha_q$. In **Chapter 3**, the activity of other G proteins was examined by a fluorescent nucleotide exchange assay. In addition, we introduce the first simplified analog of YM, WU-07047 and its potency towards $G\alpha_q$ and other G proteins was analyzed. Even though the receptor-assisted nucleotide exchange assay is a reliable way for testing the simplified analogs, it requires radio-labeled ligand and a number of accessory proteins. Hence, efforts were moved towards development of a rapid screening method utilizing the power of microelectrode arrays. The idea was to monitor binding interactions between immobilized small molecules and purified G proteins via electrochemical methods. **Chapter 4** investigates an approach to modify the array surface via the use of PEG-polymer as a means to reduce non-specific binding. In addition to the reduction of non-specific binding, the ability to incorporate PEG onto the array surface provides an opportunity to utilize PEG-polymers as a linker. These linkers move the immobilized molecule away from the array surface. In **Chapter 5**, we tested the compatibility of G proteins to the electroanalytical methods applied on microelectrode arrays. Moreover, we study a known binding interaction between a G protein and a short peptide on the arrays. Based on preliminary results, we can see specific binding interaction between them over non-specific background binding.

Chapter 1: Introduction

1.1 G protein-coupled receptors (GPCRs)

Signal transduction cascades (also known as cell signaling) mediate nearly all biological functions.[1,2,3] These cascades are paramount because they determine how the cell senses and responds to its environment. Many signal transduction pathways follow a general scheme illustrated in **Figure 1.1**. The event begins when an environmental signal ranging from photons of light to small molecules (referred to as a ligand) is received by a cell surface receptor.[3] This signal is then converted or transduced into a biological response through a series of chemical transformations.[1,2,3] The biological response can be diverse in including processes such as cell death, differentiation, and proliferation as well as metabolic changes within the cell.[1] These biological responses can arise from the activation of numerous signaling pathways which must be carefully regulated in order for the body to maintain a normal physiological balance.

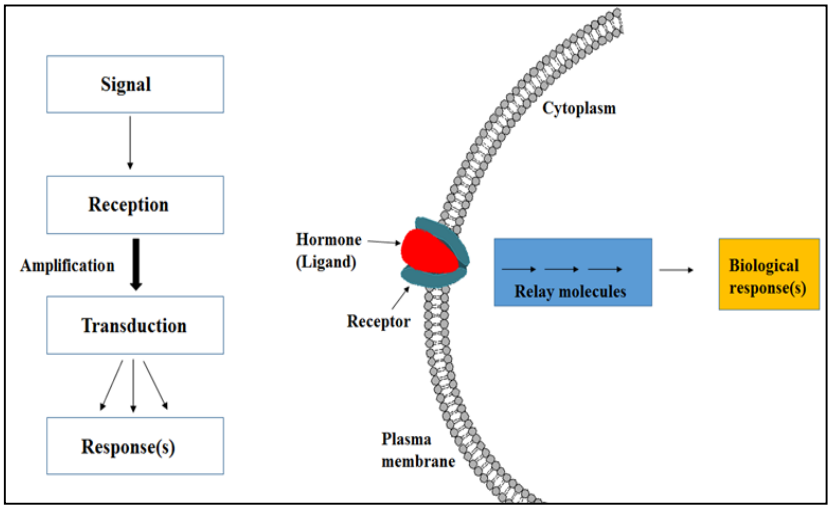

Figure 1.1. General scheme of signal transduction pathway. This figure is adapted from "Signal-Transduction pathways: An introduction to information metabolism".[1]

In this context, the majority of clinically used therapeutics modulate signaling pathways.[4] This can be done by targeting either the most upstream molecule in the pathway, the receptor [5–8] or one of the downstream chemical steps in the transduction scheme.[9] This dissertation will focus on one class of receptors known as G protein-coupled receptors (GPCRs) and the associated G proteins involved in the signal transduction pathway.

GPCRs comprise of the largest class of cell surface signaling proteins.[10,11,7] These receptors are integral transmembrane proteins that contain a seven helix bundle that crosses a cell membrane and interacts with G proteins through an intracellular binding site. The G protein plays a key role in the signal transduction part of the signaling pathway. GPCR's and their associated G proteins are essential in numerous physiological and pathological processes.[7,12,13] Most of the human GPCRs can be classified into five main families: Rhodopsin (701 members), Adhesion (24 members), Frizzled/Taste (24 members), Secretin (15 members) and Glutamate (15 members).[14,15] Defective G protein signaling pathways lead to numerous diseases (cardiovascular, neurological, inflammation, cancer, endocrine disorders etc.).[16,17,18] It has been suggested that modulating GPCR function might postpone or end the progression of numerous cancers.[7,18,19] Since GPCRs are critical players in cell signaling, they are common pharmaceutical targets. Currently ~30-50 % of the clinically approved drugs on the market target GPCRs.[4] GlaxoSmithKline's Zantac (targets Histamine H2 receptor to treat gastric ulcers), Bristol-Myers Squibb's Plavix (targets $P2Y_{12}$ receptor and acts as antiplatelet agent), and Eli Lilly's Zyprexa (targets Serotonin receptor to treat schizophrenia[20]) are prime examples of drugs in today's market that act by binding GPCRs.[12] Most of these therapeutic strategies broadly aim to either activate GPCR signaling with the use of an agonist or inhibit GPCR signaling with the use of an inverse agonist (an agent that exerts opposite pharmacological effect of an agonist[21])

and/or antagonist (an agent that blocks agonist binding to the receptor and in itself has no intrinsic activity).[21]

1.2 Heterotrimeric G proteins

The heterotrimeric guanine nucleotide-binding proteins (G proteins) that couple to the GPCRs are molecular switches that relay signals from activated GPCRs to a wide variety of intracellular effectors.[22–24] The G proteins are referred to as molecular switches because they switch between an on and off state depending on the nucleotide they bind. A GDP-bound Gα subunit is in 'off' or inactive mode whereas a GTP-bound Gα subunit is in 'on' or active mode. Details of the G protein activation cycle are described in **Section 1.3**. G proteins play an important role in transmembrane signaling process because they take part in the sorting of incoming signals. In other words, these proteins amplify and direct incoming signals coming from multiple receptors to appropriate cytoplasmic secondary messengers. For example: one G protein, Gs protein activates adenylyl cyclase (its cytoplasmic secondary messenger) upon getting a signal from β-adrenergic receptor (a GPCR).[25,26]

G proteins are comprised of three subunits; α, β, and γ (referred to as Gα, Gβ and Gγ), which are encoded by 16, 5, and 12 genes, respectively.[27] The classification of G proteins is based on the structural and functional similarities of their Gα subunit. Gα subunits are usually 40-46 kDa in size,[28] and they fall into four main subgroups: $G\alpha_s$, $G\alpha_i$, $G\alpha_q$, $G\alpha_{12/13}$.[29] **Table 1.1** depicts these subgroups, the subfamilies that lie within the groups, and their downstream effectors and effect.

Table 1.1. Classification of Gα subunits based on their structural and functional similarities. Information presented in this table was obtained from "Regulators of G protein signaling as new central nervous system drug targets".[67]

G protein	α-subunit subfamily	Downstream effectors	Effect
G_s	$G\alpha_s$, $G\alpha_{olf}$	stimulators of adenylyl cyclase	↑ cAMP
G_i	$G\alpha_{i1-3}$, $G\alpha_o$, $G\alpha_z$,	inhibitors of adenylyl cyclase	↓ cAMP
	$G\alpha_t$	stimulates cGMP phosphodiesterase	↓ cGMP
G_q	$G\alpha_q$, $G\alpha_{11}$, $G\alpha_{14}$, $G\alpha_{16}$	activates phospholipase Cβ (PLCβ)	↑ IP_3, DAG, Ca^{2+}
G_{12}	$G\alpha_{12}$, $G\alpha_{13}$	activates RhoGEF, phospholipase Cε (PLCε)	↑ Rho A signaling[30]

The Gα subunit consists of two distinct domains: a GTPase or Ras homology domain (because of its structural resemblance to Ras superfamily of monomeric GTPases[24]) and an α helical domain. Both of these domains are connected by two flexible linkers.[31,32] The nucleotide binding pocket exists in between these two domains. The guanine nucleotide exchange is a result of the interdomain movement between these two domains. Ras domain is the nucleotide binding domain that hydrolyzes bound GTP. It also provides binding surfaces for the βγ dimer and GPCRs due to the posttranslational modifications with the fatty acid myristoate (present in all Gα subunits except $G\alpha_t$).[24] This posttranslational modification at the N-terminus of α subunit is pivotal for membrane localization and protein-protein interactions.[24] The Ras domain has three flexible loops which are known as switch I, II, and III.[24,32,33] The γ-phosphate of the bound GTP makes favorable interactions with these switches, causing overall conformational changes within

the α subunit. This new conformation attained by the subunit allows it to specifically distinguish the downstream effectors.[34–38] The helical domain is unique to Gα proteins and contains a six α helical bundle that covers and buries the bound guanine nucleotide.

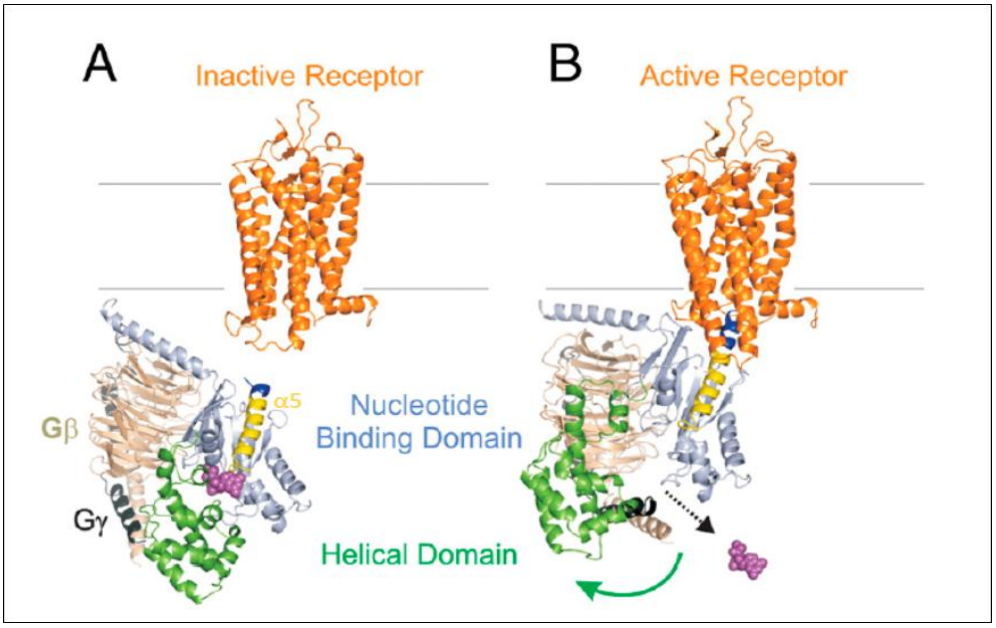

Figure 1.2. Representation of opening of the interdomain cleft. *Panel A.* The inactive receptor and G protein (PDB: 1U19). *Panel B.* Complexation of G protein with active receptor describing the reorientation of the helical domain (PDB: 3DQB). Van Eps N. *et al*. Interaction of a G protein with an activated receptor opens the interdomain interface in the alpha subunit. *Proc. Natl. Acad. Sci*. 2011; 108(23):9420-9424.

Figure 1.2 represents the opening of the interdomain cleft. Ribbon model shows α helical and Ras domains in green and light blue respectively. The C-terminal helix of the Ras domain (α5) which makes contacts with the receptor and the nucleotide binding site is represented in yellow. Prior to receptor activation, GDP (purple molecule) is bound in between the two domains. Double electron-electron resonance spectroscopy (DEER[39]) has demonstrated that even in the absence of a receptor, both domains can separate with each other in the presence of GDP.[40] This suggests that this movement is not sufficient for GDP release. Upon receptor activation, α5

displaces away from GDP which weakens the interactions between GDP and Ras domain and consequently when both domains separate, GDP releases. The catalytic G protein activation cycle will be discussed in the next section.

The Gβ and Gγ subunits exist as functional dimers and are usually referred to as Gβγ dimer. Gβ subunits are about 36 kDa and Gγ subunits are about 8 kDa in size.[41] Efforts to express these subunits separately have been rendered unsuccessful as it leads to unstable Gβ and unfolded Gγ subunits.[42] Once the dimerization has occurred, only denaturing conditions can dissociate them.[43] All Gγ subunits bind to the membrane via an isoprenyl group on their C-terminus as a result of posttranslational modification.[44] This binding interaction between Gβγ and the membrane is essential for the stability of Gα-receptor interface. Numerous studies have shown that Gβγ dimers are not just passive partners for Gα subunits. On the contrary, they are pivotal contributors in assembly and regulation of signaling pathways with the help of Gβγ binding proteins and are now potential therapeutic targets.[45–47]

1.3 G protein activation cycle

Activation of G protein can be described by the catalytic cycle in **Figure 1.3**. The cycle starts with an inactive G protein (GDP-bound Gα with Gβγ dimer) associated with the membrane-bound GPCR (Step 1). When a ligand binds to the receptor, a conformational change is induced within the receptor (Step 2). Distance between the nucleotide binding pocket of Gα subunit and the nearest receptor contact site (α5 in Ras domain) is ~30 Å.[24] An activated receptor can perturb the Ras domain of the Gα subunit and weaken the interactions this domain makes with GDP. Recent atomic-level molecular dynamics (MD) simulations of heterotrimeric G proteins with and without bound GPCRs have shown that rotation of helical domain (~90° in case of no bound GPCR and ~150° in case of bound GPCR) dramatically interrupts the interdomain nucleotide-

binding sites.[40] However, this rotation of helical domain is not sufficient for GDP dissociation which is the rate limiting step for the entire activation cycle. Conformational changes in the Ras domain initiated by an activated receptor and frequent domain separation work in conjunction to

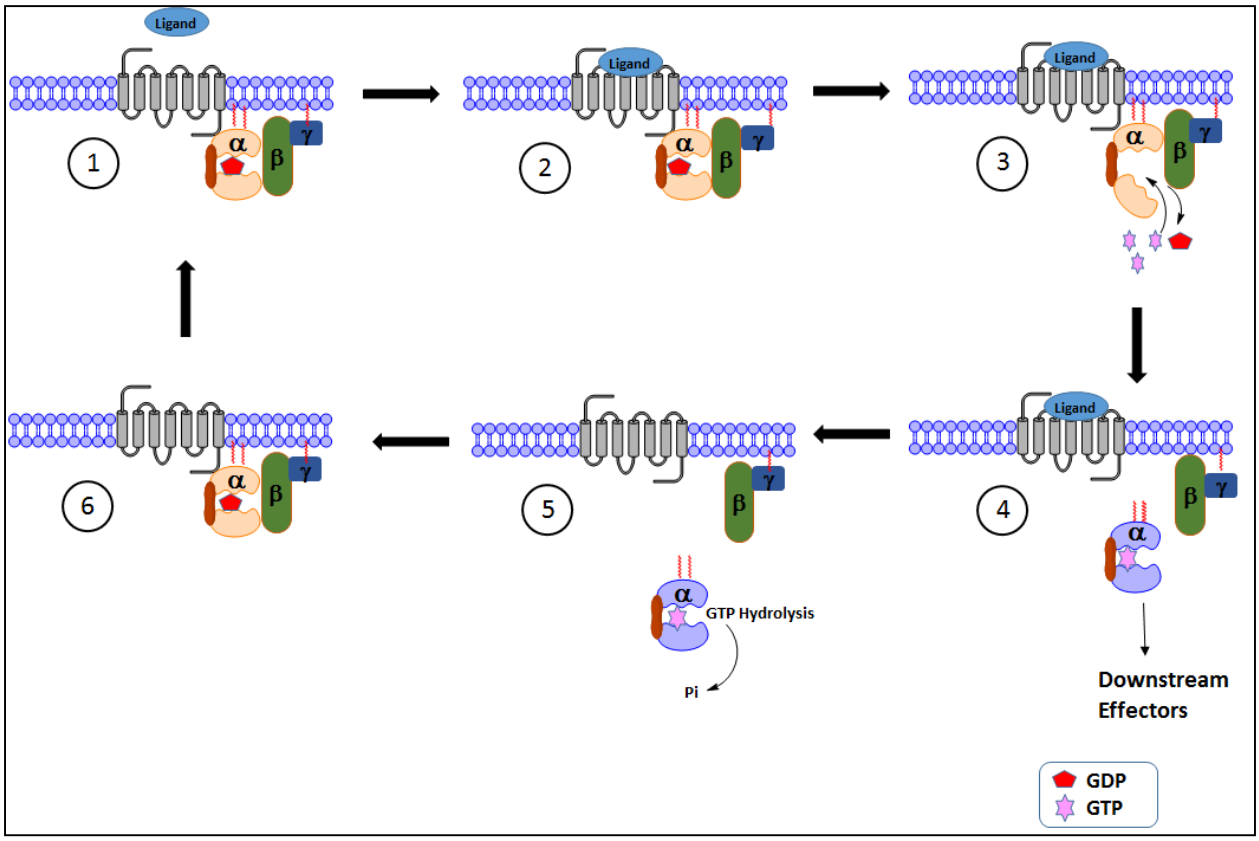

Figure 1.3. GPCR mediated G protein activation cycle. Steps of the cycle are numbered 1-6.

release GDP. The receptor stabilizes the unstable and short-lived nucleotide-free Gα subunit until a GTP binds the nucleotide pocket. Since cellular concentration of GTP (mM) exceeds that of GDP by several orders of magnitude, GTP binding is almost instant.[24] The receptor catalyzes the process of guanine nucleotide exchange (Step 3). Once GTP binds to the Gα subunit (now regarded as active Gα subunit), it initiates a structural rearrangement of Gα eliminating Gβγ binding surfaces. This causes the Gα to dissociate from the receptor and Gβγ dimer. Gα utilizes

the binding energy of GTP in order to form a conformation that will allow its interaction with specific downstream effectors (Step 4).[31] Intrinsic GTPase activity of Gα subunit mediates GTP hydrolysis resulting in GDP and Pi consequently making Gα return to its resting state. GDP-bound Gα subunit associates with Gβγ and turns off the signaling (Steps 5 and 6).

1.4 Diversity of GPCRs elicited signaling

Figure 1.3 shows a simplified description of canonical G protein signaling. The real process is much more complex. Although all GPCRs have a similar architecture of seven membrane spanning α helices, variability within the structure arises from the carboxyl terminus and amino terminus.[15] A single extracellular stimulus can activate multiple signaling pathways. For example, Serotonin, a small molecule, can bind 13-16 different GPCR family members that are expressed and coupled to separate signaling pathways.[12,41] As mentioned previously, GPCRs are targeted by the majority of pharmaceutical drugs as a means to regulate the signaling pathways but the successful development of therapeutic strategies have been hampered due to the complexities associated with these receptors. For example, **Table 1.2** lists GPCRs that couple to one class of G proteins, $G\alpha_q$. Complete inhibition of $G\alpha_q$ mediated signaling would require a ligand that would abrogate activity of all GPCRs capable of coupling to $G\alpha_q$. In other words, a ligand that would block one receptor might not be effective because an output signal can still appear due to the activation by other receptors. Another example is $G\alpha_i$ coupled μ-opioid receptor: OPRM1 which is known to regulate the analgesic and euphoric effects of opioid drugs like morphine.[49,50] OPRM1 receptor activates extracellular signal-regulated kinase (ERK) pathway which phosphorylates ERK. Morphine, etorphine and fentanyl are some of the known agonists of this receptor which activate ERK phosphorylation with similar potencies. The difference, however, is that morphine uses the Protein Kinase C (PKC) pathway and etorphine

uses β-arrestin pathway to phosphorylate ERK.[51] Hence, the same endpoint can be achieved through different pathways by different ligands with similar potencies. The functional utility of this redundancy constructed by nature into GPCR signaling pathways is a mystery.

Table 1.2. List of GPCRs that couple to $G\alpha_q$ family of G proteins

Gq family	Subfamily	Receptors
Gq	α_q	Alpha-1 adrenergic receptor, Vasopressin type 1 receptor, 5-HT2 serotonergic receptors, Angiotensin II receptor type 1, Calcitonin receptor, Histamine H1 receptor, Metabotropic glutamate receptor (group 1), M1, M3, M5 muscarinic receptors

Despite the amount of information that is known concerning GPCRs and their G protein coupling partners, little is known about their specificity. For example, the TSH receptor can activate all known G protein subfamilies[52] expressed in the thyroid. Why does one GPCR specifically couple to one G protein whereas the other GPCRs couple to multiple G proteins? Is this complexity evolved only to create a 'fail safe back-up' option? A clear understanding of the coupling specificity between GPCRs and G proteins would require an investigation at the level of G protein and receptor coupling interface. Given this intertwining between a single receptor and multiple G proteins, it is difficult to understand the chemistry of G proteins via GPCRs.

In contrast to the large number of genes encoding these receptors (more than 800 known GPCRs), fewer genes encode the heterotrimeric G proteins. There are 48 potential Gβγ dimer combinations calculated from 4 Gβ (there are weak or nonexistent dimer formation between $G\beta_5$ and Gγ subunits[53,54]) and 12 Gγ subunits. However, as mentioned previously, Gα subunits are

encoded by only 16 genes so it is much easier to target and learn about G protein signaling pathway via these α subunits.

1.5 Activation of G proteins by accessory proteins

Regulation of G proteins independently of GPCRs by other players regarded collectively as accessory proteins has also been recently identified.[55] These accessory proteins can be categorized in 4 sets: guanine nucleotide exchange factors (GEFs), guanine nucleotide dissociation inhibitors (GDIs), GTPase-activating proteins (GAPs) and Gβγ interacting proteins.[56–59] These accessory proteins provide additional signal input to G proteins in the absence of GPCRs or they can act as binding partners for G proteins to serve functions that are not yet clear. Recent findings suggest that accessory proteins are essential for the regulation of cardiovascular system.[56,55,60] The accessory proteins can be briefly described as:

1. GEFs for the Gα subunit: This class of accessory proteins catalyzes the guanine nucleotide exchange from the Gα subunit in the same manner as an activated GPCR would. Certain groups have reported AGS1 (activator of G protein signaling 1)[61] and Ric8 (resistance to inhibitors of cholinesterase)[62–64] as GEFs for certain Gα subunits.
2. GDIs for the Gα subunit: This class of accessory proteins share a common structural domain known as GPR (G protein regulatory) domain or GoLoco motif. This domain interacts with the GDP-bound conformation of Gα subunit and prevents nucleotide exchange resulting in the inhibition of Gα mediated signaling.[65,66] AGS3 (activator of G protein signaling 3) and Rap1GAP (Ras-related protein 1GAP)[65,66] are examples of signaling proteins that contain GoLoco motifs that can act as GDIs.

3. GAPs for the Gα subunit: This class of accessory proteins accelerate the GTPase activity of Gα subunit.[67–69] Most of the proteins in this class contain an RGS (regulator of G protein signaling) homology domain. RGS2 is a GAP for $G\alpha_q$.[70]
4. Gβγ interacting proteins: This class comprises proteins that deactivate Gβγ signaling by making contacts similar to Gα subunit. Gβγ can signal via its effector molecules (GRK2, GIRK, calcium channels etc.) only upon its dissociation from Gα subunit because effector molecules and Gα subunit share an overlapping surface present on Gβγ.[71] Phosducin and phosducin like proteins (PhLP) are examples of proteins that belong to this class.[72]

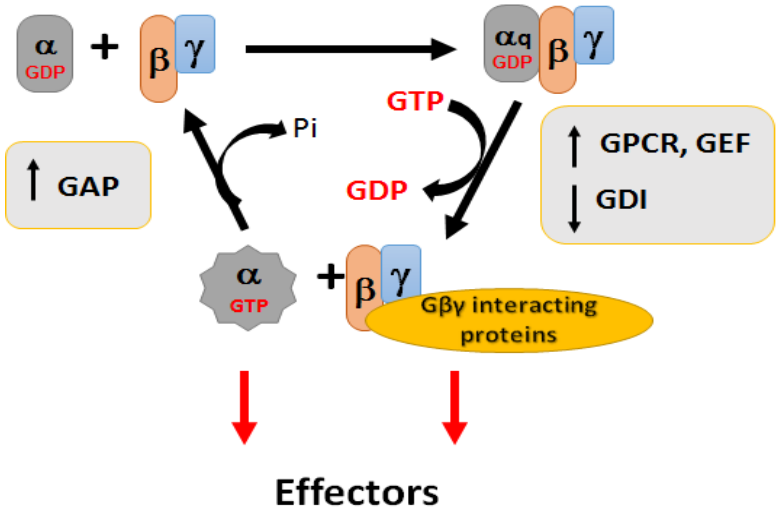

Figure 1.4. Effect of accessory proteins on activation/deactivation of G proteins. This figure is adapted from "Accessory proteins for heterotrimeric G-protein: Implication in the cardiovascular system"[60] with permission from Circulation journal. GPCR mediated G protein activation cycle.

1.6 Role of Gα proteins in diseases

$G\alpha_s$ was the first G protein to be associated with a human genetic disorder.[73] Mutations inactivating $G\alpha_s$ causes prototypical hormone resistance disorder known as

pseudohypoparathyroidism,[74] whereas somatic mutations activating $G\alpha_s$ have been associated with sporadic endocrine tumors.[73,74] Mutations that activate $G\alpha_s$ occur at Arg201 to either Cys or His inhibiting intrinsic GTPase activity which in turn results in a constitutively active $G\alpha_s$ and constitutive cAMP production.[19,75] A variety of mutations at Arg201 have also been linked to McCune-Albright syndrome (MAS), a rare disease causing skin pigmentation, bone disorder and autonomous hyperactivity of several endocrine glands.[75] Another G protein, $G\alpha_o$ with mutations at Arg243 to His was found in breast cancers.[76] Somatic mutations were found in both $G\alpha_q$ and $G\alpha_{11}$ (proteins that activate intra cellular calcium mediated signaling) that cause uveal melanoma.[77,78] Gln209 to Leu (Q209L) and Arg183 to Cys (R183C) were the identified mutations and out of the two, Q209L mutation is more frequent in uveal melanoma cells.[19] These examples mentioned above depict how gain of function or loss of function mutations in genes encoding for G proteins are associated with complex pathologies such as cancer. It is also clear that G proteins are not just simple signal transducers but are an essential part of a complex machine. Dissection of intracellular signaling networks can have substantial impacts on several aspects of both basic research and clinical medicine. However due to the redundancy in GPCR-G protein coupling mentioned in **Section 1.4**, any effort to gain a better understanding of molecular biology of signal transduction and explore more disease causing G protein mutations, requires approaches that directly modulate the G proteins.

1.7 Application of mouse models as a way to study G protein mediated signaling

The complex nature of GPCRs, GPCR independent G protein signaling via accessory proteins, and the direct role of G proteins in diseases provides us with a clear rationale for targeting G proteins. One way to deduce role of specific G proteins is through conditional or classical gene targeting technique which allows alteration of definitive genes.[79–81] Homologous

recombination is a DNA repair mechanism employed to introduce an engineered mutation into a mouse and is usually utilized to create a "loss of function" mutation (or an inactive gene).[80] The knockout mouse has been an invaluable tool for the geneticists to explore functions of genes. Through classical knockouts of certain genes, complete loss of activity is attained which helps in the inference of that gene's functional utility from a physiological context. Offermans and colleagues have elucidated the role of $G\alpha_{12/13}$ mediated signaling beyond the cellular and subcellular structures through their use of these types of mouse models.[82,83] The function of $G\alpha_q$ protein in platelet activation was also explored with the use of mouse models.[82,84] In addition, pathophysiological roles of multiple Gα proteins have been explored through these genetically engineered mice strategies, strategies that offer great advantages because of their *in vivo* applications.[82,85,86] These genetic approaches potentially have high target selectivity. Despite these advantages, the use of mouse models has its own inherent set of limitations as well.[87] For one, generating conditional mice lines is time consuming and expensive. It can take years to produce a functional mice line. Second, a single G protein can have multiple close homologs. Therefore, the classical knockout strategy can be rendered useless if it results in compensatory regulation of other genes.[88,89] Finally, knockout or knockdown of a protein interacting with a receptor may affect function of other proteins along with that specific receptor. For example: arrestin (a family of signaling proteins) has a dual function in receptor signaling, and it also serves as a scaffolding protein involved in cell migration and cytoskeletal reorganization[91]. Therefore, any knockout or knockdown of arrestin might not simply point towards its role in receptor signaling.[92]

There are other alternatives for studying G protein mediated signaling: knockdown of selected genes via RNA interference (RNAi),[93,94] selective inhibition via antibodies,[95,96] selective

activation via constitutively active mutants,[97] and selective regulation using chemical probes.[98–100] Chemical probes are small molecules that can be used as tools to regulate and learn about G proteins. These molecules are not yet drugs but they can mimic the function of a drug or its role in studying a physiological mechanism. This dissertation will focus on the use of novel chemical probes for direct modulation of G proteins.

1.8 Utilization of novel chemical probes as G protein inhibitors

Development of G protein selective inhibitors to study the underlying mechanisms of G protein activation and function, both *in vitro* and *in vivo,* appears to be of great pharmacological significance. For example, pertussis toxin, an enzyme complex produced by the bacterial pathogen *Bordetella pertussis,* selectively inhibits $G\alpha_i$ class[101,102] whereas *Pasteurella multocida* selectively activates $G\alpha_q$ protein.[103] In other studies, peptide based inhibitors potentially disrupt the GPCR-G protein interface and prevent activation.[68,104,105,106]

For our part, we are particularly interested in the development of small molecule inhibitors that serve as chemical probes for Gα subunits. The goal is to develop methods for a better understanding of biochemistry of these key players in the cell signaling pathway. To achieve decent *in vivo* binding affinities (low nM or better), a small molecule must form multiple non-covalent interactions with the protein of interest. This strategy will work efficiently if the target protein is not flat with limited surface topology. The α subunit of heterotrimeric G proteins has structural features consisting of a catalytic site and numerous clefts that could potentially bind to small molecules.[24,107,108] X-ray crystallographic, DEER spectroscopic studies have provided many of the mechanistic details regarding receptor-mediated GDP dissociation.[40] These structural and mechanistic details provide an opportunity to target GDP release with a small

molecule. For example, one can envision the inhibition of Gα subunits by blocking the inter-domain movements necessary for GDP release using a small molecule.

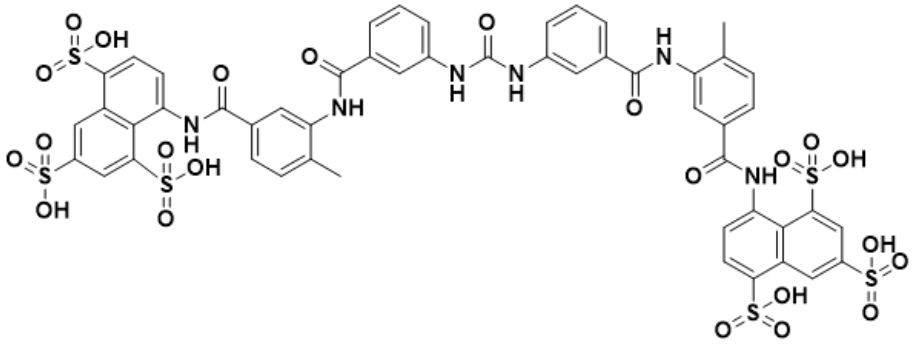

Figure 1.5. Suramin, $G\alpha_s$ family inhibitor

Numerous small molecules have been developed that target specific G proteins by preventing GDP release. The molecules work by blocking the inter-domain movement. Suramin **(Figure 1.5)** is a symmetric polysulfonated napthylaminebenzamide derivative that can directly interfere with receptor-G protein coupling.[109,110] This compound was originally introduced in 1916 by Bayer and was developed to treat African sleeping sickness and river blindness.[19] Suramin has been shown to block the receptor-mediated activation of $G\alpha_s$ (IC_{50}~250nM). It also inhibits guanine nucleotide exchange on $G\alpha_i$ and $G\alpha_o$ at higher concentrations (20 and 10 fold higher for $G\alpha_i$ and $G\alpha_o$ respectively).[110] One drawback of this compound is its sulfonated groups. Suramin has six negative charges which prevents it from passing through the plasma membrane. Characterization of this molecule is done using purified components (purified G proteins and adenylyl cyclase etc.).[109] Regardless of its inability to traverse through the plasma membrane, this compound is the first example of a small molecule inhibitor of G protein signaling. In efforts to learn more about this compound, researchers have derivatized this molecule and developed analogs (**Figure 1.6)** that are more selective towards $G\alpha_s$ in comparison to $G\alpha_i$ or $G\alpha_o$.[110,111,112]

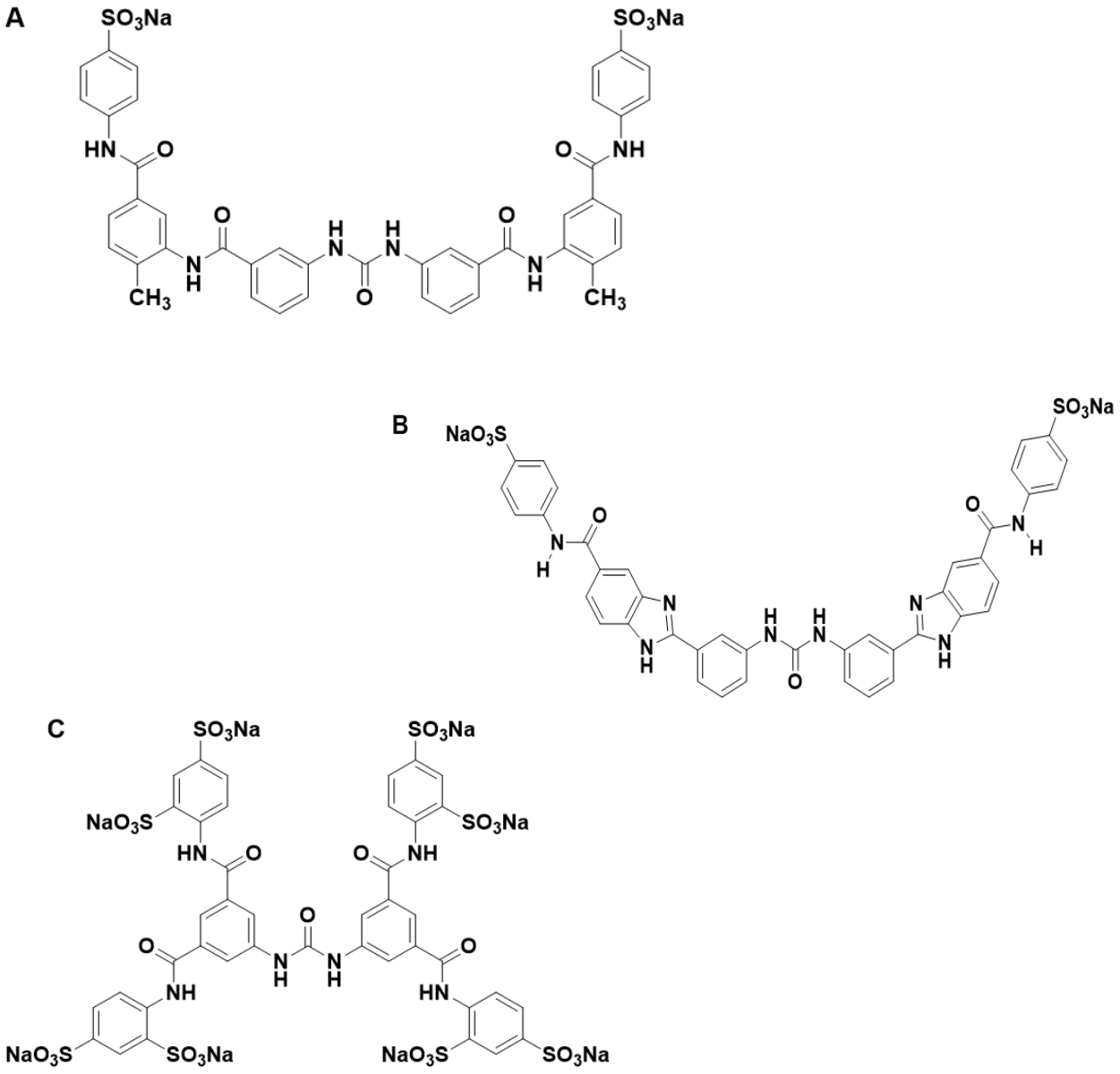

Figure 1.6. Suramin analogs (**A**: **NF062***;* **B**: **NF503**; **C: NF449**)

Another G protein modulator is BIM-46174 (**Figure 1.7**) which has been identified as a 'pan-G protein' inhibitor. Pan inhibitors couple to multiple G proteins and can be used as potential

cancer therapy agents.[19] BIM-46174 was identified in a differential screening library using human cancer MCF-7 cells. This library was established to categorize compounds that would inhibit the heterotrimeric G protein complex. This imidazo-pyrazine derivative halts GPCR signaling mediated by all four classes of G proteins ($G\alpha_s$, $G\alpha_{i/o}$, $G\alpha_q$ and $G\alpha_{12}$).[98,99] It acts directly on the G protein/receptor complex and not on any downstream signaling proteins.[99]

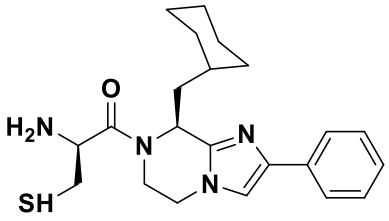

Figure 1.7. BIM-46174 ($G\alpha_s$, $G\alpha_{i/o}$, $G\alpha_q$ inhibitor)

This dissertation is concentrated on a specific $G\alpha_q$ inhibitor, YM-254890 **(Figure 1.8)**. YM-254890 (abbreviated as YM) is a cyclic depsipeptide derived from *Chromobacterium sp.* It is the first and only known compound to specifically inhibit the $G\alpha_q$ mediated signaling pathway.[113–115] In addition, YM exhibits antithrombotic and thrombolytic effects in rat models.[115,116]

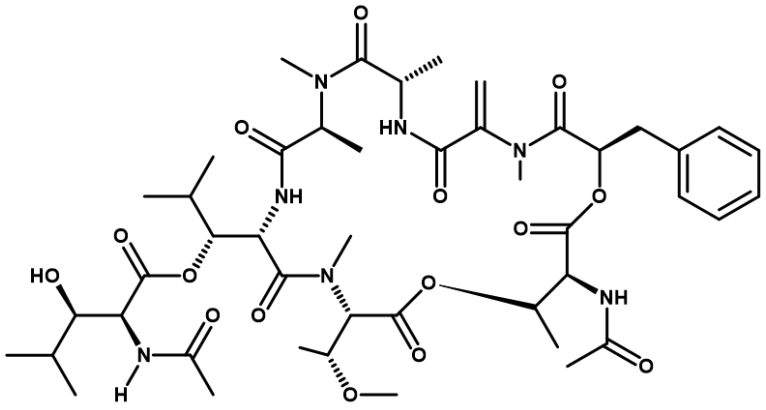

Figure 1.8. YM-254890, $G\alpha_q$ inhibitor

An X-ray crystal structure of the heterotrimeric G protein ($G\alpha_q\beta_1\gamma_2$) complexed with YM (PDB ID: 3AH8) has provided insight into the molecule's mechanism of action at the atomic level.[19] **Figure 1.9** illustrates specific binding of YM to $G\alpha_q$ using PyMOL software (The PyMOL Molecular Graphics System, Version 1.3 Schrödinger, LLC). In order to simplify the ribbon model drawing, $G\beta_1\gamma_2$ sequences have been eliminated. According to the crystal structure, YM molecule (grey line diagram) makes extensive contacts (represented in red**)** with both GTPase (also known as Ras-like domain) and helical domains and places itself between Switch I (represented in orange) and Linker 1 (represented in magenta) which reduces the hinge motion of the interdomain linkers as shown in **Figure 1.9**. Once bound, YM compound exhibits an overall folded V-shaped conformation and its aromatic phenyl group docks into a small hydrophobic pocket (yellow phenyl ring in **Figure 1.9**). YM compound behaves as an "interfacial inhibitor" which binds to both domains and forms a dead-end complex.

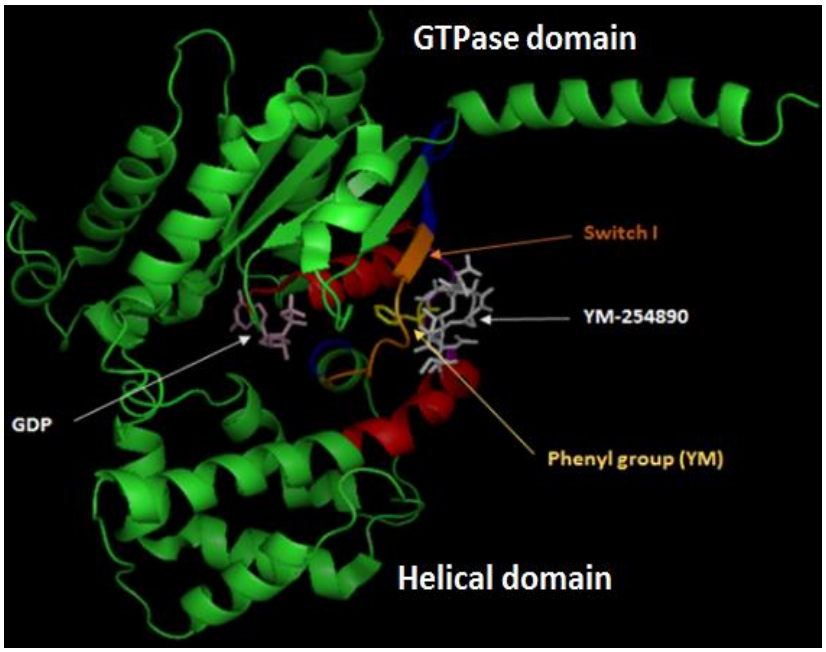

Figure 1.9. Specific binding of YM to $G\alpha_q$. Ribbon models were reconstructed using PyMOL (PDB ID: 3AH8). Nishimura. *et al*. Structural basis for the specific inhibition of heterotrimeric G_q protein by a small molecule. *Proc. Natl. Acad. Sci.* **2010**, 107, 13666–13671.

In this way, YM provides a potential lead compound for developing new inhibitors for $G\alpha_q$ and potentially other partially homologous Gα proteins as well. This has led to an intense interest in YM. However, these efforts are being hindered by two reasons. First, YM is not commercially available, and second its complex cyclic depsipeptide core structure has hampered its *de novo* synthesis. For this reason, we sought to overcome these obstacles by initially synthesizing simplified YM analogs that retain the ability to selectively inhibit $G\alpha_q$ signaling and eventually developing analogs that selectively inhibit other Gα proteins. The goals of the work are to understand what makes YM specific to only one class of G proteins and then capitalize on that information. Is it possible to ruin the selectivity of YM for $G\alpha_q$ and then reengineer in new selectivity? What controls the selectivity of the molecule? Is it a function of molecular conformation, or does it relate to the specific groups used to comprise the pharmacophoric regions of the molecule?

In order to address these questions, we need to synthesize analogs of YM, isolate and purify the $G\alpha_q$ protein, identify *in vitro* biochemical assays that allow us to determine the activity of analogs synthesized, and then develop a cost effective method for rapidly screening newly synthesized YM analogs in real-time for their potential activity towards $G\alpha_q$.

1.9 Goals of this dissertation

The work described here will focus on the last three tasks in the list presented above. Namely, methods for the isolation and purification of several Gα proteins will be described along with biochemical assays that capitalize on the proteins for probing the biochemistry of YM analogs. Along the way, we would like to ask certain questions that will assist us in gaining a comprehensive biochemical characterization of YM molecule. Once we simplify the YM molecule, does it loose its specificity towards $G\alpha_q$? In addition, we will describe efforts to take

advantage of microelectrode arrays for the rapid screening of small molecule-Gα protein interactions.

1.10 References

(1) Berg, J.; Tymoczko, J.; Stryer, L. Chapter 15 Signal-Transduction Pathways: An Introduction to Information Metabolism - Biochemistr... Page 1 of 4 http://www.ncbi.nlm.nih.gov/books/NBK21205/.

(2) Persidis, A. *Nat. Biotechnol.* **1998**, *16*, 1082–1083.

(3) Cornell, T. T.; Shanley, T. P. *Crit. Care Med.* **2005**, *33*, S410–S413.

(4) Brunton, L.; Parker, K.; Blumenthal, D.; Buxton, I. *Goodman & Gilman's: Manual of Pharmacology and Therapeutics*; **2008**; Vol. 95.

(5) Ghanemi, A. *Saudi Pharm J*, **2013**; 2, 115-129.

(6) Koelink, P. J.; Overbeek, S. A.; Braber, S.; De Kruijf, P.; Folkerts, G.; Smit, M. J.; Kraneveld, A. D. *Pharmacology and Therapeutics*, **2012**, *133*, 1–18.

(7) Lappano, R.; Maggiolini, M. *Nat. Rev. Drug Discov.* **2011**, *10*, 47–60.

(8) Wise, A.; Gearing, K.; Rees, S. *Drug Discovery Today*, **2002**, *7*, 235–246.

(9) Atalay, G.; Cardoso, F.; Awada, A.; Piccart, M. J.. *Annals of Oncology*, **2003**, *14*, 1346–1363.

(10) Lagerström, M. C.; Schiöth, H. B. *Nat. Rev. Drug Discov.* **2008**, *7*, 339–357.

(11) Pierce, K. L.; Premont, R. T.; Lefkowitz, R. J. *Nat. Rev. Mol. Cell Biol.* **2002**, *3*, 639–650.

(12) Filmore, D. *Mod. drug Discov.* **2004**, *7*, 24–27.

(13) Lania, A. G.; Mantovani, G.; Spada, A. *Nat. Clin. Pract. Endocrinol. Metab.* **2006**, *2*, 681–693.

(14) Fredriksson, R.; Lagerström, M. C.; Lundin, L.-G.; Schiöth, H. B. *Mol. Pharmacol.* **2003**, *63*, 1256–1272.

(15) Kobilka, B. K. *Biochim. Biophys. Acta* **2007**, *1768*, 794–807.

(16) Zolk, O.; Kouchi, I.; Schnabel, P.; Böhm, M. *Can. J. Physiol. Pharmacol.* **2000**, *78*, 187–198.

(17) Melien, O. *Methods Mol. Biol.* **2007**, *361*, 119–144.

(18) Dorsam, R. T.; Gutkind, J. S. *Nat. Rev. Cancer* **2007**, *7*, 79–94.

(19) Smrcka, A. V. *Trends Pharmacol Sci*, **2013**, *34*, 290–298.

(20) Digitale, E. *Nobel Prize work on G-protein-coupled receptors paves way for drug discoveries*; **2012**.

(21) Vilardaga, J.-P.; Steinmeyer, R.; Harms, G. S.; Lohse, M. J. *Nat. Chem. Biol.* **2005**, *1*, 25–28.

(22) Neves, S. R.; Ram, P. T.; Iyengar, R. *Science* **2002**, *296*, 1636–1639.

(23) Milligan, G.; Kostenis, E. *Br. J. Pharmacol.* **2006**, *147 Suppl* , S46–S55.

(24) Oldham, W. M.; Hamm, H. E. *Nat. Rev. Mol. Cell Biol.* **2008**, *9*, 60–71.

(25) Ross, E. M. *Neuron* **1989**, *3*, 141–152.

(26) May, D. C.; Ross, E. M.; Gilman, A. G.; Smigel, M. D. *J. Biol. Chem.* **1985**, *260*, 15829–15833.

(27) Downes, G. B.; Gautam, N. *Genomics* **1999**, *62*, 544–552.

(28) Graziano, M. P.; Freissmuth, M.; Gilman, A. G. *J. Biol. Chem.* **1989**, *264*, 409–418.

(29) Simon, M. I.; Strathmann, M. P.; Gautam, N. *Science* **1991**, *252*, 802–808.

(30) Siehler, S. *Br. J. Pharmacol.* **2009**, *158*, 41–49.

(31) Sprang, S. R. *Annu. Rev. Biochem.* **1997**, *66*, 639–678.

(32) Lambright, D. G.; Noel, J. P.; Hamm, H. E.; Sigler, P. B. *Nature* **1994**, *369*, 621–628.

(33) Mixon, M. B.; Lee, E.; Coleman, D. E.; Berghuis, A. M.; Gilman, A. G.; Sprang, S. R. *Science* **1995**, *270*, 954–960.

(34) Johnston, C. A.; Siderovski, D. P. *Mol. Pharmacol.* **2007**, *72*, 219–230.

(35) Tesmer, V. M.; Kawano, T.; Shankaranarayanan, A.; Kozasa, T.; Tesmer, J. J. G. *Science* **2005**, *310*, 1686–1690.

(36) Tesmer, J. J. G.; Sunahara, R. K.; Gilman, A. G.; Sprang, S. R. *Science (80).* **1997**, *278*, 1907–1916.

(37) Slep, K. C.; Kercher, M. A.; He, W.; Cowan, C. W.; Wensel, T. G.; Sigler, P. B. *Nature* **2001**, *409*, 1071–1077.

(38) Chen, Z.; Singer, W. D.; Sternweis, P. C.; Sprang, S. R. *Nat. Struct. Mol. Biol.* **2005**, *12*, 191–197.

(39) Jeschke, G. *Annu. Rev. Phys. Chem.* **2012**, *63*, 419–446.

(40) Dror, R. O.; Mildorf, T. J.; Hilger, D.; Manglik, A.; Borhani, D. W.; Arlow, D. H.; Philippsen, A.; Villanueva, N.; Yang, Z.; Lerch, M. T.; Hubbell, W. L.; Kobilka, B. K.; Sunahara, R. K.; Shaw, D. E. *Science (80).* **2015**, *348*, 1361–1365.

(41) Gies, J. P.; Landry, Y. *The Practice of Medicinal Chemistry*; **2008**; pp. 85–105.

(42) Higgins, J. B.; Casey, P. J. *J. Biol. Chem.* **1994**, *269*, 9067–9073.

(43) Schmidt, C. J.; Thomas, T. C.; Levine, M. A.; Neer, E. J. *J. Biol. Chem.* **1992**, *267*, 13807–13810.

(44) Zhang, F. L.; Casey, P. J. *Annu. Rev. Biochem.* **1996**, *65*, 241–269.

(45) Sadja, R.; Alagem, N.; Reuveny, E. *Proc. Natl. Acad. Sci.* **2002**, *99*, 10783–10788.

(46) Khan, S. M.; Sleno, R.; Gora, S.; Zylbergold, P.; Laverdure, J.-P.; Labbé, J.-C.; Miller, G. J.; Hébert, T. E. *Pharmacol. Rev.* **2013**, *65*, 545–577.

(47) Lin, Y.; Smrcka, A. V. *Mol. Pharmacol.* **2011**, *80*, 551–557.

(48) Takeda, S.; Kadowaki, S.; Haga, T.; Takaesu, H.; Mitaku, S. *FEBS Lett* **2002**, *520*, 97–101.

(49) Deb, I.; Chakraborty, J.; Gangopadhyay, P. K.; Choudhury, S. R.; Das, S. *J. Neurochem.* **2010**, *112*, 486–496.

(50) Xin, L.; Wang, Z. J. *AAPS PharmSci* **2002**, *4*, E23.

(51) Zheng, H.; Loh, H. H.; Law, P.-Y. *Mol. Pharmacol.* **2008**, *73*, 178–190.

(52) Laugwitz, K. L.; Allgeier, A.; Offermanns, S.; Spicher, K.; Van Sande, J.; Dumont, J. E.; Schultz, G. *Proc. Natl. Acad. Sci.* **1996**, *93*, 116–120.

(53) Dingus, J.; Hildebrandt, J. D. *Subcell. Biochem.* **2012**, *63*, 155–180.

(54) McIntire, W. E. *Neurosignals.* **2009**, *17*, 82–99.

(55) Sato, M.; Blumer, J. B.; Simon, V.; Lanier, S. M. *Annu. Rev. Pharmacol. Toxicol.* **2006**, *46*, 151–187.

(56) Sato, M. *Circ J* **2013**, *77*, 2455–2461.

(57) Sato, M.; Kataoka, R.; Dingus, J.; Wilcox, M.; Hildebrandt, J. D.; Lanier, S. M. *J. Biol. Chem.* **1995**, *270*, 15269–15276.

(58) Marjamaki, A.; Sato, M.; Bouet-Alard, R.; Yang, Q.; Limon-Boulez, I.; Legrand, C.; Lanier, S. M. *J. Biol. Chem.* **1997**, *272*, 16466–16473.

(59) Sato, M.; Cismowski, M. J.; Toyota, E.; Smrcka, A. V; Lucchesi, P. A.; Chilian, W. M.; Lanier, S. M. *Proc. Natl. Acad. Sci.* **2006**, *103*, 797–802.

(60) Sato, M.; Ishikawa, Y. *Pathophysiology*, **2010**, *17*, 89–99.

(61) Cismowski, M. J.; Ma, C.; Ribas, C.; Xie, X.; Spruyt, M.; Lizano, J. S.; Lanier, S. M.; Duzic, E. *J. Biol. Chem.* **2000**, *275*, 23421–23424.

(62) Wright, S. J.; Inchausti, R.; Eaton, C. J.; Krystofova, S.; Borkovich, K. a. *Genetics* **2011**, *189*, 165–176.

(63) Kataria, R.; Xu, X.; Fusetti, F.; Keizer-gunnink, I.; Jin, T.; Haastert, P. J. M. Van. *Proc. Natl. Acad. Sci.* **2013**, 110, 6424-9.

(64) Thomas, C. J.; Tall, G. G.; Adhikari, A.; Sprang, S. R. *J. Biol. Chem.* **2008**, *283*, 23150–23160.

(65) Blumer, J. B.; Oner, S. S.; Lanier, S. M. *Acta Physiologica*, **2012**, *204*, 202–218.

(66) Blumer, J. B.; Smrcka, A. V.; Lanier, S. M. *Pharmacology and Therapeutics*, **2007**, *113*, 488–506.

(67) Neubig, R. R.; Siderovski, D. P. *Nat. Rev. Drug Discov.* **2002**, *1*, 187–197.

(68) Kimple, A. J.; Bosch, D. E.; Gigue, P. M.; Siderovski, D.P. *Pharmacol Rev* **2011**, *63*, 728–749.

(69) Sjgren, B.; Blazer, L. L.; Neubig, R. R. *Prog. Mol. Biol. Transl. Sci.* **2010**, *91*, 81–119.

(70) Heximer, S. P.; Watson, N.; Linder, M. E.; Blumer, K. J.; Hepler, J. R. *Proc. Natl. Acad. Sci.* **1997**, *94*, 14389–14393.

(71) Smrcka, A. V. *Cell. Mol. Life Sci.* **2008**, *65*, 2191–2214.

(72) Schröder, S.; Lohse, M. J. *Proc. Natl. Acad. Sci.* **1996**, *93*, 2100–2104.

(73) Spiegel, A. M. *N. Engl. J. Med.* **2013**, *368*, 2515–2516.

(74) Spiegel, A. *Endocrine Development*; **2007**; Vol. 11, 133–144.

(75) Weinstein, L. S.; Shenker, A.; Gejman, P. V; Merino, M. J.; Friedman, E.; Spiegel, A. M. *N. Engl. J. Med.* **1991**; Vol. 325, pp. 1688–1695.

(76) Kan, Z.; Jaiswal, B. S.; Stinson, J.; Janakiraman, V.; Bhatt, D.; Stern, H. M.; Yue, P.; Haverty, P. M.; Bourgon, R.; Zheng, J.; Moorhead, M.; Chaudhuri, S.; Tomsho, L. P.; Peters, B. A.; Pujara, K.; Cordes, S.; Davis, D. P.; Carlton, V. E. H.; Yuan, W.; Li, L.; Wang, W.; Eigenbrot, C.; Kaminker, J. S.; Eberhard, D. A.; Waring, P.; Schuster, S. C.; Modrusan, Z.; Zhang, Z.; Stokoe, D.; de Sauvage, F. J.; Faham, M.; Seshagiri, S. *Nature* **2010**, *466*, 869–873.

(77) Van Raamsdonk, C. D.; Griewank, K. G.; Crosby, M. B.; Garrido, M. C.; Vemula, S.; Wiesner, T.; Obenauf, A. C.; Wackernagel, W.; Green, G.; Bouvier, N.; Sozen, M. M.; Baimukanova, G.; Roy, R.; Heguy, A.; Dolgalev, I.; Khanin, R.; Busam, K.; Speicher, M. R.; O'Brien, J.; Bastian, B. C. *N. Engl. J. Med.* **2010**, *363*, 2191–2199.

(78) Van Raamsdonk, C. D.; Bezrookove, V.; Green, G.; Bauer, J.; Gaugler, L.; O'Brien, J. M.; Simpson, E. M.; Barsh, G. S.; Bastian, B. C. *Nature* **2009**, *457*, 599–602.

(79) Lindeberg, J. *Ups. J. Med. Sci.* **2003**, *108*, 1–23.

(80) Hall, B.; Limaye, A.; Kulkarni, A. B. *Current Protocols in Cell Biology*, **2009**.

(81) Capecchi, M. R. *Nat. Rev. Genet.* **2005**, *6*, 507–512.

(82) Wettschureck, N.; Moers, A.; Offermanns, S. *Pharmacology and Therapeutics*, **2004**, *101*, 75–89.

(83) Worzfeld, T.; Wettschureck, N.; Offermanns, S. *Trends in Pharmacological Sciences*, **2008**, *29*, 582–589.

(84) Offermanns, S. *Circulation Research*, **2006**, *99*, 1293–1304.

(85) Offermanns, S. *Oncogene* **2001**, *20*, 1635–1642.

(86) Wettschureck, N.; Offermanns, S. *Physiol Rev* **2005**, 1159–1204.

(87) Eisener-Dorman, A. F.; Lawrence, D. A.; Bolivar, V. J. *Brain, Behavior, and Immunity*, **2009**, *23*, 318–324.

(88) Sprossmann, F.; Pankert, P.; Sausbier, U.; Wirth, A.; Zhou, X. B.; Madlung, J.; Zhao, H.; Bucurenciu, I.; Jakob, A.; Lamkemeyer, T.; Neuhuber, W.; Offermanns, S.; Shipston, M. J.; Korth, M.; Nordheim, A.; Ruth, P.; Sausbier, M. *FEBS J.* **2009**, *276*, 1680–1697.

(89) Benes, J.; Varejkova, E.; Farar, V.; Novakova, M.; Myslivecek, J. *Naunyn. Schmiedebergs. Arch. Pharmacol.* **2012**, *385*, 1161–1173.

(90) Birnbaumer, L. *Biochimica et Biophysica Acta - Biomembranes*, **2007**, *1768*, 756–771.

(91) Min, J.; Defea, K. *Mol. Pharmacol.* **2011**, *80*, 760–768.

(92) Michel, M. C.; Seifert, R. *Am. J. Physiol. - Cell Physiol.* **2015**, *308*, C505–C520.

(93) Andreeva, A. V; Vaiskunaite, R.; Kutuzov, M. A.; Profirovic, J.; Skidgel, R. A.; Voyno-Yasenetskaya, T. *Mol. Pharmacol.* **2006**, *69*, 975–982.

(94) Birukova, A. A.; Birukov, K. G.; Smurova, K.; Adyshev, D.; Kaibuchi, K.; Alieva, I.; Garcia, J. G. N.; Verin, A. D. *FASEB J.* **2004**, *18*, 1879–1890.

(95) Aragay, A. M.; Collins, L. R.; Post, G. R.; Watson, A. J.; Feramisco, J. R.; Brown, J. H.; Simon, M. I. *J. Biol. Chem.* **1995**, *270*, 20073–20077.

(96) Gohla, A.; Harhammer, R.; Schultz, G. *J. Biol. Chem.* **1998**, *273*, 4653–4659.

(97) Wu, E. H. T.; Tam, B. H. L.; Wong, Y. H. *FEBS J.* **2006**, *273*, 2388–2398.

(98) Schmitz, A.-L.; Schrage, R.; Gaffal, E.; Charpentier, T. H.; Wiest, J.; Hiltensperger, G.; Morschel, J.; Hennen, S.; Häußler, D.; Horn, V.; Wenzel, D.; Grundmann, M.; Büllesbach, K. M.; Schröder, R.; Brewitz, H. H.; Schmidt, J.; Gomeza, J.; Galés, C.; Fleischmann, B. K.; Tüting, T.; Imhof, D.; Tietze, D.; Gütschow, M.; Holzgrabe, U.; Sondek, J.; Harden, T. K.; Mohr, K.; Kostenis, E. *Chem. Biol.* **2014**, *21*, 890–902.

(99) Ayoub, M. A.; Damian, M.; Gespach, C.; Ferrandis, E.; Lavergne, O.; De Wever, O.; Banères, J.-L.; Pin, J.-P.; Prévost, G. P. *J. Biol. Chem.* **2009**, *284*, 29136–29145.

(100) Prévost, G. P.; Lonchampt, M. O.; Holbeck, S.; Attoub, S.; Zaharevitz, D.; Alley, M.; Wright, J.; Brezak, M. C.; Coulomb, H.; Savola, A.; Huchet, M.; Chaumeron, S.; Nguyen, Q.-D.; Forgez, P.; Bruyneel, E.; Bracke, M.; Ferrandis, E.; Roubert, P.; Demarquay, D.; Gespach, C.; Kasprzyk, P. G. *Cancer Res.* **2006**, *66*, 9227–9234.

(101) Casey, P. J.; Gilman, A. G. *J. Biol. Chem.* **1988**, *263*, 2577–2580.

(102) Fields, T. A.; Casey, P. J. *Biochem. J.* **1997**, *321 (Pt 3*, 561–571.

(103) Wilson, B. A.; Ho, M. *Reviews of Physiology, Biochemistry and Pharmacology*, **2004**, *152*, 93–109.

(104) Scott, J. K.; Huang, S. F.; Gangadhar, B. P.; Samoriski, G. M.; Clapp, P.; Gross, R. A.; Taussig, R.; Smrcka, A. V. *EMBO J.* **2001**, *20*, 767–776.

(105) Higashijima, T.; Uzu, S.; Nakajima, T.; Ross, E. M. *J. Biol. Chem.* **1988**, *263*, 6491–6494.

(106) Higashijima, T.; Burnier, J.; Ross, E. M. *J. Biol. Chem.* **1990**, *265*, 14176–14186.

(107) Wall, M. A.; Coleman, D. E.; Lee, E.; Iñiguez-Lluhi, J. A.; Posner, B. A.; Gilman, A. G.; Sprang, S. R. *Cell* **1995**, *83*, 1047–1058.

(108) Lambright, D. G.; Sondek, J.; Bohm, A.; Skiba, N. P.; Hamm, H. E.; Sigler, P. B. *Nature* **1996**, *379*, 311–319.

(109) Beindl, W.; Mitterauer, T.; Hohenegger, M.; Ijzerman, A. P.; Nanoff, C.; Freissmuth, M. *Mol. Pharmacol.* **1996**, *50*, 415–423.

(110) Freissmuth, M.; Boehm, S.; Beindl, W.; Nickel, P.; Ijzerman, A. P.; Hohenegger, M.; Nanoff, C. *Mol. Pharmacol.* **1996**, *49*, 602–611.

(111) Hohenegger, M.; Waldhoer, M.; Beindl, W.; Böing, B.; Kreimeyer, A.; Nickel, P.; Nanoff, C.; Freissmuth, M. *Proc. Natl. Acad. Sci.* **1998**, *95*, 346–351.

(112) Kassack, M. U.; Högger, P.; Gschwend, D. A.; Kameyama, K.; Haga, T.; Graul, R. C.; Sadée, W. *AAPS PharmSci* **2000**, *2*, E2.

(113) Takasaki, J.; Saito, T.; Taniguchi, M.; Kawasaki, T.; Moritani, Y.; Hayashi, K.; Kobori, M. *J. Biol. Chem.* **2004**, *279*, 47438–47445.

(114) Uemura, T.; Kawasaki, T.; Taniguchi, M.; Moritani, Y.; Hayashi, K.; Saito, T.; Takasaki, J.; Uchida, W.; Miyata, K. *Br. J. Pharmacol.* **2006**, *148*, 61–69.

(115) Nishimura, A.; Kitano, K.; Takasaki, J.; Taniguchi, M.; Mizuno, N.; Tago, K.; Hakoshima, T.; Itoh, H. *Proc. Natl. Acad. Sci.* **2010**, *107*, 13666–13671.

(116) Kawasaki, T.; Taniguchi, M.; Moritani, Y.; Uemura, T.; Shigenaga, T.; Takamatsu, H. *Br J Pharmacol* **2005**, 184–192.

Chapter 2: Expression and Purification of $G\alpha_q$ from Insect Cells

2.1 Introduction

G proteins receive signals from a variety of integral transmembrane cell receptors (G protein-coupled receptors, GPCRs) and transmit them to numerous intracellular downstream effectors.[1] Purified, recombinant G proteins have been paramount reagents in advancing our knowledge of G protein structure, function and signaling pathways.[2–4] For example, the cross-disciplinary research involving biochemical and crystallographic characterization requires homogenous functional G protein subunits in large amounts. As mentioned in the first chapter, our lab is interested in learning about G protein-mediated signaling pathways *via* novel chemical probes, in particular, simplified analogs of a $G\alpha_q$ specific inhibitor known as YM-254890. In order to test the activity of synthesized analogs, large amounts of purified $G\alpha_q$ protein will be necessary.

Gα subunits can be commonly classified into four classes: $G\alpha_s$, $G\alpha_{i/o}$, $G\alpha_q$, and $G\alpha_{12/13}$.[5] Large scale production of two classes of Gα subunits ($G\alpha_s$, $G\alpha_{i/o}$) has been well established using bacterial cell expression system (*E.coli* expression system).[4,6] *E.coli* expression system is the simplest and least expensive heterologous expression system which can be scaled up easily.[7] However, α subunits of $G\alpha_q$ and $G\alpha_{12/13}$ class cannot be expressed from bacterial cells as functional proteins due to unclear reasons. Fortunately, insect cell expression systems have made it possible for these α subunits to be expressed and purified as active proteins. This chapter will discuss expression, purification and characterization of $G\alpha_q$ protein from insect cells using a new

approach, which utilizes Baculovirus-Infected Insect Cells (BIICs) and Titerless Infected-cells Preservation and Scale up (TIPS).

2.1.1 Insect cell expression system

Recombinant protein technology has made impressive advances over the past decades. A variety of expression systems have been developed, but the *E.coli* expression system continues to dominate the bacterial expression system and is the first choice for heterologous protein production.[7] However, many eukaryotic proteins require folding chaperones and various covalent modifications following translation in order to become functional and/or adapt proper structure. Bacterial expression systems are not capable of carrying out these events. Fortunately, there are other expression systems which can overcome these limitations and provide active protein. With respect to mammalian cells, insect cells are the second best host in terms of their ability to produce fully processed and biologically active recombinant proteins.[8] This is because insect cells are eukaryotic and are able to fold proteins in a manner that closely resembles mammalian cells. Subsequently, chances of proteins expressed from insect cells having normal biological activity in comparison to proteins expressed from bacterial cells will be greater. In addition, insect cell expression system is a popular choice because it allows expression of recombinant proteins in large scale whereas large scale protein expression can be cumbersome and expensive in mammalian cells.[9] Sf9 and sf21 cells from the fall armyworm *spodoptera frugiperda* are the most frequently used cell lines. Cell lines from *Trichoplusia ni* (commercially available as High-Five™) are also insect cell lines and have been used to give high yields of recombinant proteins.[8,10] Stable cell lines from all the insect larvae are obtained from embryonic cells and represent undifferentiated cells. Recombinant baculoviruses are used as expression vectors to produce foreign proteins in cultured insect cells. These baculoviruses are double-stranded, circular, supercoiled DNA molecules in a

rod shaped capsid.[11] *Autographa californica* multiple nuclear polyhedrosis virus (AcMNPV) and *Bombyx mori* (silkworm) nuclear polyhedrosis virus (BmNPV) are the two most commonly used baculovirus for gene expression.[12,13] The genome of the baculovirus contains a foreign nucleic acid sequence, a cDNA encoding protein of interest under the transcriptional control of the polyhedrin promoter.[12,14] This chimeric gene constituting of the polyhedrin promoter and the protein of interest is present in place of the non-essential (not required for the replication of baculoviruses[15]) and wild-type polyhedrin gene.[14] The recombinant virus can then be used to infect cultured insect cells and eventually express the protein of interest (instead of naturally occurring polyhedrin protein) by taking over the gene expression machinery of the host cell.[16] Baculoviruses are nonpathogenic to plants and mammals[17] and therefore can be safely used with minimal containment conditions.[13] Since its introduction in 1983, Baculovirus Expression Vector Systems (BEVS) technology has improved and now emerged as a state of the art technique to make recombinant proteins.[12–14,18,19] Details about insect cell lines and expression methods are available from Life Technologies instruction manual titled "Guide to Baculovirus Expression Vector Systems (BEVS) and insect cell culture techniques".

2.1.2 Why insect cells for G protein expression?

Heterotrimeric G proteins are peripheral membrane proteins and require proper folding and lipid modification to interact with other proteins and for plasma membrane localization.[23,24] All Gα subunits are modified at or near N terminus via covalent attachment of fatty acids, myristate (a C_{14} saturated acid attached through an amide bond to a glycine residue) and/or palmitate (a C_{16} saturated acid attached through a thioester bond to a cysteine residue).[25,26] All Gα subunits undergo reversible S-palmitoylation. Some Gα subunits are palmitoylated at one site ($G\alpha_s$ and $G\alpha_{12}$) and some at two sites ($G\alpha_q$ and $G\alpha_{13}$),[27] but only members of the $G\alpha_{i/o}$ family undergo an irreversible

co-translational myristoylation along with reversible palmitoylation. The myristoylation is carried out by an enzyme known as N-myristoyl transferase (NMT).[28] Studies have shown that these lipid modifications are not sufficient for plasma membrane localization, and that heterotrimer formation is also necessary. As a result, Gα subunits need to interact with βγ dimer.[29–32] As yet, no evidence has emerged that depicts β subunits undergoing lipid modifications, however, γ subunits are lipid modified by covalent attachment of a prenyl moiety.[33,34] As mentioned previously, only the $G\alpha_s$ and $G\alpha_i$ can be expressed and purified from *E.coli* as functional proteins among all G proteins. Another major consideration during expression of Gα subunits in bacterial cells is that the Gα subunit should be present in the soluble fraction of cell lysates. If not, Gα subunits need to be solubilized and/or refolded which can easily lead to inactive protein.[24]

The sf9-baculovirus expression system (a type of BEVS) can overcome these limitations and offer great advantages. Sf9 cells provide a variety of posttranslational modification mechanisms such as palmitoylation, myristoylation and prenylation (lipid modifications essential for interaction of G proteins with other proteins and receptors[36,37]). In concert with providing an array of posttranslational modifications, the sf9 expression system can be employed for the production of multiprotein subunit complexes.[13,20] Multiple baculoviruses encoding α, β and γ subunits of the G proteins have been coinfected in cultured sf9 insect cells to express the desired G protein heterotrimer.[35] Earlier expression studies of $G\alpha_q$ in sf9 cells, without co-expression of βγ subunits, resulted in misfolded and aggregated $G\alpha_q$ protein.[37,38] Hence a new procedure was developed which required co-expression of His_6-tagged Gγ subunit (6-His-Gγ) with the desired Gα subunit and β subunit.[35] The His_6 affinity tag consists of six consecutive histidine residues bound to the N-terminus of Gγ subunit. The presence of this tag results in high affinity binding of the heterotrimer to a resin containing chelated Nickel (Ni^{2+}).[35] Hence, the Gα subunit was recovered by treatment

with aluminum fluoride which reversibly activates α subunit and results in its dissociation from βγ dimer[35] (fluoroaluminates have been shown to activate GDP bound Gα by mimicking the γ-phosphate of GTP in its binding site).[39,40] Although this method successfully provides homogenous functional Gα subunits but the laborious procedure limits its application.[24,35,41]

2.1.3 Production of protein using BEVS

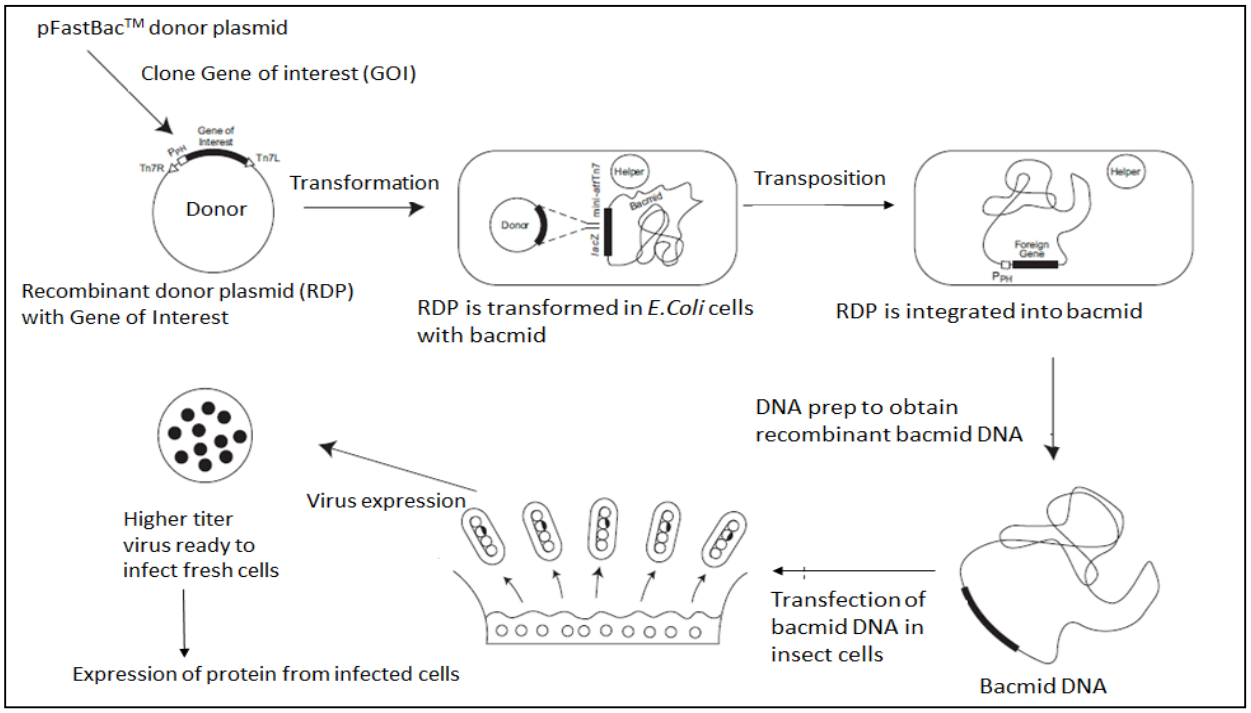

Figure 2.1. Generation of recombinant baculovirus and gene expression using Bac-to-Bac Baculovirus Expression Vector System. This figure is adapted from the user manual titled "Bac-to-Bac® Baculovirus Expression System, An efficient site-specific transposition system to generate baculovirus for high-level expression of recombinant proteins", Publication Number MAN0000414, pg 12. (Life Technologies).

Protein production using BEVS is a two-step process. During the first step, the insect cells are grown to a desired concentration (usually $1x10^6$-$2x10^6$ viable cells/mL). The second step is the infection of cultured cells with a baculovirus. Once the baculovirus takes control of the gene expression machinery of the host cell, it results in production of the target protein.[14,18–20] One of

the widely used BEVS is the Bac-to-Bac® baculovirus expression vector system.[21] A detailed description of this system is provided by Life Technologies in a manual titled "Bac-to-Bac® Baculovirus Expression System, An efficient site-specific transposition system to generate baculovirus for high-level expression of recombinant proteins". This description will not be repeated in this dissertation. However, a simplified summary explaining the generation of recombinant baculovirus is provided.

Figure 2.1 shows a general scheme depicting production of recombinant baculovirus using Bac-to-Bac® BEVS. In order to make baculovirus containing the desired target protein, the donor plasmid has to be transformed into an intermediary bacterial host (in most cases DH10Bac). This host contains a bacmid (baculovirus shuttle vector) and a helper plasmid. The helper plasmid assists the transfer of essential sequences from the donor plasmid to the bacmid (a process referred to as transposition) to generate recombinant bacmid which can be isolated by commercially available DNA purification kits (Life technologies, Carlsbad, CA). Transposition then places the gene of interest under the control of the polyhedrin promoter, a promoter which can be recognized by host cell machinery. The recombinant bacmid DNA is then used to infect cultured insect cells which generates a small scale, low titer stock of baculovirus (generally referred to as P1). P1 is then used to infect insect cells and amplified to a higher titer baculovirus (contains more viral particles and denoted as P2). Another round of amplification can be done in a similar way to produce even higher titer stock of baculovirus (denoted as P3). This titer stock is then used to infect insect cells to test expression of target recombinant protein. Finally, the highest titer stock, P4 is then used for large scale protein production. Additional rounds of amplification can increase the probability of defective interfering particles which reduces the efficiency of viral expression.[22] Hence, most protein expressions are carried out using either P3 or P4.

2.1.4 Expression and purification of recombinant Gα subunits using Ric-8

In order to simplify the production of recombinant G proteins in insect cells, another method was introduced which utilizes a mammalian protein called Resistance to Inhibitor of Cholinesterase 8 (Ric-8).[42,43] There are two mammalian homologs of Ric-8, named Ric-8A and Ric-8B, which are hypothesize to function as guanine nucleotide exchange factors (GEF) and folding chaperones for G proteins.[44,38] Ric-8A specifically interacts with $G\alpha_i$, $G\alpha_q$ and $G\alpha_{13}$ class of G proteins[39] whereas Ric-8B is specific towards $G\alpha_s$[48]. Ric-8 assisted expression and purification method of Gα subunits works by co-expression of GST-tagged Ric-8A or Ric-8B with untagged Gα subunit in cultured Hi5 insect cells.[42] Since Ric-8 is GST tagged, Ric-8: Gα complex can be isolated from glutathione-sepharose resin. In order to recover Gα subunits, the protein bound matrix can then treated with aluminum fluoride. One of the most significant results from this method was the yield of Gα obtained comparing to the one obtained from Gβγ co-expression. The yields from GST-Ric-8 co-expression method increased ~20 fold for $G\alpha_q$, ~25 fold for $G\alpha_{13}$, ~8 fold for $G\alpha_{i1}$ and ~11 fold for $G\alpha_{s\ short}$ (a variant of $G\alpha_s$ protein).[42] Besides impressive yields, what makes this method so appealing is its applicability to all four classes of Gα subunits.[42]

No matter what co-expression method is utilized to obtain the protein, a high titer baculovirus is required to infect cultured cells. As discussed in **Section 2.1.3**, both P2 and P3 baculovirus stocks are considered amplified viral stocks but one of the two will express higher amounts of protein without reducing the efficiency of viral expression. An important piece of technical information that has not been introduced so far is how to determine the titer of baculovirus stock. In other words, how is the strength of virus determined? The most frequently used methods for titration of baculovirus are end-point dilution and plaque formation assays, which are lengthy and challenging to perform and can take 4-7 days after virus infection.[49] In addition, stability of

baculovirus is affected over time due to several factors such as storage temperature, virus concentration and freeze-thaw cycles.[50] Infectivity of baculovirus can significantly decrease upon exposure to light.[51] Baculovirus stored at 4 °C (covered with foil) can be stable for about 100 days but its potency can decrease after that.[50] Studies have shown that a virus stored at -80 °C can be stable for at least 300 days but will suffer significantly after every freeze-thaw cycle.[50] Hence, a method that eliminates the need to titer baculovirus and preserves it for longer periods of time would be of great value.

2.1.5 Using BIICS and TIPS method to express $G\alpha_q$

Baculovirus-Infected Insect cells (BIICs) are insect cells that allow replication of the baculovirus within themselves followed by cryopreservation. In other words, these cells are first infected with the virus and then prior to cell lysis, the newly replicated virus is cryopreserved within the cell. BIICs are stored at -80 °C and are stable for at least 60 months without loss of viability.[52] BIICs technology was established for long term storage of baculovirus and was used in conjunction with the Titerless Infected-cells Preservation and Scale up (TIPS) method. BIICs technology and TIPS method was first developed and patented by David J. Wasilko, S. Edward Lee and William Hermans (Pfizer Global Research and Development).[53] But now the concept has been harnessed by Contract research organizations for large scale production of proteins from baculovirus expression.[54] The TIPS method allows for direct infection of cultured insect cells from BIICs stocks eliminating the need for high titer virus stock. Since the titer of the virus is stable for years, one can get reproducible protein expression. Optimization of protein expression on small scale and then easy scale up (upto 100 L) makes this technique extremely attractive.[52] Hence, after a certain period of trial and error, we selected this system for use in our efforts.

2.2 Results and discussion

2.2.1 Baculovirus technology allows the expression of $G\alpha_q$

Baculovirus technology has been increasingly popular in numerous academic and industrial laboratories for expression of recombinant proteins that require posttranslational modifications.[13] **Figure 2.2** illustrates the entire process from gene cloning to protein production in a flowchart.

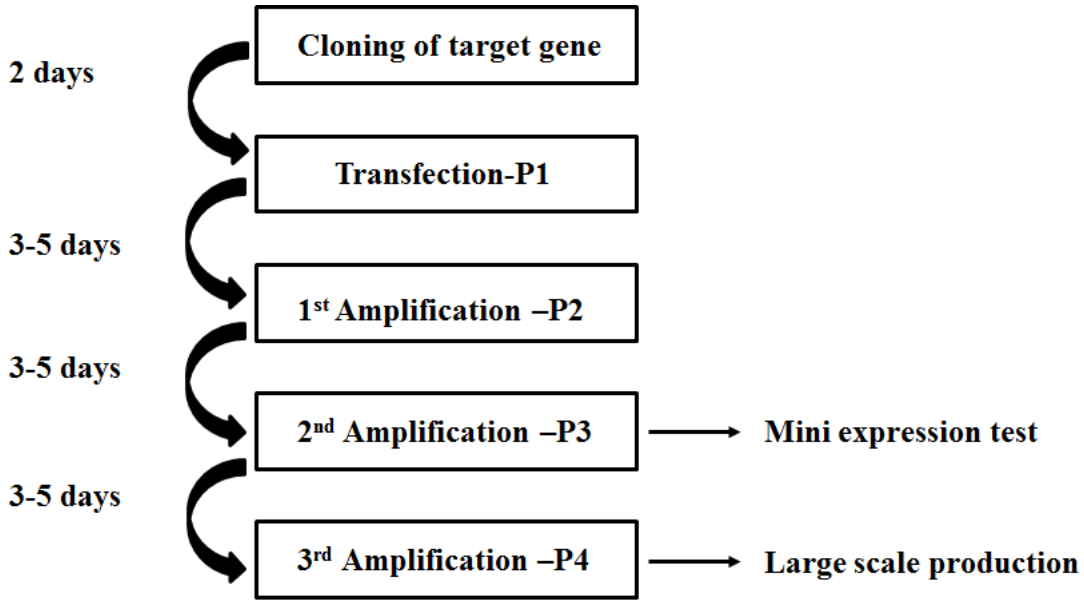

Figure 2.2. A general outline depicting the process and time scale from gene cloning to protein production in insect cells.

As mentioned previously, overexpression of wild type $G\alpha_q$ in insect cells results in insoluble, aggregated protein and requires co-expression of $G\beta\gamma$ dimer.[37,38] Another solution to this problem is a chimeric $G\alpha_{i/q}$ protein described by Tesmer *et.al*.[56] This chimera replaced the wild-type N-terminal helix with that of $G\alpha_{i1}$ and allowed expression of a soluble and functional $G\alpha_q$. Nishimura *et. al.* had used this $G\alpha_q$ chimera to show inhibitory effects of YM-254890 (now abbreviated as

YM) on $G\alpha_q$.[58] Along with this protein, numerous mutant forms of $G\alpha_q$ protein were used to explore the effectiveness of YM and one of them was $G\alpha_q$ I190N (containing one site mutation of isoleucine to asparagine). According to the authors, this mutant $G\alpha_q$ reduces the sensitivity of the YM compound (730 fold decrease in potency). With this in mind, we generated two baculoviruses encoding $G\alpha_q$ and $G\alpha_q$ I190N to produce large quantities of homogenous purified proteins in order to test the activity of simplified YM analogs. Using the BEVS, we were able to incorporate $G\alpha_q$ and mutant $G\alpha_q$ separately into two plasmids that can be recognized by insect cells and produce baculovirus that can express $G\alpha_q$ and mutant $G\alpha_q$ protein upon infection.

Clones for $G\alpha_q$ and mutant $G\alpha_q$ (WT-7`, WT-11 for $G\alpha_q$ and Mut-3 and Mut-8 for mutant $G\alpha_q$) were selected for transfection in cultured sf9 cells. Both clones for $G\alpha_q$ were successfully transfected but only one for mutant $G\alpha_q$ was transfected as shown in **Figure 2.3**. Both proteins are histidine-tagged and thus western blot was probed with anti-His antibody. Both proteins are ~44 kDa in size and the relevant bands are highlighted with the red box. Unfortunately, the protein molecular weight marker did not transfer well. The additional bands on the blot are probably

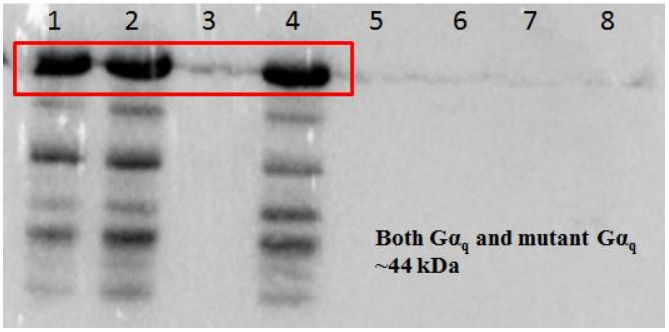

Figure 2.3. Western blot showing transfection results of $G\alpha_q$ and mutant $G\alpha_q$. Lanes 1-5 are WT-7`, WT-11, Mut-3, Mut-8, non-transfected sf9 cells respectively. Lanes 6-8 contain sample buffer only. Essential bands are indicated within the red box.

degraded protein bands. Successfully transfected clones were then amplified as described in experimental section (**Section 2.4.2**).

2.2.2 TIPS method can be applied for expression of $G\alpha_q$

In order to utilize TIPS method for protein production, it was essential to attain optimal conditions. It was decided to evaluate this method based on two factors: the amount of BIICs used to infect cells and the incubation time. This titration experiment (96-h study) was performed using $G\alpha_q$-BIICs stock (**Section 2.4.3** provides experimental details on the production of BIICs stock). Fresh sf9 cells (cell viability > 95 %) were infected with varying amounts of BIICs and a 2 mL sample was obtained after 24 h intervals. Cell count and viability was monitored throughout the experiment. It was observed that cell count doubled in the initial 24 h but slowed after that (doubling time for sf9 cells is 24 h). As far as viability is concerned, it was not affected greatly until 48 h (viability remained > 90 %) and thus it was concluded that cells so far showed no signs of infection. This was consistent with the literature report.[52] However, after 48 h, the dynamics changed dramatically for flasks that were infected with higher amounts of BIICs (1500 and 2000 BIICs/mL). Cell viability dropped to 65 % for 1500 BIICs/mL sample and 75 % for 2000 BIICs/mL flasks. Cell viability for 500 BIICs/mL and 1000 BIICs/mL was ~85 %. During the last time point (96 h), all flasks had cell viability below 50 %. **Figure 2.4** shows western blots illustrating the time course aspect of this experiment along with the effect of titration of BIICs on $G\alpha_q$ expression. Western blots were exposed to Anti-His antibody. A positive control was loaded to ensure that antibody was functional.

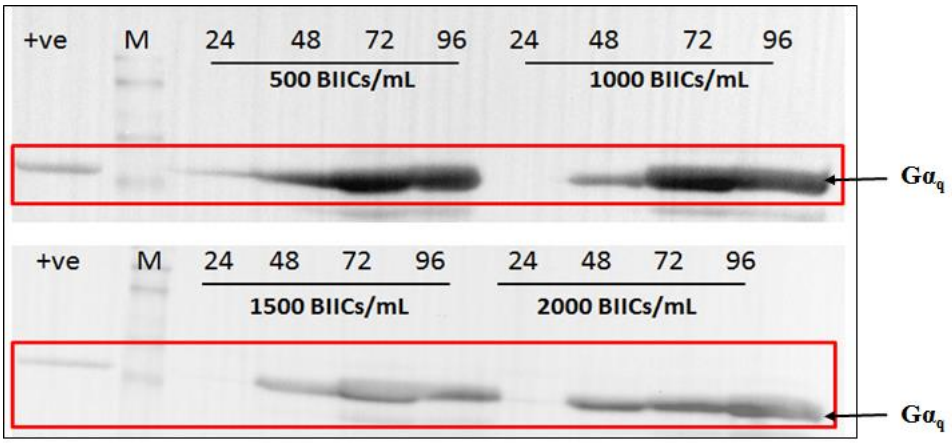

Figure 2.4. Effect of incubation time and varying amounts of BIICs on expression of $G\alpha_q$ in sf9 cells. Positive control (+ve); protein molecular weight marker (M); time point samples collected at 24, 48, 72, 96 h for sf9 cells infected with final concentration of 500 BIICs/mL or 1000 BIICs/mL (***upper blot***) or 1500 BIICs/mL or 2000 BIICs/mL (**l*ower blot***). MW= ~ 44 kDa.

The cell viability results suggested that expression had not started until 48 h; a conclusion that was supported by western blot analysis as well. Minimal amount of protein was expressed within 24 h of infection for all samples. Although the infection process was the same in every case, varying BIICs concentration produced unique protein expression results. Upper western blot (showing results from sf9 cells infected with either 500 or 1000 BIICs/mL) in **Figure 2.4** indicated similar expression kinetics for 72 and 96-h time points whereas cells infected with highest amounts of BIICs (1500 BIICs/mL) did not show increased protein expression after 48 h demonstrating that more BIICs does not necessarily result in more protein. Both western blots (assuming equal cell loading) showed that the infections done with either 500 or 1000 BIICs/mL (final concentration) and infection period between 72 and 96 h gave the most amount of expressed protein. Even though calculations were made to ensure equal cell loading and both blots had similar exposure times, there can be variabilities. Therefore, in order to confirm this result, another western blot (**Figure 2.5**) was carried out using all samples from the 72-h time point.

2.2.3 Protein expression from TIPS method was similar to traditional virus infection method

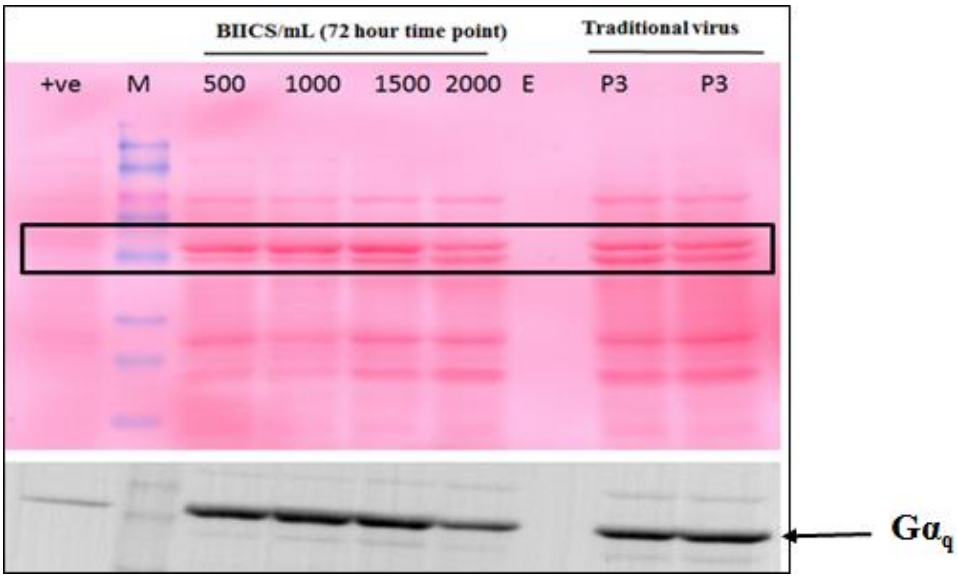

Figure 2.5. Comparison of infection by BIICs vs traditional virus. Positive control (+ve); protein molecular weight marker (M); varying BIICs amounts (500, 1000, 1500, 2000); sample buffer (E); amplified baculovirus encoding $G\alpha_q$ (P3). Ponceau stained blot (***upper blot)*** to demonstrate equal cell loading. Western blot (***lower* blot**). MW= ~ 44 kDa.

Figure 2.4 showed that TIPS method can be used to express $G\alpha_q$ protein. But the question remains as to how the method is compared to the protein expression using traditional virus stock. To answer this question, fresh sf9 cells were infected with original P3 viral stock and infected cells were harvested after 48 h. The cell pellet was saved for western blot analysis (**Figure 2.5**). In order to ensure equal cell loading, it was incubated in Ponceau stain before blocking the blot with milk. The ponceau stain is used for rapid reversible staining of protein bands on nitrocellulose or PVDF membranes. This stain is not specific towards any protein and is therefore representative of the overall amount of protein loaded. In **Figure 2.5**, only one band within the black box is the desired $G\alpha_q$ protein band. It was hard to deduce which band was the correct one using Ponceau stained blot but western blot probed with an anti-His antibody followed by HRP-conjugated secondary

antibody detected relevant his-tagged G protein bands. Western blot showed similar protein expression from all BIICs concentration (for 72 h time point) except that the expression was slightly lower in case of cells infected with 2000 BIICs/mL. Also it was observed that protein expression from BIICs was comparable to expression from traditional virus infection.

This comparative analysis showed that TIPS could be an effective alternative method to express $G\alpha_q$ protein. One of the biggest advantages of using TIPS method is its reproducibility and easy scale up. If one considers the impediments associated with traditional viral stock discussed in **Section 2.1.5** (stability, titer, scale-up etc.), TIPS method is more than just a failsafe option.

This method was also applied to express mutant $G\alpha_q$. The mutant form includes a mutation of isoleucine to asparagine at site 190. No titration-time course study was performed and it was expressed using similar BIICs concentration and incubation time (1000 BIICs/mL and 72 h incubation time).

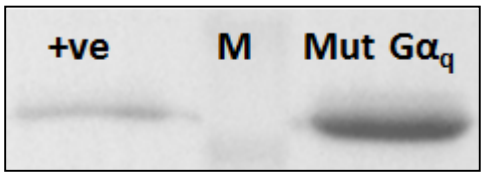

Figure 2.6. Western blot showing expression of mutant $G\alpha_q$ using TIPS method. Positive control (+ve); protein molecular weight marker (M); mutant $G\alpha_q$ (Mut $G\alpha_q$). MW= ~ 44 kDa.

2.2.4 TIPS method can be used to express other proteins as well

Resistance to inhibitors of cholinesterase 8-A (Ric-8A) has been shown to act as a chaperone and a GEF (guanine nucleotide exchange factor) for $G\alpha_q$ to catalyze nucleotide exchange.[42] Details regarding Ric8-A-assisted nucleotide exchange assay will be discussed in **Section 3.2.3**. We intended to test generality of TIPS method to express proteins other than G proteins. Hence, we

decided to express GST-Ric-8A. Similar titration-time course study was performed (as described in **Section 2.4.5** for $G\alpha_q$) to obtain optimal protein expression conditions. **Figure 2.7** shows the western blots illustrating the time course aspect of this experiment along with the effect of titration of BIICs on Ric-8A expression. A positive control was loaded to ensure that GST antibody was functional. Other bands in the gel are probably protein degradation products. Just like in the $G\alpha_q$ titration-time course study, the 72 h incubation time seemed to lead to optimal expression of the protein. We used 1500 BIICs/mL (final concentration) and a 72 h incubation time for large scale production of Ric-8A. The success of this experiment showed the ubiquity and appealing application of BIICs and TIPS method.

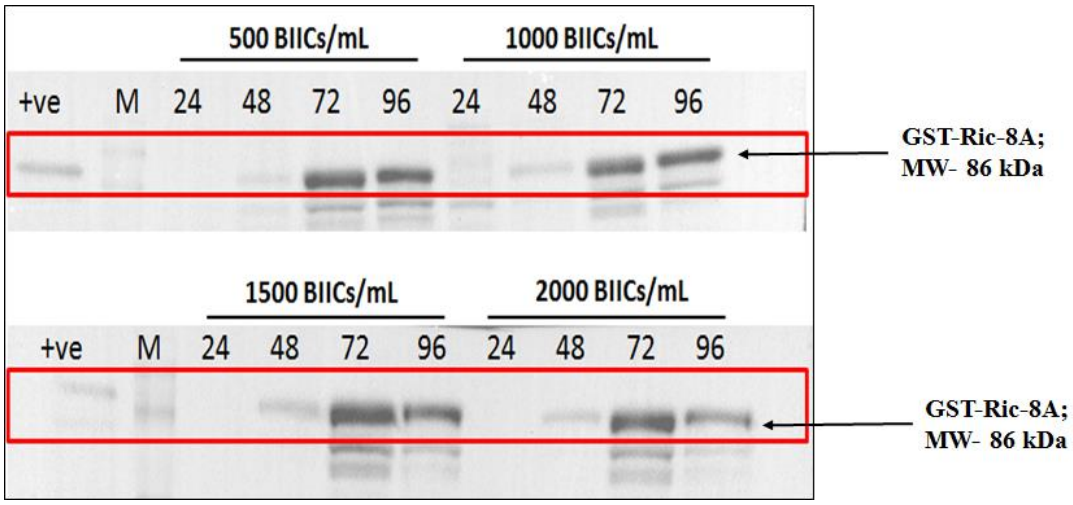

Figure 2.7. Effect of incubation time and varying amounts of BIICs on expression of Ric-8A in sf9 cells. Positive control (+ve); protein molecular weight marker (M); time point samples collected at 24, 48, 72, 96 h for sf9 cells infected with the final concentrations of 500 BIICs/mL or 1000 BIICs/mL (***upper blot***) or 1500 BIICs/mL or 2000 BIICs/mL (***lower blot***). MW= ~ 86 kDa.

2.2.5 Ni-NTA affinity chromatography provided purified $G\alpha_q$ and mutant $G\alpha_q$

Even though both the $G\alpha_q$ and mutant $G\alpha_q$ proteins expressed well in insect cells, purification was a bit challenging. Since detergents like Triton X 100 (usually used to lyse insect cells) can

affect nucleotide exchange activity of these G proteins,[59] other methods had to be used for lysis. After numerous optimizations, the final purification protocol described in experimental **Section 2.4.8** was used. Since both proteins were His-tagged, Ni-NTA chromatography was employed for their isolation. This technique takes advantage of the high affinity of the immobilized Ni-NTA resin for the hexahistidine tag.

Purification of $G\alpha_q$:

Figure 2.8 summarizes the results for $G\alpha_q$ purification using a coomassie-stained SDS-PAGE (upper panel) and a western blot (lower panel). A major portion of the expressed protein was in the pellet. We reckon that this portion of the protein was aggregated and even if we were to isolate it, it would be inactive. Additionally, aggregated protein, if not removed, might skew our future bioactivity results. Following cell lysis and a high speed centrifugation spin, the supernatant was loaded onto a Ni-NTA resin column (T) and incubated for 3 h at 4 °C. After the incubation period, the contents were filtered and the flow through (F) was saved for gel analysis. Ni-NTA column was washed once with lysis buffer (W1) and then with higher concentration of sodium chloride (W2 and W3) to remove proteins that were non-specifically bound to the resin. Protein was eluted from the resin using elution buffer containing high concentrations of imidazole which competes with the hexahistidine tag (E1, E2, and E3). Upon elution of the protein in elution buffer containing imidazole, it is essential to perform an overnight dialysis to remove imidazole.

The presence of imidazole can interfere with the activity assays. Dialyzed protein was then concentrated and stored in dialysis buffer in smaller aliquots at -80 °C. Concentration of a purified protein can be quantified in two ways. One of the simplest and fastest methods of total protein quantification is Bradford assay which is a colorimetric assay measuring proportional binding of

the coomassie brilliant blue dye to proteins.[57] However, if the eluted protein has additional impurities, this method might not provide accurate quantification of the desired protein because the dye binds non-specifically to all proteins. In that case, quantification is done by a coomassie-stained SDS-PAGE quantification method. This method provides quantification of the protein of interest relative to a known standard protein (BSA). Since our eluted protein did not show a lot of impurities (E1, E2 and E3 lanes in **Figure 2.8**), purified protein samples were quantified using a Bradford assay.[57] This preparation yielded 2 mg of purified protein. In our experience, purified $G\alpha_q$ yields range from 1-2.7 mg from a 750 mL culture.

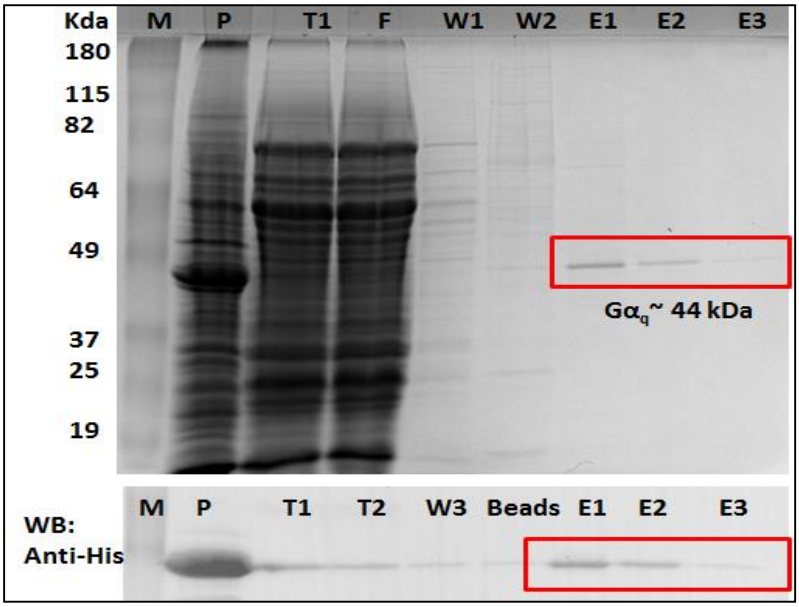

Figure 2.8. Ni-NTA affinity purification of $G\alpha_q$. Protein molecular weight marker (M); pellet obtained after ultracentrifugation (P); total lysate before filtration (T1); total lysate after filtration (T2); flow through (F); wash with lysis buffer (W1); wash with wash buffer (W2 and W3); resin after elution (Beads); eluted protein fractions (E1, E2 and E3). ***Upper panel:*** coomassie-stained SDS-PAGE. ***Lower panel:*** Western blot analysis.

Purification of Mutant $G\alpha_q$:

Figure 2.9 summarizes the results for purification of mutant $G\alpha_q$. The same procedure was used as described above. Unlike $G\alpha_q$, the eluted fraction for the mutant $G\alpha_q$ contained several

impurities as seen by additional bands in the coomassie-stained SDS-PAGE gel. Additional purification methods such as size exclusion column chromatography can be used to obtain highly purified protein. However, this purification was sufficient for our protein requirements (biochemical assays discussed in **Chapter 3**). The next step was to determine the concentration of the eluted protein. Since additional impurities were visible (E1, E2 and E3 lanes in **Figure 2.9**), quantification of the desired protein was done by coomassie-stained SDS-PAGE quantification method. **Figure 2.10** shows coomassie-stained SDS-PAGE and the standard curve obtained from band density (integrated pixel intensity from BSA bands). A 1.5 L mutant $G\alpha_q$ infected cell culture yielded 1 mg protein. Bradford assay provided E1 concentration as 3.3 mg/mL and E2 concentration as 3.9 mg/mL. Concentrations of E1 (~1.2 mg/mL) and E2 (~2.1 mg/mL) were obtained through SDS-PAGE quantification.

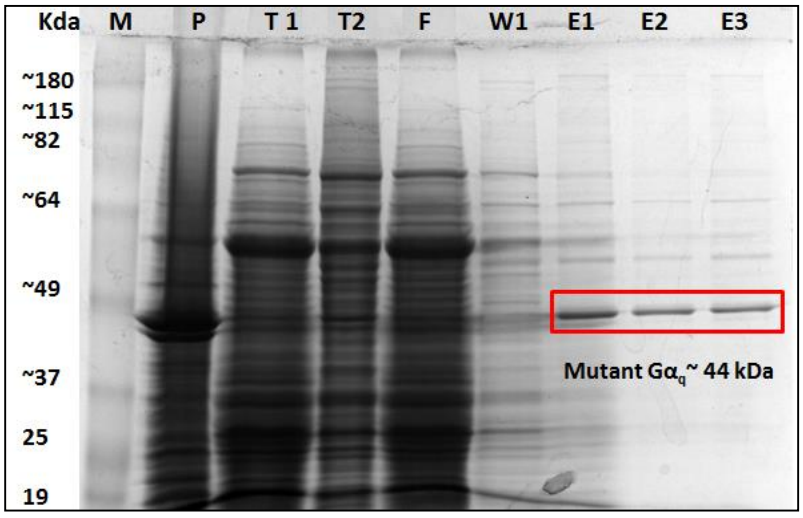

Figure 2.9. Coomassie-stained SDS-PAGE analyzing Ni-NTA affinity purification of mutant $G\alpha_q$. Protein molecular weight marker (M); pellet obtained after ultracentrifugation (P); total lysate before filtration (T1); total lysate after filtration (T2); flow through (F); wash with lysis buffer (W1); eluted protein fractions (E1, E2 and E3).

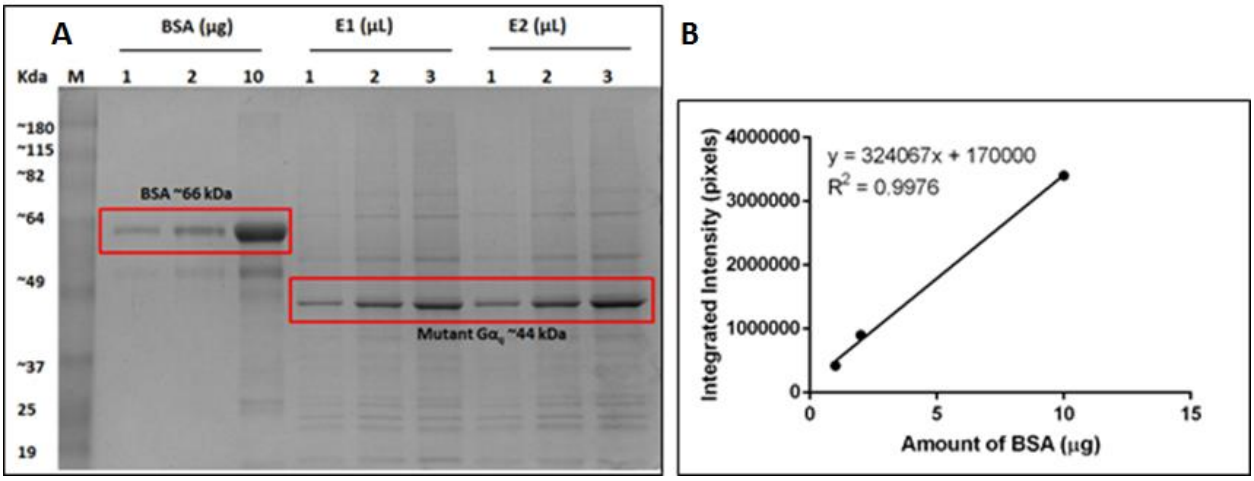

Figure 2.10. Purified mutant $G\alpha_q$ gel quantification. ***Panel A.*** Purified proteins resolved on 12 % SDS-PAGE stained with coomassie blue. ***Panel B.*** Quantification of BSA in a standard curve.

2.2.6 Glutathione-sepharose chromatography purification of GST-Ric-8A

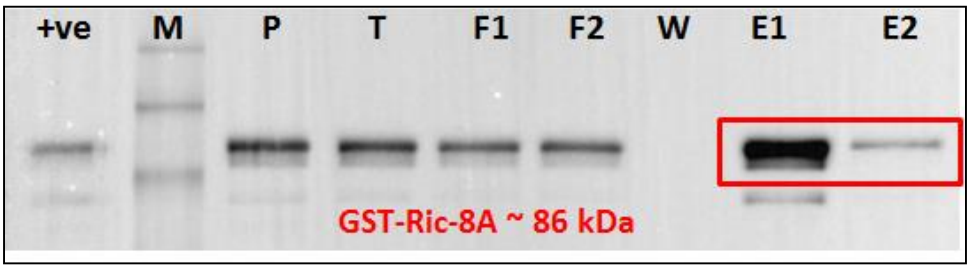

Figure 2.11. Western blot probed with Anti-GST-HRP conjugate antibody analyzing glutathione-sepharose affinity purification of GST-Ric-8A. Positive control (+ve); protein molecular weight marker (M); pellet obtained after ultracentrifugation (P); total lysate (T); first flow through (F1); second flow through (F2); wash with lysis buffer (W1); eluted protein fractions (E1& E2).

Ric-8A has been shown to catalyze nucleotide exchange activity of $G\alpha_q$.[42] Therefore, it would be beneficial to have purified Ric-8A so that it could be used in our biochemical activity assays for $G\alpha_q$. Hence, Ric-8A was purified based on the published protocols.[42] Further details regarding the mechanism would be discussed in **Chapter 3. Figure 2.11** summarizes the purification of Ric-

8A using glutathione-sepharose resin beads. A significant portion of protein did not bind to the resin beads (F1) even after reloading onto the beads (F2) which could denote the fraction of protein that was misfolded. Quantification of purified Ric-8A was done by coomassie-stained SDS PAGE gel (data not shown).

2.2.7 Expression and purification of other G proteins ($G\alpha_{i1}$ & $G\alpha_o$)

YM compound is known to be specific towards only one class of G proteins ($G\alpha_q$). Will simplified analogs of the molecule lose this specificity towards $G\alpha_q$? In order to answer this question, we needed other purified G proteins as well. Hence, we purified $G\alpha_{i1}$ and $G\alpha_o$ (both these proteins belong to one class of G proteins, $G\alpha_i$). Unlike $G\alpha_q$, both $G\alpha_{i1}$ and $G\alpha_o$ can be easily expressed and purified from *E.coli* (as discussed in the **Section 2.1.2**). Established protocols have been published discussing expression and purification of these two proteins.[23] Recombinant protein expression in *E.*coli can result in the formation of highly aggregated protein known as inclusion bodies. Greentree *et. al* demonstrated that in order to reduce the formation of inclusion bodies and get better expression of soluble $G\alpha_{i1}$ and $G\alpha_o$, it is necessary to express the proteins at lower temperature (30 °C) and with lower IPTG (reagent used to induce protein expression) concentration (100µM). To this end, both proteins were expressed in *E.coli* as described in **Section 2.4.10**. After expression, cell lysates were prepared and purified over a Ni-NTA affinity column.[23] **Figure 2.12** shows SDS-PAGE and western blot analyzing the purification of His-tagged $G\alpha_{i1}$ (denoted as $G\alpha_{i1}$, ***panels A and B***) and His-tagged $G\alpha_o$ (denoted as $G\alpha_o$, ***panels C and D***) respectively. **Figure 2.13** summarizes coomassie-stained SDS-PAGE and standard curve obtained from band density (integrated pixel intensity from BSA bands) for $G\alpha_{i1}$ (concentrations of E1 (~8 mg/mL) and E2 (~4 mg/mL) were obtained through SDS-PAGE quantification). Similar analysis

was done for $G\alpha_o$ for its quantification (data not shown). For both $G\alpha_{i1}$ and $G\alpha_{o,}$ a 1 L culture generally yields 4-7 mg protein based on our experience.

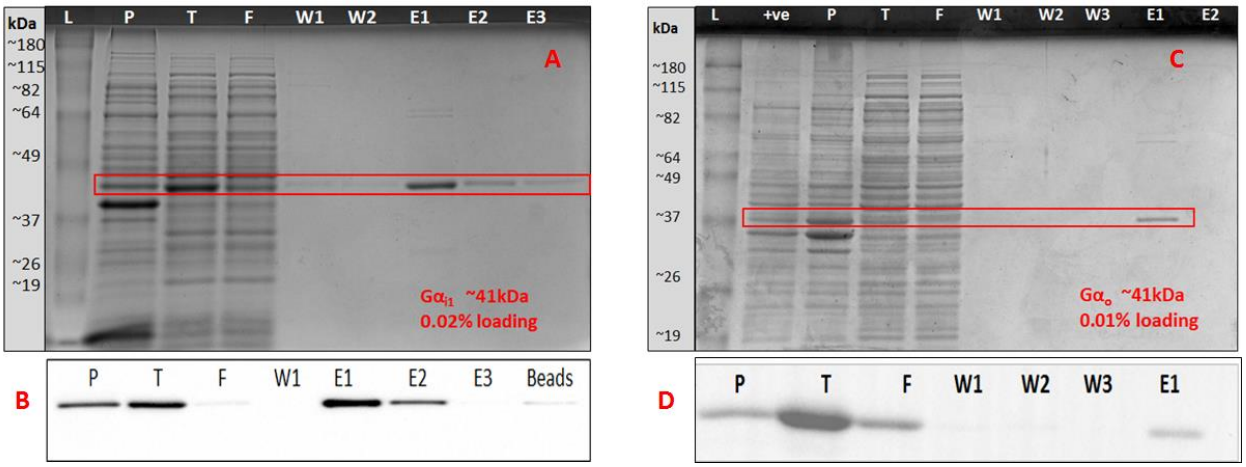

Figure 2.12: ***Panel A & C.*** SDS-PAGE analysis of $G\alpha_{i1}$ and $G\alpha_o$ purification using Ni-NTA resin beads. Cell pellet (P) after ultracentrifugation, total cell lysate (T), flow-through (F), wash with lysis buffer (W1), wash with wash buffer (W2 & W3) followed by elution of protein in three fractions (E1, E2, E3). Beads were boiled to ensure that protein was eluted successfully (Beads). Protein molecular weight marker (L) is shown on the left for both gels. ***Panel B &D.*** Western blot probed with Anti-His.

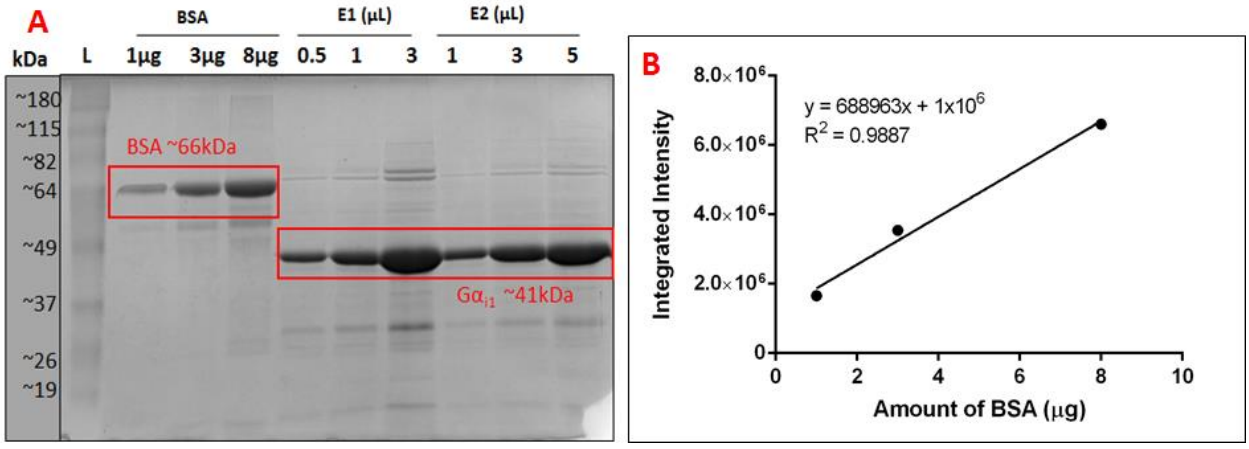

Figure 2.13: Purified $G\alpha_{i1}$ gel quantification. ***Panel A.*** Purified proteins resolved on 12 % SDS-PAGE stained with coomassie blue. ***Panel B.*** Quantification of BSA in a standard curve

2.3 Conclusions

In conclusion, a new application of the TIPS method toward the expression of G proteins from insect cells was introduced. This method uses Baculovirus-Infected Insect cells (BIICs) to express recombinant proteins. The use of BIICs eliminates the need to titer the virus and can provide reproducible protein expression. Based on our studies, protein expression using BIICs was similar to that of traditional virus. In other words, insect cells infected from BIICs had comparable expression profile to that of cells infected with traditional baculovirus. Hence, two G proteins ($G\alpha_q$ and mutant $G\alpha_q$) were expressed using TIPS method. In addition, another protein known as Ric-8A was expressed using the same technology. Other G proteins ($G\alpha_{i1}$ and $G\alpha_o$) were expressed and purified from *E.coli*. All proteins were purified utilizing affinity tag chromatography and characterized using coomassie-stained gels and western blots.

Prior to investigating effects of simplified YM analogs on these purified G proteins, it is imperative to test their activity. Purification process can be rigorous and, if not carried out accurately, can affect the activity of proteins. In order to study function of G protein, nucleotide exchange assays are performed. **Chapter 3** will focus on different approaches that can determine whether the purified G proteins are functional.

2.4 Experimental section

Unless noted otherwise, all chemicals were ordered from Sigma Aldrich (St. Louis, MO). All other vendor information is noted in the experimental section.

2.4.1 Insect cell culture

Freshly thawed sf9 cells were grown in SF-900^{TM} II SFM (Life technologies, Carlsbad, CA) containing 0.5X antibiotic-antimycotic (Life technologies, Carlsbad, CA). Since the cells were adapted to serum free conditions, media was not supplemented with any serum. Cells were cultured in a 125 mL tissue culture flask at 27 °C with constant shaking between 127-130 rpm. Stock cell cultures were passaged every 2 days and maintained at a cell density between $0.8x10^6$ -$2x10^6$ cell/mL (usually cell density was maintained close to $1x10^6$ cells/mL).

2.4.2 Generation of $G\alpha_q$ and mutant $G\alpha_q$ (I190N) recombinant baculovirus

$G\alpha_q$: Plasmid encoding chimeric His-$G\alpha_{i/q}$ (will now be abbreviated as $G\alpha_q$) was kindly provided by Tohru Kozasa (University of Chicago, IL). DNA encoding chimeric $G\alpha_{i/q}$ has a N-terminal His_6 tag, followed by a TEV cleavage site, amino acids 1-28 of rat $G\alpha_{i1}$, an Arg and Ser linker followed by amino acid residues 37-359 of mouse $G\alpha_q$[55] This plasmid was used to create recombinant baculovirus after transfection of cultured sf9 cells (cell density = $0.8x10^6$ cell/mL) according to the manufacturer's instructions (Bac-to-Bac Baculovirus expression system, Life technologies, Carlsbad, CA). The transfection viral supernatant (P1) was harvested after 72 h (swollen cells is considered a positive sign for a successful transfection) by centrifuging at 500 g for 5-10 min and then stored at 4 °C in a tube covered with aluminum foil until the amplification step. A 50 µL cell pellet was saved at -80 °C for western blot to test the expression. **Figure 2.3** shows transfection results from western blot.

For amplification of P1 viral stock, 10 mL sf9 cells (cell density = $1.0x10^6$-$1.5x10^6$ cell/mL) were plated in a T25 cm^2 flask equipped with a filter cap and infected with 250 µL P1 viral stock. The infection viral supernatant (P2) was harvested in a similar manner as P1 after 72 h. Another

round of amplification was performed to obtain P3 by infecting 30 mL sf9 cells (cell density = $1.0x10^6$-$1.5x10^6$ cell/mL) with 250 µL P2 viral stock in a T75 cm^2 flask equipped with a filter cap. The infection viral supernatant (P3) was harvested after 48 h and stored at 4 °C in 15 mL conical tubes (10 mL aliquots) covered with aluminum foil.

Mutant $G\alpha_q$: I190N, one site mutation was introduced into the original plasmid mentioned above by site-directed PCR mutagenesis. Site-directed PCR mutagenesis is used to carry out specific changes to the DNA sequence of a gene and was performed by Kevin Kaltenbronn (Washington University School of Medicine, MO). Recombinant baculovirus for this plasmid was generated using the exact same procedure mentioned above. **Figure 2.3** shows transfection results from western blot.

2.4.3 Preparation of $G\alpha_q$ and mutant $G\alpha_q$ BIICs stock

Freezing media used to cryopreserve infected cells contains 8 parts (or 90 %) SF-900™ II SFM media containing 1X antibiotic-antimycotic, one part (or 1 % final or 100 mg/mL in SF-900 II media) BSA (Sigma Aldrich, St. Louis, MO) and one part DMSO (or 10 % final).

Sf9 cells (50 mL at cell density of $1.8x10^6$ cells/mL) were infected with 500 µL P3 $G\alpha_q$ or P3 mutant $G\alpha_q$ and incubated at 27 °C for 24 h. Before cryopreserving infected cells, viability was checked using 0.4 % Trypan blue solution (Sigma Aldrich, St. Louis, MO). High cell viability (>95 % viability) is recommended for cryopreservation. Infected cells were centrifuged at 500 g for 10 min. Cell pellet was re-suspended in freezing media (final cell density of $1x10^7$ viable cells/mL) and transferred into 1.8 mL clear cryovials in 300 µL aliquots. The cryopreservation process was started by slowly by cooling the vials in a Styrofoam box overnight at -80 °C and then storing the vials in a storage box at -80 °C or in liquid nitrogen for long term storage.

Note: All BIICs stocks were prepared from untitered liquid viral stocks (a liquid viral stock prepared from a culture with a maximum density of $1x10^6$ sf9 cells/mL was presumed to contain at least $1x10^8$ plaque forming units (pfu)/mL).[52]

2.4.4 Preparation of GST-Ric-8A BIICs stock

Baculovirus encoding GST-Ric-8A (P3) was kindly provided by Gregory Tall (University of Rochester Medical Center, NY) and BIICs for GST-Ric-8A were prepared from P3 viral stock as mentioned above.

2.4.5 Production of $G\alpha_q$ protein using TIPS method

Expression of $G\alpha_q$ was evaluated based on two parameters: BIIC-to-volume ratios (500, 1000, 1500, and 2000 BIICs/mL) and time of infection.

Titration-time course experiment

The $G\alpha_q$ BIIC stock (300 µL) was quickly thawed in a 37 °C water bath and diluted into 30 mL (1:100) cell-free medium (media used to culture cells). Four culture flasks, each containing fresh sf9 cells (50mL at cell density = $1x10^6$ cells/mL), were infected with varying amounts of BIICs from diluted BIICs stock. The final BIIC density in each flask was 500 BIICs/mL (flask 1), 1000 BIICs/mL (flask 2), 1500 BIICS/mL (flask 3) and 2000 BIICS/mL (flask 4). Infected cultures were incubated at 27 °C with constant shaking between 127-130 rpm. After infection, 2 mL cell pellet samples were collected from each flask at 24 h intervals and saved for western blot. In addition, cell count (using hemocytometer) and viability (using 0.4 % Trypan blue solution) was monitored at 24 h intervals. Western blot samples were centrifuged at 500 g for 5 min and cell pellets were re-suspended in 1x Laemmli sample buffer containing 10 % β-mercaptoethanol. The samples were heated for 10 min at 100 °C and 10 µL of each sample (calculations were done in

order to ensure equal cell loading) was electrophoresed on a 12 % SDS-PAGE and transferred onto a polyvinylidene difluoride (PVDF) membrane. Membrane was blocked in TBST (20 mM Tris-HCl pH 7.6, 137 mM NaCl, 0.1 % Tween 20) containing 5 % non-fat milk for 1 h. Blocked membrane was probed with an anti-His antibody (H-15, sc-803, Santa Cruz Biotechnology (Santa Cruz, CA)) (1:1,000 dilution) and washed three times in TBST followed by incubating in HRP-conjugated secondary antibody diluted in TBST for 1 h. Upon washing the membrane three times with TBST, it was incubated in Amersham ECL western blotting detection reagent (Enhanced chemiluminescence, GE healthcare, Buckinghamshire, UK) and visualized using ChemiDoc imaging system (Bio-Rad laboratories Inc., Richmond, CA). **Figure 2.4** shows the western blot analysis of the titration-time course experiment.

Large scale expression of $G\alpha_q$ using TIPS method

The $G\alpha_q$ BIIC stock (300 µL) was quickly thawed in a 37 °C water bath and diluted into 30 mL (1:100) cell-free medium (media used to culture cells). Three sf9 cell cultures with viability of >95 % (743 mL each at cell density = ~$1.5x10^6$ cells/mL) were infected with 7.5 mL of diluted BIICs media (final concentration: 1000 BIICs/mL). All infected cultures were incubated at 27 °C with constant shaking at 127-130 rpm for 72 h. After the incubation period was over, cells were harvested by centrifuging at 500 g for 10 min. The cell pellet was flash frozen in liquid nitrogen and then stored at -80 °C until ready for purification. A 2 mL cell pellet was saved to test expression before purification.

Large scale expression of mutant $G\alpha_q$ using TIPS method

Exact same procedure was applied for large scale expression of mutant $G\alpha_q$ (**Figure 2.6**).

2.4.6 $G\alpha_q$ protein from BIICs vs traditional P3 viral stock

Two sf9 cultures (50mL each at cell density = $2x10^6$) were infected with traditional P3 viral stock (10 mL virus /L of sf9 cells). Both cultures were incubated at 27 °C with constant shaking between 127-130 rpm. Both culture flasks were harvested after 48 h by centrifuging at 500 g for 10 min. A 2 mL cell pellet was saved for western blot analysis whereas the rest of the cell pellet was stored at -80 °C. Western blot was performed as mentioned in the section above. Except before blocking the PVDF membrane with milk, it was stained by Ponceau stain (Sigma Aldrich, St. Louis, MO). **Figure 2.5** shows western blot comparing expression of $G\alpha_q$ from two different infection methods: BIICs vs traditional virus.

2.4.7 Production of GST-Ric-8A protein using TIPS method

A titration time course study (similar to one described in **Section 2.4.5** for $G\alpha_q$) was carried out for GST-Ric-8A in order to obtain optimal condition for its expression. Western blot was carried out as mentioned in **Section 2.4.5** except for using anti-GST HRP conjugate antibody (GE healthcare life science, Buckinghamshire, UK). GST tagged to Ric-8A leads to a molecular weight of 86 kDa. **Figure 2.7** summarizes the results from the titration-time course study for Ric-8A.

Large scale expression using TIPS method: The GST-Ric-8A BIICs stock (300 µL) was quickly thawed in a 37 °C water bath and diluted into 30 mL (1:100) cell-free medium (media used to culture cells). Two sf9 cell cultures with viability of >95 % (743 mL at cell density = ~$1.5x10^6$ cells/mL) were infected with 7.5 mL of diluted BIICs media (final concentration: 1500 BIICs/mL). All infected cultures were incubated at 27 °C with constant shaking at 127-130 rpm for 72 h. After the incubation period was over, cells were harvested by centrifuging at 500 g for 10 min. The cell

pellet was flash frozen in liquid nitrogen and then stored at -80 °C until ready for purification (**Section 2.4.9**). Cell pellet (2 mL) was saved to test expression before purification.

2.4.8 Ni-NTA metal chromatography to purify $G\alpha_q$

His-tagged $G\alpha_q$ was purified as previously described with minor modifications.[56] All purification steps were performed at 4 ^{0}C. Frozen cell pellets were thawed and suspended in cold lysis buffer (20 mM HEPES pH 8.0, 100 mM NaCl, 10 mM β-mercaptoethanol, 0.1 mM EDTA, 3 mM magnesium chloride, 10 µM GDP and 1X EDTA-free protease inhibitors). Cells were lysed using a dounce homogenizer followed by sonication. Sonicated cell lysates were spun at 186,000 g for 1 h and the cloudy supernatant (T1) was passed through a glass fiber filter (GF/D, Whatman). Filtered supernatant (T2) was then added to a 50 mL polypropylene tube containing 2 mL Ni-NTA agarose resin (Qiagen, Valencia, CA) pre-equilibrated with lysis buffer, mixed gently by rotation at 4 ^{0}C for 2-3 h, and loaded onto a Bio-Rad disposable column. The flow through (F) was saved for analysis. Ni-NTA resin was washed with 40 mL lysis buffer (W1) followed by two washes with wash buffer (lysis buffer with 300 mM NaCl and 20 mM imidazole pH 8.0) (W2 and W3). $G\alpha_q$ was eluted with elution buffer (lysis buffer with 200 mM imidazole pH 8.0) and dialyzed overnight against dialysis buffer (20 mM HEPES pH 8.0, 100 mM NaCl, 1 mM magnesium chloride, 10 µM GDP and 2 mM DTT). Resin beads were incubated in lysis buffer and loaded on the gel to check if all protein was eluted (Beads). Dialyzed protein was concentrated 20 folds to 500 µL using Vivaspin 20 column (Fisher Scientific, Waltham, MA), was flash frozen in liquid nitrogen, and stored at -80 °C in aliquots to avoid repeated freeze-thaws. No further purification steps were performed. Eluted protein fractions (E1, E2 and E3) were analyzed by SDS-PAGE and western blot (His-probe antibody H-15, Santa Cruz Biotechnology, Dallas, TX). This preparation

yielded 2 mg of purified protein as quantified by Bradford assay.[57] **Figure 2.8** summarizes the results of $G\alpha_q$ purification from BIICs infected sf9 cells.

Ni-NTA metal chromatography to purify mutant $G\alpha_q$

Exact same procedure was followed to purify mutant $G\alpha_q$ except purification analysis was done by coomassie-stained SDS-PAGE (details provided in **Section 2.4.9**). Figure **2.9** summarizes the results of mutant $G\alpha_q$ purification from BIICs infected sf9 cells.

2.4.9 Glutathione-Sepharose Chromatography to purify GST-Ric-8A

GST-Ric-8A was isolated from whole cell lysates over a glutathione-sepharose resin column as per published protocols with minor modifications.[42] All purification steps were performed at 4 °C. Frozen cell pellets were thawed and suspended in 185 mL cold lysis buffer (20 mM HEPES, 150 mM NaCl, 1 mM EDTA, 1 mM DTT, and 1X EDTA-free protease inhibitors). Cells were lysed using a dounce homogenizer followed by sonication. Sonicated cells were centrifuged for 1 h at 100,000 g. Clear supernatant (T) was loaded onto 2 mL glutathione-sepharose 4b resin (GE healthcare, Buckinghamshire, UK) pre-equilibrated with lysis buffer, mixed gently by rotation at 4 °C for 2-3 h. After incubation, contents were loaded onto a Bio-Rad disposable column. The first flow-through (F1) was passed through the resin again and the second flow-through (F2) was saved for gel analysis. The resin was then washed with 50 mL lysis buffer (W1) followed by two washes with wash buffer (lysis buffer with 300 mM NaCl) (W2 & W3). GST-Ric-8A was first eluted with 7 mM reduced glutathione (E1) followed by a second elution with 20 mM reduced glutathione (E2) and dialyzed overnight again dialysis buffer (20 mM HEPES, 150 mM NaCl, 1 mM EDTA and 1 mM DTT). The resin beads were incubated in lysis buffer and loaded onto the gel to ensure that all the protein was eluted (Beads). Dialyzed protein was concentrated using Vivaspin 20

column (Fisher Scientific, Waltham, MA), flash frozen in liquid nitrogen and stored at -80 °C in aliquots to avoid repeated freeze-thaws. No further purification steps were performed. Purification was analyzed by western blot probed with Anti-GST HRP conjugated antibody (GE healthcare life science, Buckinghamshire, UK) (**Figure 2.11**). Protein was quantified using the coomassie-stained SDS PAGE gel quantification method described in **Section 2.4.10.**

2.4.10 Expression and purification of $G\alpha_{i1}$

Plasmids encoding His_6-$G\alpha_{i1}$ and His_6-$G\alpha_o$ were kindly provided by Maurine E. Linder (Cornell University, NY). N-terminally His_6 tagged $G\alpha_o$ and $G\alpha_{i1}$ were expressed and purified as described previously with slight modifications.[23]

The pT7-5 plasmid encoding His_6-$G\alpha_{i1}$ (will be referred to as $G\alpha_{i1}$) was transformed into *Escherichia Coli* BL21 (DE3) one shot cells (Life technologies, Carlsbad, CA) following the instructions provided by the company. Varying amounts of transformed cells (5 µL, 10 µL and 30 µL) were plated on Luria Broth (LB) plates containing 100 µg/mL ampicillin and grown overnight in 37 °C incubator. A single colony was picked to inoculate two 5 mL LB cultures containing 100 µg/mL ampicillin and grown overnight by shaking at 225 rpm in a 37 ^{0}C shaker incubator. Overnight cultures were used to inoculate two 500 mL LB containing 100 µg/mL ampicillin. Cells were grown at 30 °C with gentle shaking at 200 rpm until the OD_{600} reached 0.5-0.7. IPTG was added to the culture at a final concentration of 100 µM to induce expression of protein. Cells were allowed to grow at 30 °C with gentle shaking at 200 rpm for 9-12 h. Cells were harvested by centrifugation at 3000 g for 10 min at 4 °C. Cell pellet was stored at -80 °C until purification.

All steps were performed on ice unless otherwise mentioned. The cell pellet was suspended in 80 mL of cold lysis buffer (50 mM Tris-HCl pH 8.0, 20 mM β-mercaptoethanol, 10 mM imidazole,

25 µM GDP, 1X EDTA-free protease inhibitor cocktail tablets (Roche, Basel, Switzerland). The contents were gently stirred for 10 min or until cell pellet was thawed. Clumps of cells that occur can be broken by passing contents through a 21½-gauge needle. Lysozyme was added to a final concentration of 0.2 mg/mL and contents were gently stirred for 15 min. Magnesium chloride (final concentration 5 mM) and 3 mg DNase I was added and contents were gently stirred for 15 min or until the viscosity of the solution diminished. The cells were further lysed by sonication (15 s on, 15 s off, total process time- 1 min 30 s, amplitude- 3-5) on ice using a Q700 sonicator (Qsonica, LLC, Newton, CT). Post sonication, lysate was incubated on ice for 10 min followed by ultracentrifugation at 100,000 g in a 50.2 Ti rotor (Beckman coulter, Brea, CA) at 4 °C. Supernatant was loaded on Ni-NTA agarose resin (1.25 mL) (Qiagen, Valencia, CA) washed with lysis buffer (3x5 mL). Contents were incubated at 4 °C under gentle rotation for 3 h. Pellet was dissolved in 10 mL lysis buffer and saved for gel analysis. Upon completion of incubation period, the contents were loaded on a 20 mL disposable column (Bio-Rad laboratories Inc., Richmond, CA) and the flow-through (F) was saved for gel analysis. Resin was washed with lysis buffer (1x50 mL, W1) and then with lysis buffer containing 500 mM sodium chloride (2x50 mL, W2 and W3). The protein was eluted in three fractions (5 mL each) by addition of lysis buffer containing 150 mM imidazole and 10 % glycerol (3x5 mL, E1, E2 and E3). E2 and E3 elutions were pooled together and labeled as E2. The beads were re-suspended in 5 mL elution buffer (Beads). Both E1 and E2 elutions were dialyzed in dialysis buffer (50 mM HEPES pH 8.0, 1 mM EDTA, 1 mM DTT, 10 % glycerol) using a 12-14 kD cutoff dialysis membrane (Spectrum laboratories, Inc. Rancho Dominguez, CA) overnight. Dialyzed protein was concentrated down to 500 µL using vivaspin^{TM} 20 centrifugal concentrators (Thermo Fisher Scientific, Waltham, MA). Total protein quantification was obtained by Bradford protein assay.[57] Concentrated protein was flash frozen in

liquid nitrogen and stored at -80 °C in aliquots to avoid repeated freeze-thaws and was used without additional purification steps.

Purification analysis

Purification steps were analyzed via SDS-PAGE analysis. Samples were electrophoresed on a 12 % SDS-PAGE and stained with coomassie blue. For western blot, samples were electrophoresed on a 12 % SDS-PAGE and transferred onto a polyvinylidene difluoride (PVDF) membrane. Membrane was blocked in TBST (20 mM Tris-HCl pH 7.6, 137 mM NaCl, 0.1 % Tween 20) containing 5 % non-fat milk for 1 h. Blocked membrane was probed with an anti-His antibody (H-15, sc-803, Santa Cruz Biotechnology, Santa Cruz, CA) (1:1,000 dilution) and washed three times in TBST followed by incubation in HRP-conjugated secondary antibody diluted in TBST for 1 h. Upon washing the membrane three times with TBST, it was incubated in Amersham ECL western blotting detection reagent (Enhanced chemiluminescence, GE healthcare, Buckinghamshire, UK) and visualized using ChemiDoc imaging system (Bio-Rad laboratories Inc., Richmond, CA).

2.4.11 Expression and purification of $G\alpha_o$

His_6-$G\alpha_o$ will be referred to as $G\alpha_o$. Exact same procedure was applied to express and purify $G\alpha_o$ except the post- IPTG induction time was 16-18 h.

2.5 References

(1) Cabrera-Vera, T. M.; Vanhauwe, J.; Thomas, T. O.; Medkova, M.; Preininger, A.; Mazzoni, M. R.; Hamm, H. E. *Endocr. Rev.* **2003**, *24*, 765–781.

(2) Sprang, S. R. *Annu. Rev. Biochem.* **1997**, *66*, 639–678.

(3) Gilman, A. G. *Annu. Rev. Biochem.* **1987**, *56*, 615–649.

(4) Lee, E.; Linder, M. E.; Gilman, A.G. *Methods Enzymol.* **1994**, 237, 146-64.

(5) Simon, M. I.; Strathmann, M. P.; Gautam, N. *Science* **1991**, *252*, 802–808.

(6) Linder, M. E.; Ewald, D. A.; Miller, R. J.; Gilman, A. G. *J. Biol. Chem.* **1990**, *265*, 8243–8251.

(7) Chen, R. *Biotechnol. Adv.* **2012**, *30*, 1102–1107.

(8) Altmann, F.; Staudacher, E.; Wilson, I. B.; März, L. *Glycoconj. J.* **1999**, *16*, 109–123.

(9) Ikonomou, L.; Schneider, Y.-J.; Agathos, S. N. *Appl. Microbiol. Biotechnol.* **2003**, *62*, 1–20.

(10) Davis, T. R.; Schuler, M. L.; Granados, R. R.; Wood, H. A. *In Vitro Cell. Dev. Biol. Anim.* **1993**, *29A*, 842–846.

(11) Summers, M. D.; Anderson, D. L. *J. Virol.* **1972**, *9*, 710–713.

(12) Kost, T. A.; Condreay, J. P. *Current Opinion in Biotechnology*, **1999**, *10*, 428–433.

(13) Kost, T. A.; Condreay, J. P.; Jarvis, D. L. *Nat. Biotechnol.* **2005**, *23*, 567–575.

(14) Jarvis, D. L. *Methods Enzymol.* **2009**, *463*, 191–222.

(15) Smith, G. E.; Fraser, M. J.; Summers, M. D. *J. Virol.* **1983**, *46*, 584–593.

(16) Xue, J.; Qiao, N.; Zhang, W.; Cheng, R.-L.; Zhang, X.-Q.; Bao, Y.-Y.; Xu, Y.-P.; Gu, L.-Z.; Han, J.-D. J.; Zhang, C.-X. *J. Virol.* **2012**, *86*, 7345–7359.

(17) Thiem, S. M.; Cheng, X. W. *Virologica Sinica*, **2009**, *24*, 436–457.

(18) Luckow, V. A.; Summers, M. D. *Bio/Technology*, **1988**, *6*, 47–55.

(19) Possee, R. D. *Current Opinion in Biotechnology*, **1997**, *8*, 569–572.

(20) Berger, I.; Fitzgerald, D. J.; Richmond, T. J. *Nature biotechnology*, **2004**, *22*, 1583–1587.

(21) Ciccarone, V. C.; Polayes, D. A.; Luckow, V. A. *Methods Mol. Med.* **1998**, *13*, 213–235.

(22) Contreras-Gómez, a; Sánchez-Mirón, a; García-Camacho, F.; Molina-Grima, E.; Chisti, Y. *Biotechnol. Prog.* **2013**, *30*, 1–18.

(23) Greentree, W. K.; Linder, M. E. *Methods Mol. Biol.* **2004**, *237*, 3–20.

(24) Kozasa, T. *Methods Mol. Biol.* **2004**, *237*, 21–38.

(25) Mumby, S. M.; Heukeroth, R. O.; Gordon, J. I.; Gilman, A. G. *Proc. Natl. Acad. Sci. U. S. A.* **1990**, *87*, 728–732.

(26) Linder, M. E.; Middleton, P.; Hepler, J. R.; Taussig, R.; Gilman, A. G.; Mumby, S. M. *Proc. Natl. Acad. Sci. U. S. A.* **1993**, *90*, 3675–3679.

(27) Chen, C.A.; Manning, D. R. *Oncogene* **2001**, *20*, 1643–1652.

(28) Johnson, D. R.; Bhatnagar, R. S.; Knoll, L. J.; Gordon, J. I. *Annu. Rev. Biochem.* **1994**, *63*, 869–914.

(29) Gotta, M.; Ahringer, J. *Nat. Cell Biol.* **2001**, *3*, 297–300.

(30) Song, J.; Hirschman, J.; Gunn, K.; Dohlman, H. G. *J. Biol. Chem.* **1996**, *271*, 20273–20283.

(31) Michaelson, D.; Ahearn, I.; Bergo, M.; Young, S.; Philips, M. *Mol. Biol. Cell* **2002**, *13*, 3294–3302.

(32) Takida, S.; Wedegaertner, P. B. *J. Biol. Chem.* **2003**, *278*, 17284–17290.

(33) Maltese, W. A.; Robishaw, J. D. *J. Biol. Chem.* **1990**, *265*, 18071–18074.

(34) Wedegaertner, P. B.; Wilson, P. T.; Bourne, H. R. *J.Biol. Chem.* **1995**, *270*, 503–506.

(35) Kozasa, T.; Gilman, A. G. *J. Biol. Chem.* **1995**, *270*, 1734–1741.

(36) Iñiguez-Lluhi, J. A.; Simon, M. I.; Robishaw, J. D.; Gilman, A. G. *J. Biol. Chem.* **1992**, *267*, 23409–23417.

(37) Hepler, J. R.; Kozasa, T.; Smrcka, A. V; Simon, M. I.; Rhee, S. G.; Sternweis, P. C.; Gilman, A. G. *J. Biol. Chem.* **1993**, *268*, 14367–14375.

(38) Kozasa, T. *Proc. Natl. Acad. Sci.*, **1993**, *90*, 9176–9180.

(39) Sarvazyan, N. A.; Remmers, A. E.; Neubig, R. R. *J. Biol. Chem.* **1998**, *273*, 7934–7940.

(40) Bigay, J.; Deterre, P.; Pfister, C.; Chabre, M. *FEBS Lett.* **1985**, *191*, 181–185.

(41) Singer, W. D.; Miller, R. T.; Sternweis, P. C. *J. Biol. Chem.* **1994**, *269*, 19796–19802.

(42) Chan, P.; Gabay, M.; Wright, F. a; Kan, W.; Oner, S. S.; Lanier, S. M.; Smrcka, A. V; Blumer, J. B.; Tall, G. G. *J. Biol. Chem.* **2011**, *286*, 2625–2635.

(43) Tall, G. G.; Gilman, A. G. *Methods Enzymol.* **2004**, *390*, 377–388.

(44) Tall, G. G.; Krumins, A. M.; Gilman, A. G. *J. Biol. Chem.* **2003**, *278*, 8356–8362.

(45) Tall, G. G. **2010**, http://az9194.vo.msecnd.net/pdfs/100401/EB10S4.c.pdf.

(46) Thomas, C. J.; Tall, G. G.; Adhikari, A.; Sprang, S. R. *J. Biol. Chem.* **2008**, *283*, 23150–23160.

(47) Wright, S. J.; Inchausti, R.; Eaton, C. J.; Krystofova, S.; Borkovich, K. A. *Genetics* **2011**, *189*, 165–176.

(48) Chan, P.; Gabay, M.; Wright, F. a; Tall, G. G. *J. Biol. Chem.* **2011**, *286*, 19932–19942.

(49) L.A., K.; R.D, P. *The Baculovirus Expression System: A laboratory Guide*; 1992; Chapman and Hall, London

(50) Jorio, H.; Tran, R.; Kamen, A. In *Biotechnology Progress*; **2006**; Vol. 22, pp. 319–325.

(51) Jarvis, D. L.; Garcia, A. *Biotechniques* **1994**, *16*, 508–510.

(52) Wasilko, D. J.; Lee, S. E.; Stutzman-Engwall, K. J.; Reitz, B. a; Emmons, T. L.; Mathis, K. J.; Bienkowski, M. J.; Tomasselli, A. G.; Fischer, H. D. *Protein Expr. Purif.* **2009**, *65*, 122–132.

(53) Wasilko, D. J.; Lee, S. E.; Hermans, W. R. Cryogenically Protected Viral Delivery Systems and Related Manufacture and Use. WO2004040976 A1, 2004.

(54) Hanna, A.; Hermans, W. R.; Garceau, N. Essential Technologies for a Baculovirus Expression CRO http://www.blueskybioservices.com/blog/essential-technologies-for-a-baculovirus-expression-cro/

(55) Tesmer, V. M.; Kawano, T.; Shankaranarayanan, A.; Kozasa, T.; Tesmer, J. J. G. *Science* **2005**, *310*, 1686–1690.

(56) Tesmer, V. M.; Kawano, T.; Shankaranarayanan, A.; Kozasa, T.; Tesmer, J. J. G. *Science* **2005**, *310*, 1686–1690.

(57) Ernst, O.; Zor, T. *J. Vis. Exp.* **2010**, 1–6.

(58) Nishimura, A.; Kitano, K.; Takasaki, J.; Taniguchi, M.; Mizuno, N.; Tago, K.; Hakoshima, T.; Itoh, H. *Proc. Natl. Acad. Sci.* **2010**, *107*, 13666–13671.

(59) Kalipatnapu, S.; Chattopadhyay, A. *IUBMB Life;* **2005**, *57*, 505–512.

Chapter 3: Testing the First Simplified Analog of YM-254890

NOTE: Part of this chapter has been published as Rensing, D.T., Uppal, S., Blumer, K.J., Moeller, K.D. Toward the Selective Inhibition of G Proteins: Total Synthesis of a Simplified YM-254890 Analog. *Org. Letters* 2015 May 1; 17 (9): 2270-3.

3.1 Introduction

Our lab is interested in pursuing chemical biology approaches to investigate G protein signaling pathways and to determine the acute function of specific G proteins. Small molecule ligands that directly target selected G proteins to modulate their activity are potentially valuable as probes of biological function and as avenues to develop therapeutics.[1] The first such small molecule-$G\alpha_q$ protein inhibitor is YM-254890 (now referred to as YM). To date, two main complications have blocked efforts to develop a family of G protein inhibitors based on the structure of YM. First, YM is not readily available which impedes efforts to use the natural product itself as a platform for building derivatives. Second, YM has a complex cyclic depsipeptide core structure that has thwarted efforts to obtain a series of analogs by means of total synthesis. With this in mind, our lab is interested in synthesizing and biologically testing simplified analogs of YM. This chapter will focus on testing the first simplified analog of YM compound named WU-07047 (will be referred to as WU) for its effect on purified Gα proteins. Would simplification of YM structure result in loss of biological activity and its selectivity? This question was answered using an *in vitro* biochemical assay.

Prior to examining the activity of WU, it was essential to test whether the proteins purified in the work described in **Chapter 2** were functional. Since the activity of G proteins is studied by

their ability to exchange bound GDP for GTP, nucleotide exchange assays were used. This chapter will first briefly describe the YM compound and its mechanism of action followed by different types of GTPγS nucleotide exchange assays that are commonly used to assess the biochemical activity of G proteins and determine the efficacy of their inhibitors. The challenges associated with testing the functional activity of purified $G\alpha_q$ will also be discussed. A receptor-assisted nucleotide exchange assay will be introduced that solves these challenges. It is this assay that will be used to test WU. Finally, the specificity of WU compound will be examined using other G proteins ($G\alpha_{i1}$ and $G\alpha_o$). For these assays, a fluorescently labeled nucleotide will be employed.

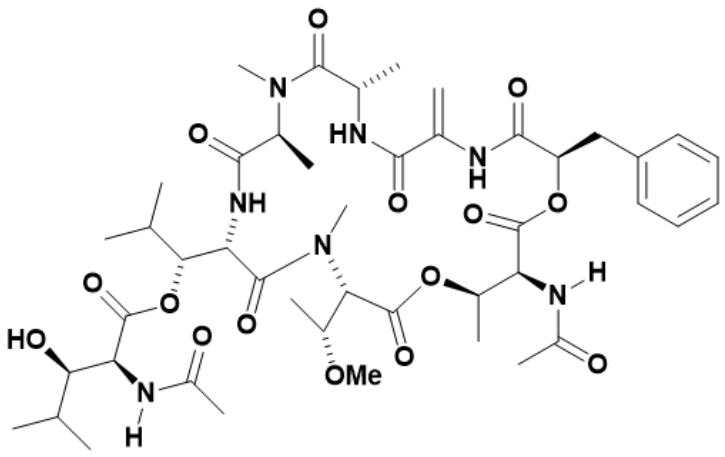

Figure 3.1. Structure of YM

3.1.1 YM, a $G\alpha_{q/11}$-specific inhibitor

The $G\alpha_q$ class of G proteins can be constituted as key players in GPCR signaling for essential agonists such as thrombin and angiotensin II.[2] Wirth *et. al* showed that their $G\alpha_q$ knockout mice have lower blood pressure,[3] providing strong evidence for the importance of $G\alpha_q$ in GPCR signaling and that $G\alpha_q$ antagonists might function as antihypertensive agents. Along these lines, YM (**Figure 3.1**) was discovered by Yamanouchi Pharmaceuticals. YM is a cyclic depsipeptide

derived from *Chromobacterium* sp. QS 3666 that potently (IC_{50} = 0.15 nM) and specifically inhibits the α subunit of the G protein class G_q.[4–6] YM has also shown blood pressure reduction,[6] thrombosis inhibition[5] and decrease in neointima formation following a vascular injury in animal models.[6] All these effects are consistent with the phenotypes of mice lacking $G\alpha_q$.[7]

3.1.2 Mechanism of action

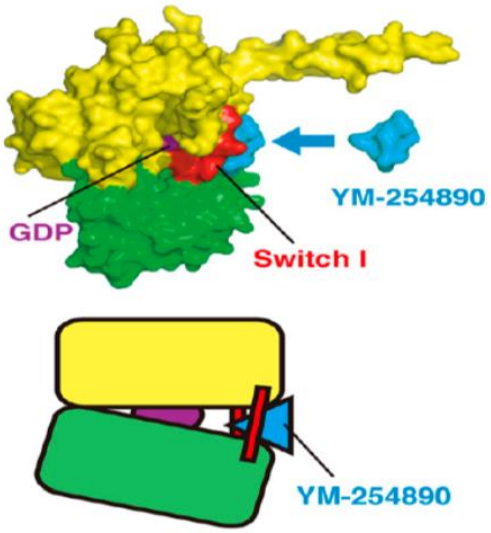

Figure 3.2. Schematic representation of YM compound (represented in blue) directly inhibiting the hinge motion that results in the rearrangement of GTPase (represented in yellow) and helical domain (represented in green) causing the release of GDP (represented in purple). Nishimura *et al*. Structural basis for the specific inhibition of heterotrimeric G_q protein by a small molecule. *Proc. Natl. Acad. Sci.* **2010**, 107, 13666–13671.

Heterotrimeric G proteins are molecular switches that can intrinsically cycle between the inactive GDP-bound to active GTP-bound state.[8] Binding of an agonist to the GPCR elicits guanine nucleotide exchange activity within G proteins which results in receptor catalyzed release of GDP by Gα subunit.[8,9] A general G protein activation cycle has been discussed in detail in **Section 1.3**. Upon receptor activation, nucleotide exchange is the key step towards the activation of G proteins which leads to the dissociation of GTP-bound Gα and Gβγ dimer, which is now able to activate its

specific effectors. This activation cycle is terminated by the intrinsic GTPase activity of Gα subunit resulting in GTP hydrolysis. The Gα (now GDP-bound) now associates with Gβγ dimer and inactive basal state is restored. The rate limiting step in the catalytic cycle described above is the release of GDP. It is this step that is inhibited by YM compound. The selectivity of YM for $G\alpha_q$ is thought to depend on the unique features of the binding pocket for YM in $G\alpha_q$. **Figure 3.2** provides a schematic representation of YM compound directly inhibiting the release of GDP by blocking the hinges that result in the rearrangement of two domains. This binding pocket itself is present in all classes of G proteins. Hence, analogs of YM that were designed to fit the pockets of other G proteins might provide selective inhibitors of those G proteins. In this way, the development of YM analogs has the potential to provide a collection of inhibitors for probing the role of specific G proteins in various physiological or disease processes. This dissertation will focus on the first simplified analog of YM, WU. The WU compound will be considered active if it is able to inhibit the ability of $G\alpha_q$ to undergo nucleotide exchange.

3.1.3 [^{35}S] GTPγS binding assay- testing functional activity of purified G proteins

Prior to testing activity of WU for $G\alpha_q$ and other G proteins, it is essential to test whether the purified G proteins (**Chapter 2**) are active. The functional activity of purified Gα proteins is measured by assessing their ability to undergo nucleotide exchange and bind GTP. Historically, the binding of [^{35}S] guanosine 5'-(gamma-thio) triphosphate (GTPγS) has been used as an approach to characterize purified G proteins.[10–12] In fact, non-hydrolyzable analogs of guanine nucleotides have been extremely important tools for elucidating the function of G proteins.[13] Along these lines, GTPγS (**Figure 3.3**) is one of the most widely used non-hydrolyzable (or slowly hydrolyzed to GDP) analogs of GTP known to activate G proteins.[13]

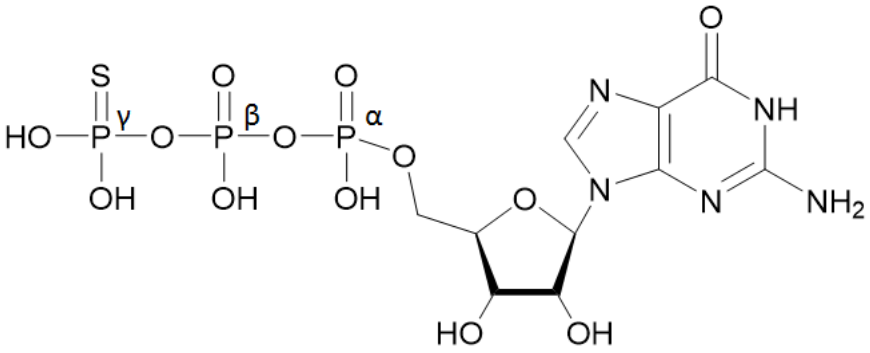

Figure 3.3. GTPγS, a non-hydrolyzable analog of GTP.

Noel *et al.* provided a comprehensive crystallographic study of a heterotrimeric G protein, $G\alpha_t$ complexed with GTPγS.[14] According to the authors, a water molecule plays an essential role in the GTPase mechanism. It serves as a nucleophile and positions itself in-line with the γ-phosphate before the attack. Conversely, the bulky sulfur atom of GTPγS shields the phosphorus atom and prevents its interaction with the active-site water molecule. The majority of GTPγS binding assays are performed using the radiolabeled version of the molecule in which the γ-phosphate is labeled with ^{35}S. Since the γ-thiophosphate bond is resistant to hydrolysis by the GTPases, G proteins cannot reform as a heterotrimer and the lifetime of the nucleotide-bound Gα protein is increased. Thus, [^{35}S] GTPγS labeled Gα subunits can be accumulated and measured by counting the amount of incorporated [^{35}S] label. The use of [^{35}S] GTPγS to directly measure G protein activation by monitoring nucleotide exchange was first described by Hilf *et al.*[15] Upon binding of the radioactive nucleotide to Gα subunits, a filtration procedure was performed to separate free radioactivity from the radioactivity that bound to the protein. This classic method for GTPγS binding can only be used in purified systems because [^{35}S] GTPγS is unable to cross cell membranes.[13] This binding method provides a sensitive tool for assessing the functional activity of purified Gα proteins. However, while these assays provide reliable and accurate results, they have limitations. For

example, the assays generate unwanted radioactive waste and are tedious to perform. Furthermore, the assays are not capable of resolving rapid kinetics of heterotrimeric G protein signaling and thus provide data at distinct intervals only.[16]

3.1.4 Fluorescent ligand based exchange assays

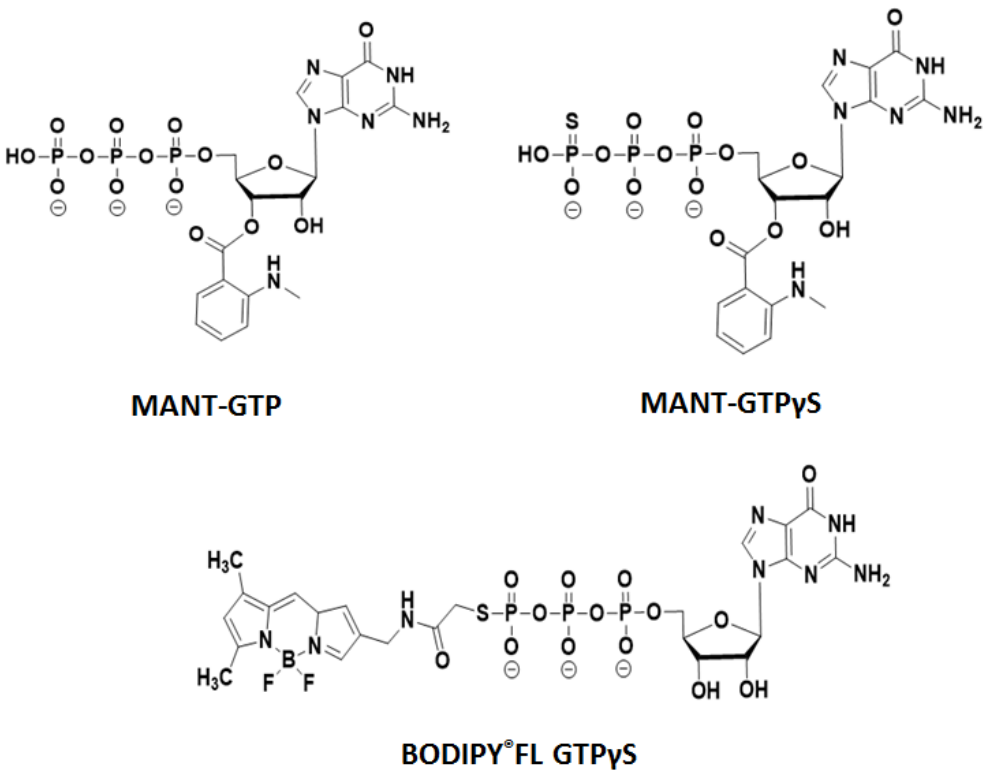

Figure 3.4. Fluorescently labeled guanine nucleotides

In an attempt to develop nonradioactive nucleotide based exchange assays which are capable of performing real time continuous measurements, several groups have reported the use of different fluorescent guanine nucleotides.[17–19] **Figure 3.4** provides two of the most widely used fluorescently labeled guanine nucleotides: N-methylanthraniloyl (MANT) conjugates of GTP and BODIPY®FL (4,4-difluoro-5,7-dimethyl-4-bora-3a,4a-diaza-*s*-indacene-3-alkyl) conjugated guanine nucleotides.[18,26] MANT conjugates of guanine nucleotides are not applicable to all classes

of Gα subunit and have behaved unpredictably for some studies.[24] Therefore, in order to test activity of our other G proteins ($G\alpha_{i1}$ and $G\alpha_o$), BODIPY®FL GTPγS was used.

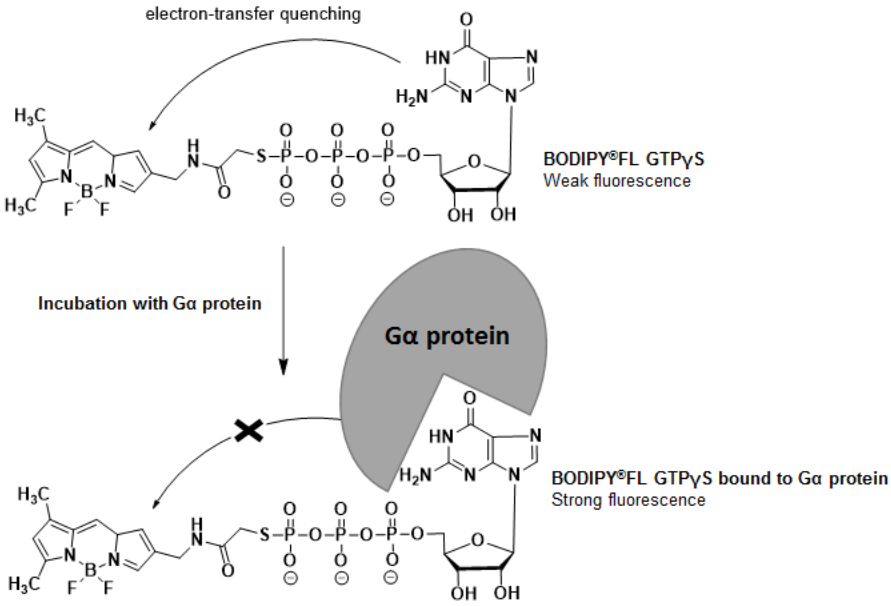

Figure 3.5. Mechanism of action of BODIPY®FL GTPγS in the presence of purified Gα.

BODIPY®FL fluorophore is linked through the γ-thiol of GTPγS. These nucleotides yield greater fluorescence enhancement in comparison to MANT labeled guanine nucleotides.[26] BODIPY®FL labeled nucleotides can be excited in the visible region and have shown to bind $G\alpha_i$ and $G\alpha_s$ class of G proteins.[26] Due to their emission and excitation spectra in the visible region, intact cell studies can be performed with minimal background (a major problem with MANT labeled nucleotides).[26] Even though BODIPY®FL GTPγS has significantly lower affinity (~10 to 100 fold) for Gα subunits than [^{35}S] GTPγS,[26] these fluorescent probes are still one of the most convenient ways to quantify the amount of functional purified G proteins for two classes of G proteins ($G\alpha_{i1}$ and $G\alpha_s$) except for $G\alpha_q$ or $G\alpha_{13}$ class of G proteins. **Figure 3.5** demonstrates the mechanism of action for BODIPY®FL GTPγS. The guanine moiety can donate electrons to the

BODIPY moiety which results in fluorescence quenching. However, once the guanine moiety is bound by the Gα subunit, there is a steric bulk around the moiety which prevents the fluorescence quenching and there is an increase in fluorescence indicative of binding of BODIPY®FL GTPγS to Gα. Unlike $G\alpha_q$, our other purified G proteins ($G\alpha_{i1}$ and $G\alpha_o$) exhibit faster spontaneous nucleotide exchange and can be assayed using fluorescent guanine nucleotides. Therefore, we utilized this convenient and easy method to access activity of purified $G\alpha_{i1}$ and $G\alpha_o$.

3.2 Results and discussion

3.2.1 [^{35}S] GTPγS and purified $G\alpha_q$ binding

The $G\alpha_q$ class of G proteins, like other G proteins, is activated by GTP binding and is deactivated upon hydrolysis of the bound GTP to GDP. Nucleotide exchange is dependent on the rate limiting step of the G protein activation cycle, release of GDP from Gα subunit. The ability of $G\alpha_q$ to exchange guanine nucleotide is reduced drastically by their separation from cell membranes.[27] Most G proteins bind nearly stoichiometrically to GTPγS within 5-30 min in the presence of micromolar nucleotide concentrations. Even in the presence of high nucleotide concentrations (0.1 to 0.2 mM), the binding of soluble $G\alpha_q$ to GTPγS is slow (more than 1 h for marginal loading).[27] Assay conditions that are considered standard for [^{35}S] GTPγS binding to other G proteins have been ineffective for monitoring purified $G\alpha_q$.[33–35] As a result, binding of reasonable quantities of GTPγS or other nucleotides to soluble purified $G\alpha_q$ has been extremely challenging. This anomalous guanine nucleotide binding behavior is not unique to $G\alpha_q$, another class of G proteins, $G\alpha_{12/13}$ also exhibit this unusual nucleotide binding characteristics upon solubilization from membranes.[36,37] Ferguson *et al.* showed that purified $G\alpha_q$ are not able to bind

GTPγS because of the slow dissociation rate of bound GDP, which is the rate limiting step for nucleotide exchange.[38]

3.2.2 Use of ammonium sulfate to accelerate GDP dissociation

Certain studies have used ammonium sulfate to accelerate the dissociation of bound GDP from $G\alpha_q$.[22,38,39] One of the classic ways to precipitate proteins is to use high concentrations of ammonium sulfate (utilizing the tendency of protein to precipitate with increasing ionic concentrations).[40,41] By taking advantage of a similar strategy, appropriate amounts of ammonium sulfate (200 mM) can promote GDP release.[27] The idea is to use 'right' amount of ammonium sulfate that would be enough to affect the stability of the Gα subunit and result in GDP release. Since concentration of GTPγS is high in the solution, as soon as GDP dissociates from the pocket, GTPγS will enter the pocket and Gα. GTPγS complex will be further stabilized by the presence of magnesium ions. Hence, we decided to use this method to see if we could accelerate the exchange of GDP for GTPγS within purified $G\alpha_q$.

$G\alpha_q$ was incubated with 225 mM ammonium sulfate and 10 μM GTPγS at 20 °C for varying periods of time. The reaction contents were then quenched with a buffer containing high concentrations of magnesium (magnesium ions can stabilize the GTPγS bound $G\alpha_q$[11]) and GTP. The quenched reactions were filtered through nitrocellulose membranes, dried and subjected to scintillation counting. Adsorption of GTPγS bound protein on the membrane will result in high radioactive counts per min. As shown in **Figure 3.6**, radioactive counts obtained from samples containing $G\alpha_q$ were similar to samples without $G\alpha_q$. This observation was consistent with $G\alpha_q$ still exchanging the nucleotides very slowly. While radioactive counts were higher at the last time point, this was also true for the control and we concluded that no GTPγS binding was observed above background. This led to the question of whether our protein might be inactive or might have

been denatured during purification. Unfortunately, we did not have any positive controls (functional and active G protein) and therefore, there was no way of testing the validity of the assay. Hence, we did not have a concrete conclusion.

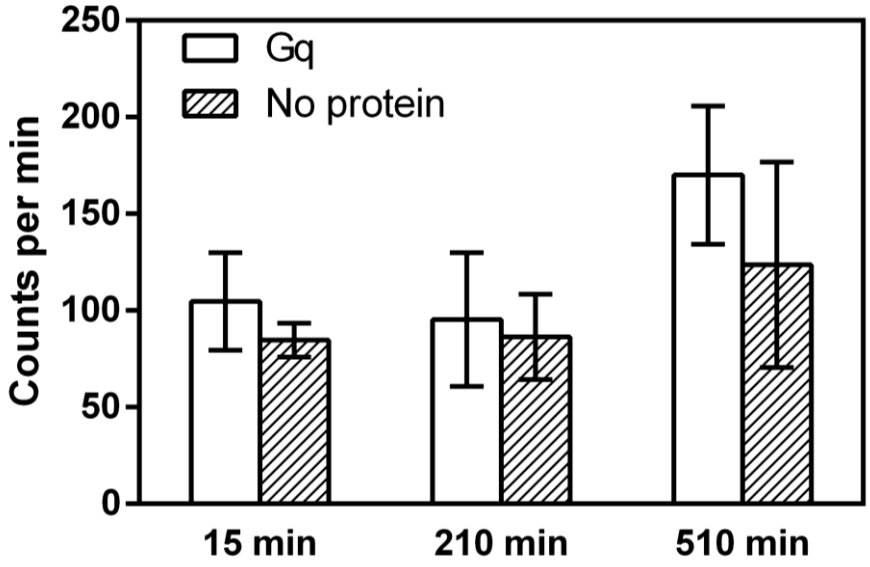

Figure 3.6. Effect of ammonium sulfate on [^{35}S] GTPγS binding to $G\alpha_q$. Binding buffer containing [^{35}S] GTPγS and ammonium sulfate was added to reactions with $G\alpha_q$ or without $G\alpha_q$. GTPγS binding was measured by quenching aliquots of each reaction at indicated times. The data represents (mean ± standard deviation) counts/min from three independent experiments.

3.2.3 Ric-8A assisted nucleotide exchange

Chan *et al.* demonstrated that homologs of the mammalian protein, resistance to inhibitors of cholinesterase 8 (Ric-8) behave as non-receptor guanine nucleotide exchange factors (non-receptor GEFs).[28] Non-receptor GEFs stimulate the release of GDP from specific Gα subunits and stabilize the nucleotide-free Gα form until GTP binding. Ric-8A stimulates the release of GDP by stabilizing a nucleotide-free form of the G protein.[33] We decided to test GTPγS binding to $G\alpha_q$ in

the presence of purified Ric-8A (**Section 2.4.7** provides experimental details regarding the expression of GST-Ric-8A).

Purified $G\alpha_q$ (100 nM) was incubated in a timed GTPγS binding reaction with Ric-8A (200 nM) or without Ric-8A as recommended by the published protocols.[33] The analysis was conducted as described above. Once again, the experiment did not show any GTPγS binding above background (data not shown). The published protocol had expressed $G\alpha_q$ complexed with Ric-8A.[28] It was thought that this might be the problem with the assay conducted. Hence, we expressed both proteins as a complex in insect cells and performed glutathione-sepharose chromatography. Ric-8A protein binds GDP-bound $G\alpha_q$ and forms a nucleotide-free Ric-8A•Gα complex. This complex is stable unless GTPγS or GDP-AlF_4^- are present.[28] Aluminum fluoride occupies the γ-phosphate binding site on the protein and makes the G protein active in the presence of GDP. In other words, since the Al-F bond length is similar to P-O bond length, aluminum fluoride acts as an analog of phosphate and mimics the oxygen bound phosphate.[42] During the purification, this aluminum fluoride activation step was performed to dissociate the complex and obtain free $G\alpha_q$ and Ric-8A. Upper panel in **Figure 3.7** shows a western blot probed with anti-His antibody ($G\alpha_q$ is His-tagged). The majority of $G\alpha_q$ remained in the cell pellet (P) (this is consistent with all our other purifications described in **Chapter 2**). $G\alpha_q$ that did not bind to the glutathione-sepharose column is denoted by F. We reckon that this amount of $G\alpha_q$ did not complex with Ric-8A. Upon washing the resin with a buffer containing aluminum fluoride (AMF-1 and AMF-2), $G\alpha_q$ dissociated from the complex and eluted as pure $G\alpha_q$. Some of the samples were loaded onto a different gel and the western blot was probed with anti-GST antibody since Ric-8A is GST-tagged (lower panel in **Figure 3.7**). Unlike $G\alpha_q$, the cell pellet (P) did not have much Ric-8A which signifies that almost all Ric-8A protein was in the supernatant and was loaded onto the glutathione-

sepharose column (T). No Ric-8A protein dissociated from the resin upon aluminum fluoride wash (AMF-1). Upon washing the resin with a buffer containing 20 mM reduced glutathione, Ric-8A eluted from the resin (reduced glutathione competes with the binding interaction of fused protein with immobilized glutathione) as seen in lanes E1 and E2. Results from this purification indicated that both proteins were functional. With this information in hand, the Ric-8A assisted GTPγS binding study was repeated using these purified proteins.

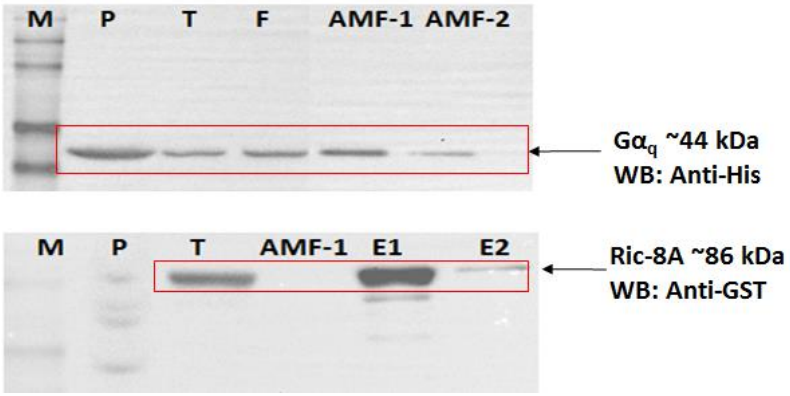

Figure 3.7. Glutathione-sepharose affinity chromatography purification. Protein molecular weight marker (M); pellet obtained after ultracentrifugation (P); total lysate (T); flow through (F); first wash with buffer containing aluminum fluoride (AMF-1); second wash with buffer containing aluminum fluoride (AMF-2); eluted protein fractions (E1& E2). Western blot probed with ***upper panel:*** Anti-His; ***lower panel:*** Anti-GST.

Figure 3.8 shows the results from three independent Ric-8A assisted GTPγS binding experiments. For all these binding assays, lower amounts of unlabeled GTPγS (1.5 µM compared to 10 µM used in experiments before) was used and as a result there was higher loading of labeled GTPγS. Use of less unlabeled GTPγS allows for incorporation of more labeled GTPγS and as result provides higher average radioactive counts for each sample. For some unexplainable reason, our control (samples with Ric-8A only) always showed slightly higher radioactive counts. Ric-8A protein does not bind GTP, therefore this result was odd. Just like the previous assay, no radioactive counts were observed above background. Something was erroneous about this assay

and no concrete conclusions regarding the activity of proteins could be derived from these experiments. What was clear was that we still needed an assay that would allow us to determine if our purified $G\alpha_q$ was active, and then determine if YM analogs were effective inhibitors of that activity.

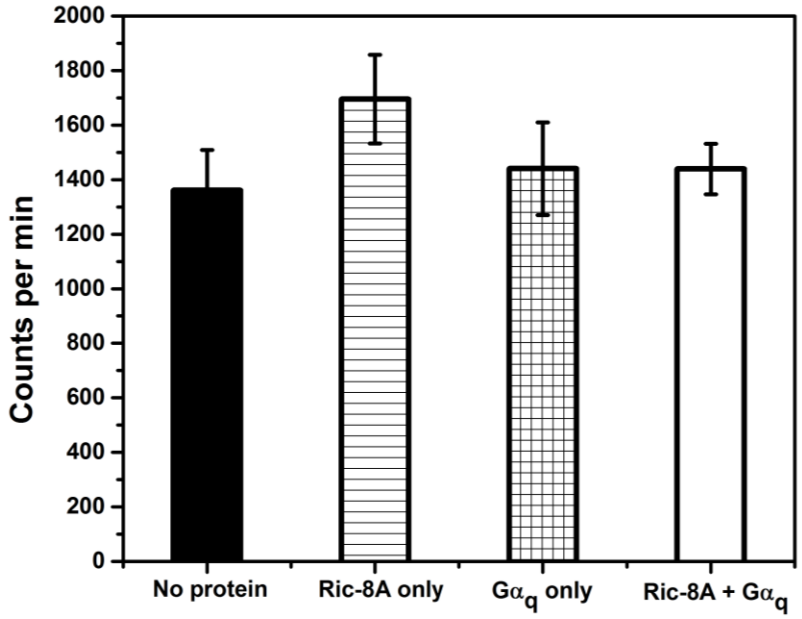

Figure 3.8. Effect of Ric-8A on binding of [^{35}S] GTPγS binding to $G\alpha_q$. Binding of GTPγS to $G\alpha_q$ was measured with or without Ric-8A. Samples containing no protein or Ric-8A only were used as controls. The data represents (mean ± standard deviation) counts/min from three independent experiments.

3.2.4 Purified $G\alpha_q$ is functional as shown by receptor-assisted [^{35}S] GTPγS binding assay

We decided to consult Dr. John Tesmer at University of Michigan, Ann Arbor. The Tesmer lab performs nucleotide exchange assays on a regular basis. Therefore I visited their lab and learned about receptor-assisted [^{35}S] GTPγS binding assays. The Tesmer lab examines the binding of [^{35}S] GTPγS to $G\alpha_q$ using Sepia rhodopsin receptor membranes. As mentioned earlier, the ability of $G\alpha_q$ to exchange guanine nucleotide is reduced drastically by their solubilization from

cell membranes.[27] In a conversation with Dr.Tesmer, he pointed out that in the presence of receptor membranes, the ability of $G\alpha_q$ to exchange nucleotides is returned to normal. However, the receptor acts on the heterotrimer and not $G\alpha_q$ alone. Therefore, receptor mediated exchange assays require $\beta\gamma$ as well.

In order to ensure stability of $G\alpha_q$, purified $G\alpha_q$ is always stored in a buffer containing excess GDP. But this excess GDP can act as a competitor during the GTPγS exchange assays. Therefore, a buffer exchange is essential before the receptor-assisted [^{35}S] GTPγS binding assay. Following the buffer exchange, $G\alpha_q$ was incubated with Sepia $\beta\gamma$ dimer to form the heterotrimer complex. Polypropylene tubes were used because they allow the least amount of non-specific protein interaction. The nucleotide exchange reaction was then initiated by the addition of a reaction mixture containing binding buffer, 100 nM Sepia rhodopsin and [^{35}S] GTPγS to all of the sample tubes. Upon completion of the incubation period, the reactions were quenched by addition of cold Tris buffer containing excess magnesium to stabilize the bound GTPγS. The contents of each sample tube were then filtered through glass fiber filters. The filters were washed extensively with the same Tris buffer containing high magnesium ions, dried and subjected to scintillation counting. **Figure 3.9** provides quantification of receptor-assisted [^{35}S] GTPγS binding experiments. Two independent experiments were conducted (each experiment had triplicates for each sample). Increased radioactive counts per min for the heterotrimer suggested [^{35}S] GTPγS binding. In order to ensure that this binding was not an artifact because of the addition of $\beta\gamma$ dimer, samples with only $\beta\gamma$ were also used (shows lower radioactive counts than heterotrimer in **Figure 3.9**). We decided to use no unlabeled GTPγS because it would decrease the overall radioactive counts. Since our control radioactive counts were always in the range of 700-1500 counts per min, we decided to use more labeled GTPγS. Besides expense, another caveat to using more labeled GTPγS is that

if filters are not washed properly, control counts will also increase. Therefore, it is essential to wash filters. In addition, we noticed that if control samples (samples containing only receptor and [^{35}S] GTPγS) were diluted with 5 mL cold buffer and filtered immediately after that, overall counts were lower. The other samples were also filtered immediately after dilution. In other words, diluted solutions should not be allowed to incubate any longer and must be filtered right away. Over the period we have gained immense knowledge about handling G proteins and may be if we were to repeat the ammonium sulfate-assisted nucleotide exchange assay with longer incubation period, it might work. That assay does not require any additional accessory proteins (e.g. Sepia rhodopsin receptor and βγ dimer). Moreover, now we have a positive control (an active $G\alpha_q$) to test the validity of the assay.

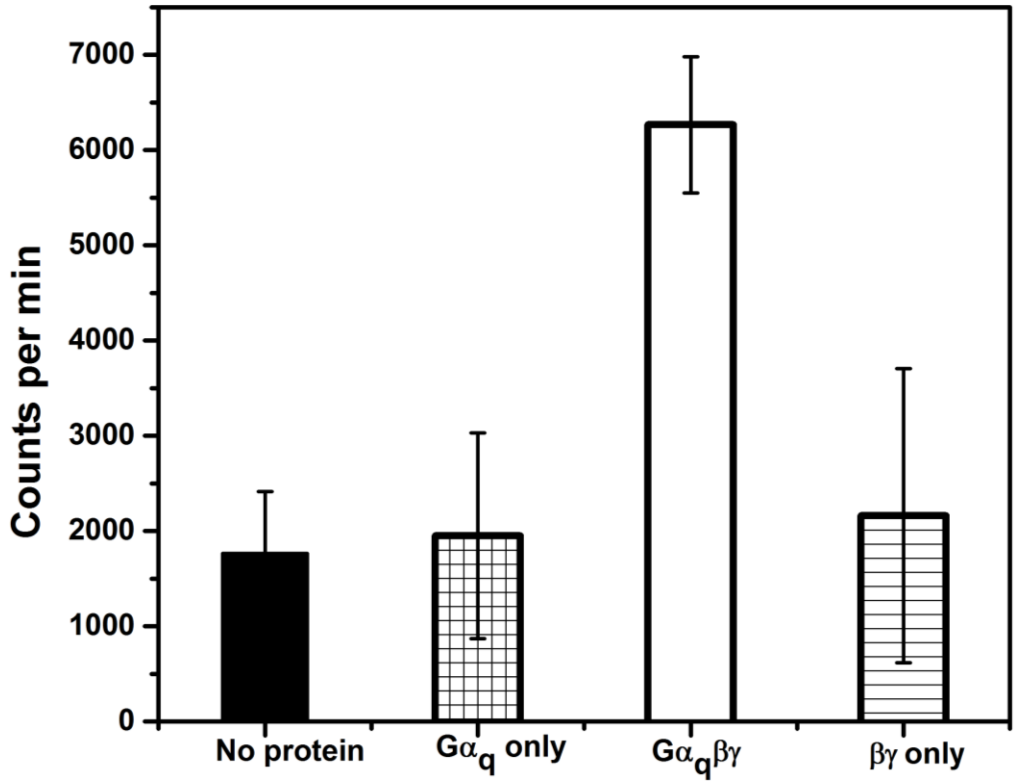

Figure 3.9. Quantification of receptor-assisted [^{35}S] GTPγS binding assay. The data represents mean (±standard deviation) counts from two independent experiments (each experiment had triplicates for each sample).

The success of this assay proved that $G\alpha_q$ purified from TIPS method is functional. Furthermore, we had a working assay to test activity of simplified YM analogs. The simplified analog, if active, would prevent [^{35}S] GTPγS binding to $G\alpha_q$ and the radioactive counts will be lower.

3.2.5 Synthetic plan for simplified YM analog, WU

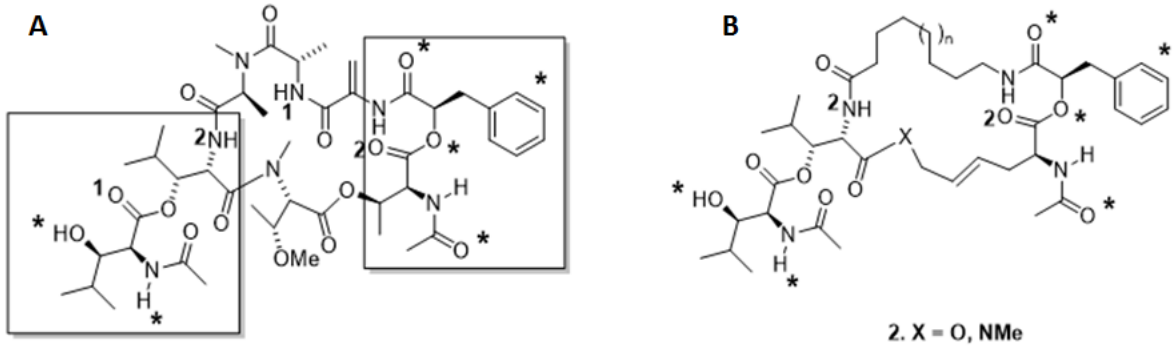

Figure 3.10. ***A.*** YM; ***B.*** WU. Boxes highlight the regions of YM that bind to $G\alpha_q$ based on the X-ray crystal structure of the YM-$G\alpha_q$ complex.[29] Asterisks signify essential points of YM that make direct contact with $G\alpha_q$ and numbers denote hydrogen bonds that impart stability to the YM-conformation involved in binding $G\alpha_q$.

Figure 3.10 (A) depicting the small molecule inhibitor of $G\alpha_q$, YM contains two regions that are highlighted along with several asterisks and a pair of numbers. The boxes highlight the regions of YM that bind to $G\alpha_q$. The points in YM that make contact with $G\alpha_q$ are marked with the asterisks, and the numbers denoted hydrogen bonds that impart stability to the YM-conformation involved in binding $G\alpha_q$ (in both **A** and **B**). Both regions are connected by two bridging groups. Since no tangible information was available about these groups making contacts with $G\alpha_q$, we reckoned to simplify the synthesis of YM analogs while allowing the molecule to still bind and inhibit $G\alpha_q$ by replacing these bridging groups with simplified chains. For a first attempt, the bridge

at the top of the molecule was replaced with an alkyl chain and the bridge at the bottom was replaced with an alkene unit. The alkene would arise from a metathesis reaction used to construct the macrocycle. The trans double bond was located in the same position as the "s-cis" ester located in the bottom bridge of YM in the YM-$G\alpha_q$ complex.[29] WU (**Figure 3.10 B**) was prepared by Derek Rensing in Moeller group. Details regarding the synthesis route have been published (Rensing, D.T., Uppal, S., Blumer, K.J., Moeller, K.D. Toward the Selective Inhibition of G Proteins: Total Synthesis of a Simplified YM-254890 Analog. *Org. Letters* 2015 May 1; 17 (9): 2270-3).

3.2.6 WU shows inhibitory activity towards $G\alpha_q$

With WU in hand, attention was turned toward determining its inhibitory activity in a receptor-assisted [^{35}S] GTPγS binding assay. Upon receptor activation, α subunit of the G_q heterotrimer exchanges bound GDP for GTP to establish an active conformation of the protein. By using [^{35}S] GTPγS, this reaction was monitored over time to obtain conditions of half-maximal exchange. Under these conditions, the ability of WU to inhibit nucleotide exchange was compared to that of another natural product closely related to YM (UBO-QIC, **Figure 3.11**)[43] relative to a vehicle (DMSO) control. UBO-QIC (or FR900359, a selective $G\alpha_q$ inhibitor) is structurally similar to YM and is commercially available.[43]

To our knowledge, inhibitory effects of UBO-QIC on $G\alpha_q$ have not been characterized in a receptor-assisted [^{35}S] GTPγS binding assay. In cell based assays, 1 μM UBO-QIC completely silenced G_q mediated signaling in comparison to 300 nM YM (UBO-QIC product description sheet provided by the manufacturer). The data in **Figure 3.12** are consistent with the inhibition of receptor-driven nucleotide exchange on $G\alpha_q$ by WU in a concentration dependent manner. The left y-axis in the figure signify the average radioactive counts obtained while the right y-axis implies

the [^{35}S] GTPγS binding from three independent experiments. Results indicated that WU and UBO-QIC displayed similar efficacy (up to 40 % inhibition in uptake of [^{35}S] GTPγS), but WU was less potent. So while WU is a greatly simplified version of YM that retained none of the functionality in the tethers connecting the regions of the molecule thought to be associated with its activity, it did retain the ability to inhibit $G\alpha_q$ activation.

This finding suggests that WU can provide a good starting point for exploring new $G\alpha_q$ inhibitors and learning more about the factors that impart selectivity to YM. For example, current efforts are underway to reinstall the hydrogen bond represented by the number 1 in **Figure 3.10.A** in order to determine its role in the selectivity and activity of the analog and to determine if the removal of the double bond in the bottom bridge improves activity.

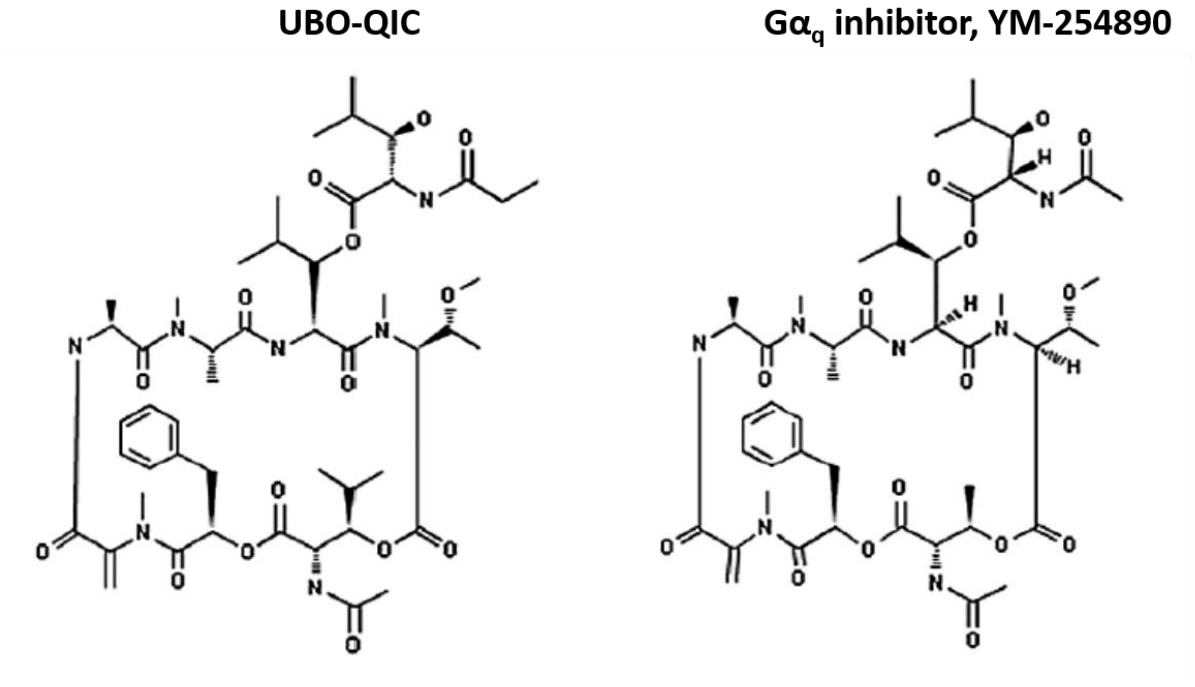

Figure 3.11. UBO-QIC (left), a closely related to YM (right). Figure obtained from product description data sheet provided by the manufacturer.

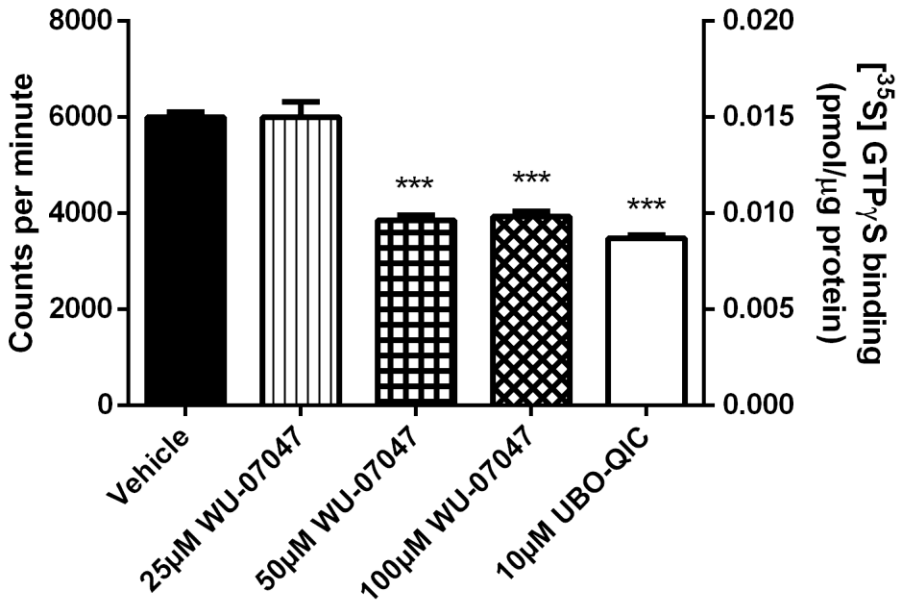

Figure 3.12. Quantification of receptor-assisted [^{35}S] GTPγS binding assay. The data represents mean (±SEM) counts from three independent experiments (n=3). Statistical significance is marked by ***, where p <0.0001 with respect to vehicle.

3.2.7 WU shows selectivity towards $G\alpha_q$

Since YM inhibits activation of $G\alpha_q$ but not $G\alpha_i$ or $G\alpha_o$, we were interested in determining whether WU displayed similar selectivity. **Chapter 2** illustrates expression and purification of both $G\alpha_{i1}$ and $G\alpha_o$ and before testing effect of WU on these proteins, it was essential to assess the activity of both proteins. Because the rate of spontaneous nucleotide exchange by $G\alpha_{i1}$ and $G\alpha_o$ is faster than $G\alpha_q$, a receptor-independent assay was used to monitor the binding kinetics of a fluorescently labeled (BODIPY® FL) GTPγS.[26,31]

The rate of nucleotide exchange in $G\alpha_o$ and $G\alpha_{i1}$ was determined by the uptake of fluorescent GTP analog, BODIPY® FL GTPγS after the release of bound GDP. In the absence of G protein, the guanine base quenches the BODIPY®FL fluorophore resulting in a low quantum yield. Upon binding of the Gα subunit, quenching is relieved and there is an increase in quantum yield that can

be measured by excitation at 485 nm and emission at 530 nm. (**Figure 3.5**). Binding kinetics of BODIPY®FL GTPγS to $G\alpha_o$ and $G\alpha_{i1}$ are different. $G\alpha_{i1}$ has a slower rate of nucleotide exchange as seen in **Figure 3.13**. In order to study the association and dissociation of the ligand, a kinetic experiment was performed using $G\alpha_o$ because of its fast nucleotide exchange (**Figure 3.14**). Fluorescence of BODIPY GTPγS was measured alone for 2 min and then nucleotide exchange was initiated by the addition of $G\alpha_o$ (association of BODIPY GTPγS). The fluorescence associated with the binding of BODIPY®FL GTPγS to $G\alpha_o$ reached saturation at ~ 10 min. The dissociation of BODIPY®FL GTPγS was then observed by the addition of excess unlabeled GTPγS only in one of the samples (blue circles). Dissociation kinetics initiated by addition of unlabeled GTPγS can be seen due to the fluorescence decrease. This is a competition assay in which the unlabeled GTPγS competes with the fluorescently labeled GTPγS. Please note that **Figure 3.14** shows raw curves and a decreased fluorescence (from 600 to 1100 s) in sample denoted by blue circles is just an artifact of the plate reader. The essential point is that the fluorescence decreases dramatically in the sample in which unlabeled GTPγS was added.

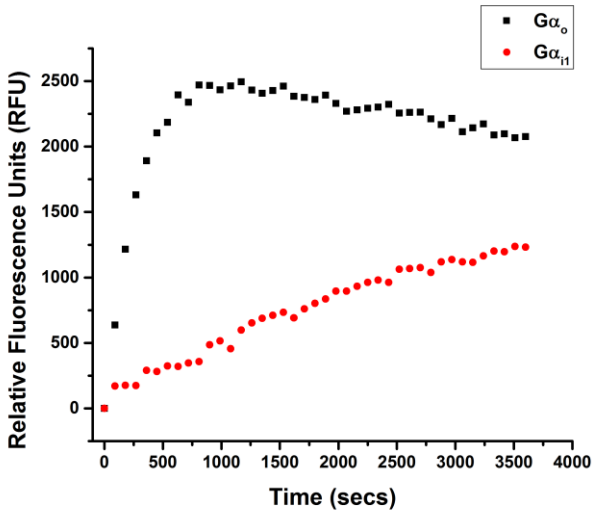

Figure 3.13. Binding kinetics of BODIPY® FL GTPγS thioether to $G\alpha_{i1}$ *(red)* and $G\alpha_o$ *(black)*. $G\alpha_{i1}$ has slower rate of nucleotide exchange.

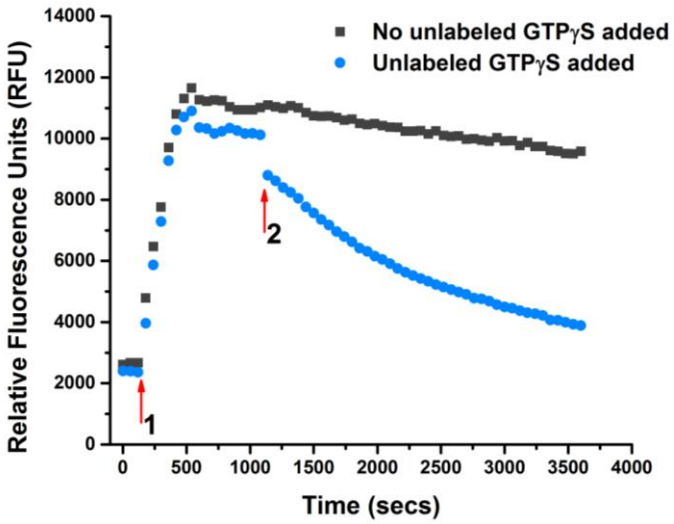

Figure 3.14. Association-dissociation kinetic experiment**.** Association and dissociation of BODIPY®FL GTPγS with $G\alpha_o$. Red arrow 1 indicates the addition of $G\alpha_o$ to both wells and red arrow 2 denotes the addition of unlabeled GTPγS only to the blue well.

In order to test validity of these assays, a positive control was used. This positive control was a peptide motif (also referred to as GPR motif) from a protein known as Activator of G protein signaling 3 (AGS3). This motif functions as a guanine nucleotide dissociation inhibitor (GDI) for $G\alpha_{i1}$ and $G\alpha_o$.[31] AGS3 motif binds strongly to all isoforms of $G\alpha_{i1}$ and weakly to $G\alpha_o$.[44] Binding of AGS3 motif blocks association of BODIPY®FL GTPγS in a concentration dependent manner. To this end, the rate of guanine nucleotide exchange on $G\alpha_{i1}$ (**Figure 3.15; left panel**) and $G\alpha_o$ (**Figure 3.15; right panel**) was assayed in the presence of varying concentrations of AGS3 motif. As mentioned previously, AGS3 peptide is a strong binder of $G\alpha_{i1}$ and thus the drop in fluorescence is greater than $G\alpha_o$ (1 µM peptide causes ~50 % decrease in fluorescence in samples with $G\alpha_o$ whereas the same amount of peptide results in ~80 % decrease in fluorescence). Thus, both proteins and peptide were behaving as expected based on literature values.[31] This assay showed that purified G proteins were functional.

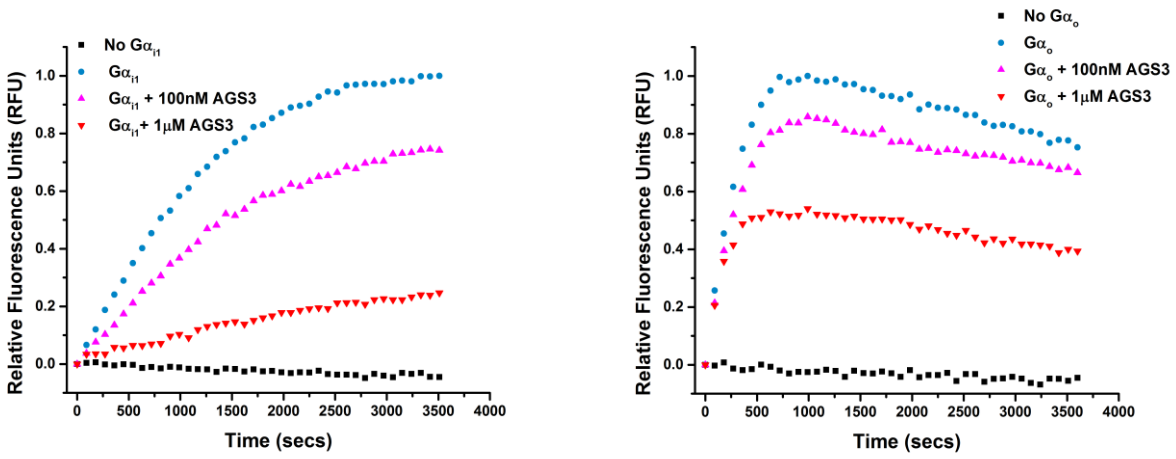

Figure 3.15. Effects of varying concentrations of AGS3 peptide on kinetics of BODIPY® FL GTPγS thioether binding to Gα. A time course of BODIPY® FL GTPγS thioether binding to Gα in the absence (*blue)* or presence *(magenta*, 100 nM; red, 1 μM*)* of AGS3. ***Left Panel:*** $G\alpha_{i1}$; ***Right Panel***: $G\alpha_o$.

Using this assay and AGS3 as a positive control, the effect of WU was examined on nucleotide exchange activity of $G\alpha_{i1}$ and $G\alpha_o$. When tested in these assays over a wide concentration range, WU displayed no ability to inhibit nucleotide exchange on $G\alpha_{i1}$ or $G\alpha_o$ (**Figure 3.16**). This data suggests that despite its simplified structure, WU maintained its selectivity towards $G\alpha_q$.

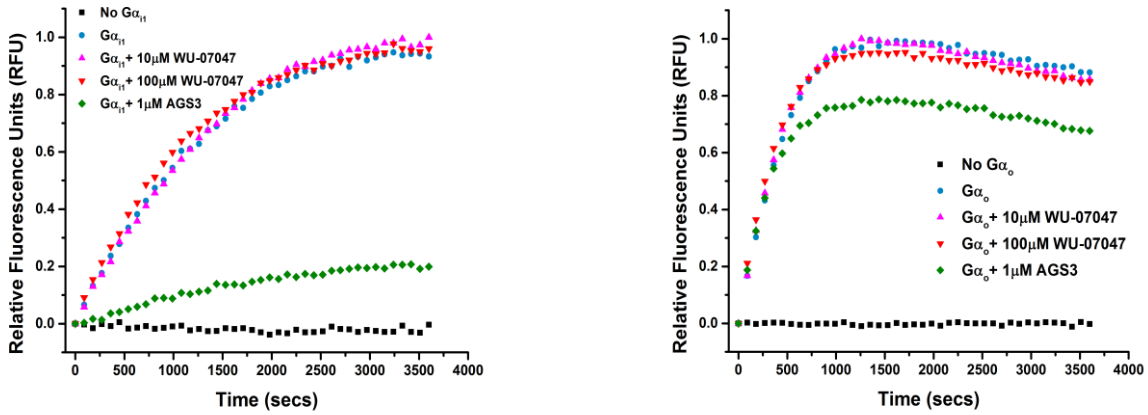

Figure 3.16. Effects of varying concentrations of WU on kinetics of BODIPY® FL GTPγS thioether binding to Gα. A time course of BODIPY® FL GTPγS thioether binding to Gα in the absence (*blue)* or presence *(magenta*, 10 μM; red, 100 μM*)* of WU. AGS3 (*green*, 1 μM*)* was used as a positive control. ***Left Panel:*** $G\alpha_{i1}$; ***Right Panel***: $G\alpha_o$.

3.3 Conclusions

In conclusion, we have shown that all purified G proteins are functional and active. The activity of $G\alpha_q$ was studied using a receptor-mediated [^{35}S] GTPγS binding assay whereas the activity of $G\alpha_{i1}$ and $G\alpha_o$ was examined using BODIPY® FL GTPγS binding assay. In addition, we have developed an *in vitro* biochemical assay to test the activity of WU, a simplified analog of YM. While this analog is not as potent as UBO-QIC, it inhibits $G\alpha_q$ and appears to retain G protein selectivity characteristics like the natural product. No substantial conclusions regarding potency of WU (in comparison to YM) can be made at this point because of the lack of YM itself. UBO-QIC compound has been compared to YM in cellular-based assays but not in an *in vitro* biochemical assay. It is possible that WU compound shows higher potency in cell-based assays.

3.4 Experimental section

Unless noted otherwise, all chemicals were ordered from Sigma Aldrich (St. Louis, MO). All other vendor information is noted in the experimental section. [^{35}S] GTPγS (catalog no. NEG030H) was purchased from Perkin Elmer (Waltham, MA).

3.4.1 [^{35}S] GTPγS binding assay using ammonium sulfate

The previously reported method was used with slight modifications.[27] Reactions were carried out in binding buffer (50 mM HEPES pH 7.5, 1 mM EDTA, 1 mM DTT, 0.9 mM $MgCl_2$, 0.05 % genapol, 225 mM ammonium sulfate and 10 μM GTPγS). [^{35}S] GTPγS was diluted 1:1000 in binding buffer so the final radioactive concentration in each sample was 0.045 μCi. Binding of 10 μM GTPγS (0.045 μCi or specific activity = 10,000 cpm/pmol) to $G\alpha_q$ was measured at 20 °C in a total volume of 100 μL. Triplicate aliquots (10 μL each) were taken from the reaction at indicated

time points and added to a conical tube containing 3 mL stop buffer (20 mM Tris-HCl pH 7.7, 100 mM NaCl, 10 mM $MgCl_2$, 0.1 mM DTT, 0.1 % genapol and 1 mM GTP), followed by filtration through nitrocellulose membranes (adsorbs $G\alpha_q$). Membranes were washed extensively with wash buffer (20 mM Tris-HCl pH 7.7, 100 mM NaCl and 2 mM $MgCl_2$). Membranes were air dried for 1 h before subjecting to scintillation counting (Tri-carb liquid scintillation counter, Perkin Elmer, Waltham, MA). Data was analyzed using MS Excel and graphed (**Figure 3.6**) using Origin 9.0 (OriginLab Corporation, Northampton, MA)

3.4.2 Disruption of nucleotide-free Ric-8A.$G\alpha_q$ complex using aluminum fluoride

Fresh sf9 cells (cell density = ~$1.8x10^6$ viable cells/mL) were infected with 1:3 $G\alpha_q$: GST-Ric-8A baculovirus P3 stocks. Cells were harvested after 48 h by centrifuging at 500 g for 10 min. Dissociation of nucleotide-free Ric-8A.$G\alpha_q$ complex was performed using published protocols.[28] **Figure 3.7** shows western blots summarizing the results from glutathione-sepharose chromatography.

3.4.3 Ric-8A assisted [^{35}S] GTPγS binding assay

Purified $G\alpha_q$ (100 nM) was incubated with purified GST-Ric-8A (200 nM) at 25 °C in GTPγS binding buffer (20 mM HEPES pH 8.0, 100 mM NaCl, 4 mM DTT, 1 mM EDTA, 10 mM magnesium chloride and 0.05 % Genapol) and 1.5 µM GTPγS (0.045 µCi or specific activity = 10,000 cpm/pmol) for 45 mins. Triplicate aliquots were taken from each reaction and quenched in 5 mL stop buffer (20 mM Tris-HCl pH 7.7, 100 mM NaCl, 4 mM DTT, 1 mM EDTA, 1 mM GTP and 0.08% genapol) and filtered through nitrocellulose filters. The filters were washed with 10 mL wash buffer (20 mM Tris-HCl pH 7.7, 100 mM NaCl and 2 mM $MgCl_2$), air dried for 1 h and then subjected to scintillation counting (Tri-carb liquid scintillation counter, Perkin Elmer, Waltham,

MA). Data was analyzed using MS Excel and graphed (**Figure 3.8**) using Origin 9.0 (OriginLab Corporation, Northampton, MA)

3.4.4 $G\alpha_q$ buffer exchange

10 µL aliquot of purified $G\alpha_q$ (stored at -80 °C) was thawed on ice. Once thawed, 10 µL of GDP-free protein dilution buffer (20 mM HEPES pH 8.0, 100 mM NaCl, 1 mM $MgCl_2$ and 2 mM DTT) was added to it. This dilution step was performed because minimum volume that can be added to the exchange buffer columns is 20 µL. Diluted protein sample was passed through micro biospin chromatography columns (Bio-Rad laboratories Inc., Richmond, CA) as per manufacturer's instructions. Concentration of the purified $G\alpha_q$ (now in GDP-free buffer) was determined using NanoDrop 2000 (Thermo Fisher Scientific, Waltham, MA).

NOTE: UV absorbance at 280 nm method for protein quantitation cannot be trusted because of the presence of GDP. Hence, Bradford assay or gel quantitation methods were applied to quantify protein before buffer exchange.

3.4.5 Storage conditions for [^{35}S] GTPγS

Fresh [^{35}S] GTPγS was diluted to 0.5 µCi/µL (final concentration) in protein dilution buffer with 4 mM DTT (final concentration) and stored in 20 µL aliquots at -80 °C. More than one freeze thaw of [^{35}S] GTPγS should be avoided.

3.4.6 Receptor-assisted [^{35}S] GTPγS binding assay

Cholate-insoluble Sepia rhodopsin and Sepia beta gamma (Sepia βγ) subunits were kindly provided by Dr. John J. Tesmer (University of Michigan, MI) who obtained it from Dr. John K. Northup (National Institutes of Health, MD).

Receptor assisted exchange of GDP for [^{35}S] GTPγS on $G\alpha_q$ was determined by modification of previously reported procedures.[27,29,30] All reactions were carried out in 5mL Falcon polypropylene tubes (Fisher Scientific) in a total assay volume of 25µL. Filter binding method was used to measure GTPγS binding to $G\alpha_q$. Purified $G\alpha_q$ was buffer exchanged into GDP-free protein dilution buffer (working stock concentration: 1 µM) (**Section 3.4.4)**. Sepia βγ was diluted (working stock concentration: 1 µM) in GDP-free protein dilution buffer containing 10 mM CHAPS detergent. Sepia rhodopsin was also diluted (working stock concentration: 1 µM) in GDP-free protein dilution buffer except no CHAPS detergent was added. Nucleotide exchange reactions were carried out in binding buffer (50 mM Tris-HCl pH 8.0, 100 mM NaCl, 5 mM $MgCl_2$, 1 mM EDTA, and 1 mM DTT). Purified $G\alpha_q$ (final concentration: 100 nM) was incubated with Sepia βγ (final concentration: 100 nM) on ice for 10 min to form heterotrimeric complex. The nucleotide exchange reaction was initiated by addition of reaction mix containing binding buffer, Sepia rhodopsin (100 nM final concentration in each sample) and [^{35}S] GTPγS (0.5 µCi or specific activity = $1.6x10^6$ cpm/pmol in each sample). After 20 min incubation at 20 ^{0}C, 4 mL cold wash buffer (50 mM Tris-HCl pH 8.0, 5 mM $MgCl_2$) was added to the tubes and the contents were filtered through glass fiber filters (GF/C, Whatman) (filters were pre wetted with wash buffer). Filters were washed further with 10 mL cold wash buffer and dried for 1 h before subjecting to liquid scintillation counting (Tri-carb liquid scintillation counter, Perkin Elmer, Waltham, MA). Data was analyzed using MS Excel and graphed (**Figure 3.9**) using Origin 9.0 (OriginLab Corporation, Northampton, MA).

3.4.7 Testing effect of WU on $G\alpha_q$ using receptor-assisted [^{35}S] GTPγS binding assay

UBO-QIC compound was purchased from the Institute of Pharmaceutical Biology, University of Bonn. WU was provided by Derek Rensing (Department of Chemistry, Washington University

in St. Louis, MO) as a brown/red colored oil. Stock solution of 25 mM was prepared in 100 % DMSO and stored in 5 µL stocks at -20 °C.

All reactions were carried out in 5mL Falcon polypropylene tubes (Fisher Scientific) in a total assay volume of 25 µL. Filter binding method was used to measure GTPγS binding to $G\alpha_q$. Purified $G\alpha_q$ was buffer exchanged into GDP-free protein dilution buffer (working stock concentration: 1 µM) (**Section 3.4.4)**. Sepia βγ was diluted (working stock concentration: 1 µM) in GDP-free protein dilution buffer containing 10 mM CHAPS detergent. Sepia rhodopsin was also diluted (working stock concentration: 1 µM) in GDP-free protein dilution buffer except no CHAPS detergent was added. Nucleotide exchange reactions were carried out in binding buffer (50 mM Tris-HCl pH 8.0, 100 mM NaCl, 5 mM $MgCl_2$, 1 mM EDTA, and 1 mM DTT). Purified $G\alpha_q$ (final concentration: 330 nM) was incubated with Sepia βγ (final concentration: 330 nM) on ice for 10 min to form heterotrimeric complex. The nucleotide exchange reaction was initiated by the addition of reaction mix containing binding buffer, 100 nM Sepia rhodopsin and [^{35}S] GTPγS ($1.6x10^6$ cpm/pmol). After 20 min incubation at 20 °C, 4 mL cold wash buffer (50 mM Tris-HCl pH 8.0, 5 mM $MgCl_2$) was added to the tubes and the contents were filtered through glass fiber filters (GF/C, Whatman). Filters were washed further with 10 mL cold wash buffer and dried for 1 h before subjecting to liquid scintillation counting (Tri-carb liquid scintillation counter, Perkin Elmer, Waltham, MA). Data was analyzed using MS Excel and graphed (**Figure 3.12**) using Prism software (Graph Pad Software Inc.).

Fluorescence based nucleotide exchange assays using BODIPY®FL GTPγS

All fluorescence measurements were made using Synergy™ H4 plate reader (BioTek Instruments, Inc. Winooski, VT). Excitation and emission wavelengths were set at 485 and 530

nm respectively (light source- xenon flash, wavelength selection- monochromator, band pass 20 nm). There was a delay of 100 ms between well readings. Costar™ 96-well black plate (Thermo Fisher Scientific, Waltham, MA) was used for all fluorescence measurements. BODIPY®FL GTPγS thioether was purchased from Molecular probes, Eugene, OR.

3.4.8 Association-dissociation kinetic experiment

BODIPY®FL GTPγS thioether (final concentration 50 nM) was diluted in 200 µL assay buffer (50 mM Tris-HCl pH 8.0, 1 mM EDTA, 10 mM Magnesium chloride). All samples were scanned immediately using a fluorescent plate reader for 2 min (1 min interval). Nucleotide exchange was initiated by addition of 200 nM $G\alpha_o$. Upon saturation (at time, t= ~20 min), unlabeled GTPγS (final concentration: 20 µM) was added to appropriate wells and mixed by manual pipetting and fluorescence intensity was measured for additional 40 min (1 min interval). Data was graphed (**Figure 3.14**) using Origin 9.0 (OriginLab Corporation, Northampton, MA).

3.4.9 BODIPY®FL GTPγS binding assay to test activity of $G\alpha_{i1}$ and $G\alpha_o$

Previously reported methods were used with slight modifications.[26,31,32] A GPR consensus peptide, AGS3 (CTMGEEDFFDLLAKSQSKRMDDQRVDLAG, purity >90 %) was purchased from Genscript (Piscataway, NJ). The C-terminus of the peptide was blocked by amidation and the N-terminus by acetylation. Peptide was delivered as a white lyophilized powder. 10 µM and 100 µM peptide stocks were prepared in 100 % dd H_2O and stored in -20 °C. This peptide was used as a control to test the validity of the biochemical assay. An aliquot of 200 nM purified protein ($G\alpha_{i1}$or $G\alpha_o$) was incubated in 200 µL assay buffer (50 mM Tris pH 8.0, 1 mM EDTA, 10 mM magnesium chloride) at 25 °C for 35 min with or without varying concentrations of AGS3 (GPR consensus peptide). After incubation, contents were transferred to Costar™ 96-well black plate

and BODIPY® FL GTPγS thioether (final concentration 75 nM) was added to each well. Contents were mixed by manual pipetting and scanned immediately in kinetics mode using a fluorescent plate reader for 1 h (90 s interval, 144 reads/well) at 30 °C. Data analysis and background subtraction of reactions without protein were performed with MS excel. Data was graphed (**Figure 3.15**) using Origin 9.0 (OriginLab Corporation, Northampton, MA).

3.4.10 Testing effect of WU on $G\alpha_{i1}$ and $G\alpha_o$ using BODIPY®FL GTPγS binding assay

Exact same procedure was used as mentioned in **Section 3.4.9** to test effect of varying concentrations of WU on $G\alpha_{i1}$ and $G\alpha_o$. DMSO was used as control vehicle and AGS3 was used as a positive control to test the validity of the assay. Data analysis and background subtraction of reactions without protein were performed with MS excel. Data was graphed (**Figure 3.16**) using Origin 9.0 (OriginLab Corporation, Northampton, MA).

3.5 References

(1) Ayoub, M. A.; Damian, M.; Gespach, C.; Ferrandis, E.; Lavergne, O.; De Wever, O.; Banères, J.-L.; Pin, J.-P.; Prévost, G. P. *J. Biol. Chem.* **2009**, *284*, 29136–29145.

(2) Bernard, R.; Thach, L.; Kamato, D.; Osman, N.; Little, P. J. *Clin. Exp. Pharmacol.* **2014**, *4*, 13–16.

(3) Wirth, A.; Benyó, Z.; Lukasova, M.; Leutgeb, B.; Wettschureck, N.; Gorbey, S.; Orsy, P.; Horváth, B.; Maser-Gluth, C.; Greiner, E.; Lemmer, B.; Schütz, G.; Gutkind, J. S.; Offermanns, S. *Nat. Med.* **2008**, *14*, 64–68.

(4) Saito, T.; Moritani, Y.; Takasaki, J. U. N.; Hayashi, K. *J Antibiot* **2003**, *56*, 358–363.

(5) Uemura, T.; Kawasaki, T.; Taniguchi, M.; Moritani, Y.; Hayashi, K.; Saito, T.; Takasaki, J.; Uchida, W.; Miyata, K. *Br. J. Pharmacol.* **2006**, *148*, 61–69.

(6) Kawasaki, T.; Taniguchi, M.; Moritani, Y.; Uemura, T.; Shigenaga, T.; Takamatsu, H. *Br J Pharmacol* **2005**, 184–192.

(7) Wettschureck, N.; Offermanns, S. *Physiol Rev* **2005**, 1159–1204.

(8) Oldham, W. M.; Hamm, H. E. *Nat. Rev. Mol. Cell Biol.* **2008**, *9*, 60–71.

(9) Johnston, C. A.; Siderovski, D. P. *Mol. Pharmacol.* **2007**, *72*, 219–230.

(10) Sternweis, P. C.; Robishaw, J. D. *J. Biol. Chem.* **1984**, *259*, 13806–13813.

(11) Higashijima, T.; Ferguson, K. M.; Sternweis, P. C.; Smigel, M. D.; Gilman, A. G. *J. Biol. Chem.* **1987**, *262*, 762–766.

(12) Bokoch, G. M.; Katada, T.; Northup, J. K.; Ui, M.; Gilman, A. G. *J. Biol. Chem.* **1984**, *259*, 3560–3567.

(13) Harrison, C.; Traynor, J. R. *Life Sciences*, **2003**, *74*, 489–508.

(14) Noel, J. P.; Hamm, H. E.; Sigler, P. B. *Nature*, **1993**, *366*, 654–663.

(15) Hilf, G.; Gierschik, P.; Jakobs, K. H. *Eur. J. Biochem.* **1989**, *186*, 725–731.

(16) Mukhopadhyay, S.; Ross, E. M. *Proc. Natl. Acad. Sci.* **1999**, *96*, 9539–9544.

(17) Remmers, A. E. *Anal. Biochem.* **1998**, *257*, 89–94.

(18) McEwen, D. P.; Gee, K. R.; Kang, H. C.; Neubig, R. R. *Methods Enzymol.* **2002**, *344*, 403–420.

(19) Eccleston, J. F.; Moore, K. J.; Brownbridge, G. G.; Webb, M. R.; Lowe, P. N. *Biochem. Soc. Trans.* **1991**, *19*, 432–437.

(20) Kimple, R. J.; Jones, M. B.; Shutes, A.; Yerxa, B. R.; Siderovski, D. P.; Willard, F. S. *Comb. Chem. High Throughput Screen.* **2003**, *6*, 399–407.

(21) Hiratsuka, T. *Biochim. Biophys. Acta* **1983**, *742*, 496–508.

(22) Remmers, A. E.; Posner, R.; Neubig, R. R. *J. Biol. Chem.* **1994**, *269*, 13771–13778.

(23) Lan, K. L.; Remmers, A. E.; Neubig, R. R. *Biochemistry* **1998**, *37*, 837–843.

(24) Zera, E. M.; Molloy, D. P.; Angleson, J. K.; Lamture, J. B.; Wensel, T. G.; Malinski, J. A. *J. Biol. Chem.* **1996**, *271*, 12925–12931.

(25) Gille, A.; Seifert, R. *J. Biol. Chem.* **2003**, *278*, 12672–12679.

(26) McEwen, D. P.; Gee, K. R.; Kang, H. C.; Neubig, R. R. *Anal. Biochem.* **2001**, *291*, 109–117.

(27) Chidiac, P.; Markin, V. S.; Ross, E. M. *Biochem. Pharmacol.* **1999**, *58*, 39–48.

(28) Chan, P.; Gabay, M.; Wright, F. a; Kan, W.; Oner, S. S.; Lanier, S. M.; Smrcka, A. V; Blumer, J. B.; Tall, G. G. *J. Biol. Chem.* **2011**, *286*, 2625–2635.

(29) Nishimura, A.; Kitano, K.; Takasaki, J.; Taniguchi, M.; Mizuno, N.; Tago, K.; Hakoshima, T.; Itoh, H. *Proc. Natl. Acad. Sci.* **2010**, *107*, 13666–13671.

(30) Greentree, W. K.; Linder, M. E. *Methods Mol. Biol.* **2004**, *237*, 3–20.

(31) Adhikari, A.; Sprang, S. R. *J. Biol. Chem.* **2003**, *278*, 51825–51832.

(32) Peterson, Y. K.; Hazard, S.; Graber, S. G.; Lanier, S. M. *J. Biol. Chem.* **2002**, *277*, 6767–6770.

(33) Chan, P.; Gabay, M.; Wright, F. A.; Tall, G. G. *J. Biol. Chem.* **2011**, *286*, 19932–19942.

(34) Blank, J. L.; Ross, A. H.; Exton, J. H. *J. Biol. Chem.* **1991**, *266*, 18206–18216.

(35) Hepler, J. R.; Kozasa, T.; Smrcka, A. V; Simon, M. I.; Rhee, S. G.; Sternweis, P. C.; Gilman, A. G. *J. Biol. Chem.* **1993**, *268*, 14367–14375.

(36) Siehler, S. *Br. J. Pharmacol.* **2009**, *158*, 41–49.

(37) Singer, W. D.; Miller, R. T.; Sternweis, P. C. *J. Biol. Chem.* **1994**, *269*, 19796–19802.

(38) Ferguson, K. M.; Higashijima, T.; Smigel, M. D.; Gilman, a. G. *J. Biol. Chem.* **1986**, *261*, 7393–7399.

(39) Ferguson, K. M.; Higashijima, T. *Methods Enzymol.* **1991**, *195*, 188–192.

(40) Mahn, A.; Ismail, M. *J. Chromatogr. B Anal. Technol. Biomed. Life Sci.* **2011**, *879*, 3645–3648.

(41) Moore, P. A.; Kery, V. *Methods Mol. Biol.* **2009**, *498*, 309–314.

(42) Wittinghofer, A. *Curr. Biol.* **1997**, *7*, R682–R685.

(43) Zaima, K.; Deguchi, J.; Matsuno, Y.; Kaneda, T.; Hirasawa, Y.; Morita, H. *J. Nat. Med.* **2013**, *67*, 196–201.

(44) Bernard, M. L.; Peterson, Y. K.; Chung, P.; Jourdan, J.; Lanier, S. M. *J. Biol. Chem.* **2001**, *276*, 1585–1593.

Chapter 4: Optimization of Microelectrode Arrays with the Use of PEG-Functionalized Diblock Copolymer Coatings

NOTE: Part of this chapter has been published as Uppal, S., Graaf, M.D., Moeller, K.D. Microelectrode Arrays and the Use of PEG-Functionalized Diblock Copolymer Coatings. *Biosensors* 2014, 4, 318-328

4.1 Introduction

Guanine nucleotide exchange is an early event in the signal transduction cascade that can be monitored using an *in vitro* receptor-assisted [^{35}S] GTPS binding assay. As mentioned in **Chapter 3**, these assays work well with $G\alpha_q$ subunits. The receptor-assisted [^{35}S] GTPS binding assay is paramount because it provides information regarding the efficacy of the small molecules in their ability to inhibit the formation of $G\alpha_q$•GTPγS complex. However, there are several impediments associated with this assay if one wants to use it as a fast method to screen the potential for activity in newly synthesized molecules. First, these assays require expensive radiolabeled ligands which require proper disposal procedures (an added expense). Second, due to the slow spontaneous nucleotide exchange, $G\alpha_q$ subunits need a large number of accessory proteins (e.g. Sepia rhodopsin receptor and Gβγ subunits). Finally, the method requires washing steps that makes it difficult to observe the binding events which occur with weaker affinities. Therefore, we sought to develop an electrochemical means to detect and monitor binding events between G proteins and potential new ligands as the events happen. Microelectrode arrays have great potential for monitoring interactions between the members of a molecular library and biological receptors because every electrode in the array is individually addressable.[1–9] Hence, if

the molecules in a library are placed (or synthesized) on a microelectrode array such that each unique member of the library is located next to a unique, addressable set of electrodes, then each member of the array can be independently monitored by the electrodes. To this end, we wanted to utilize microelectrode arrays to probe binding interactions between G proteins and small molecule inhibitors. This approach would allow us to rapidly screen small molecules that can be shortlisted as G protein binders without the need for labeled receptors. Eventually, only small molecules that show an affinity for the G proteins being targeted will be characterized for their potency using biochemical assays.

4.1.1 Microelectrode arrays- Introduction

Microarrays can play an essential role in the high-throughput screening of biological molecules, and are playing an increasingly important role in the discovery of new drugs and biological probes.[10,11] Microarrays can be defined as a collection of microscopic features that can be probed with target molecules to obtain either quantitative or qualitative analyses.[12] These arrays can use multiple technologies to immobilize different library members onto them (e.g ink-jet printing,[13] photolithography,[14] printing onto glass slides[15]). Our group is interested in use of microelectrode arrays (obtained from Combimatrix, now known as CustomArray Inc., Bothell, WA) as platforms for building molecular libraries. CustomArray Inc. has been commercializing these arrays for diagnostic purposes (as DNA or antibody microarrays). Our interest is in using them to evaluate small molecule probes for receptors.

Two types of microelectrode arrays have been made available to us from CustomArray Inc. The first is an older design 1-K array that contains 1,024 electrodes per cm^2 (**Figure 4.1**). These arrays are no longer commercially available, but are excellent tools for developing new array-based synthetic methods. The second is a 12-K array that contains 12,544 electrodes per cm^2

(**Figure 4.2**). The 12-K arrays are commercially available, and can be used for analytical electrochemical experiments because of their cyclic voltammetry capabilities. In a 1-K array, the diameter of the round platinum electrode is 92 µm and the distance between the electrodes is 245.3 µm and 337.3 µm. In a 12-K array, the diameter of the round platinum electrode is 44 µm and the distance between the electrodes is 33 µm. Complementary metal-oxide-semiconductor (CMOS) technology is used to construct electrodes that are wired in parallel.[9] Both 1-K and 12-K arrays contain a binary addressable X, Y-grid of wires and the electrodes are addressed when both a vertical and a horizontal wire are activated at the same time. All experiments discussed in this dissertation were performed on the more modern 12-K arrays.

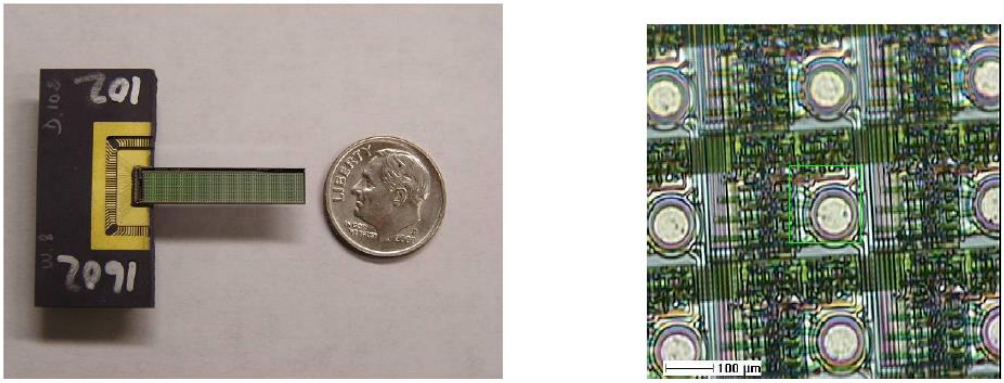

Figure 4.1. 1-K array (***left)***; zoomed image to show electrodes on the array (***right***).

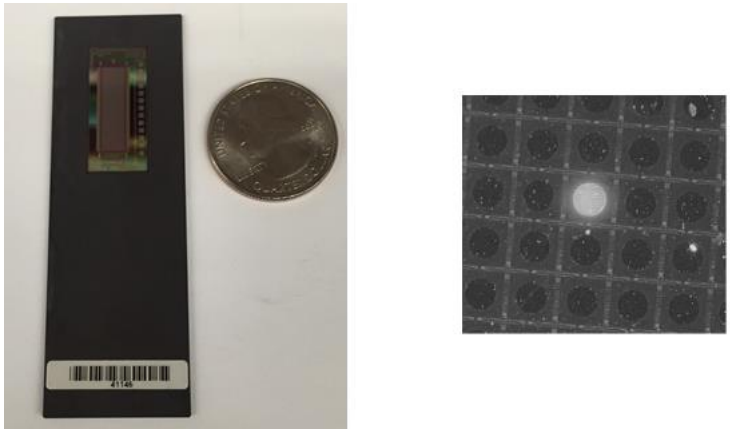

Figure 4.2. 12-K array (***left)***; zoomed image to show electrodes on the array (***right***).

In general, electrochemical reactions conducted on a 12-K array are no different from any other preparative electrolysis reaction. A basic electrochemical set up involves an anode (positive electrode that is used for oxidations), a cathode (negative electrode that is used for reductions), an electrolyte (used to reduce the resistance of the cell), and a solvent. Since the array re actions are indirect electrochemical reactions, they recycle chemical reagents at the electrodes. This allows the array reactions to take advantage of the chemical selectivity that has been built into modern synthetic methods. A computer program is used to control the reaction time, the potential of the electrodes in the array relative to a counter electrode, and select specific electrodes which are used for a reaction. In all reactions run on the array, the platinum electrodes in the array are used as the working electrodes, and a remote Pt-electrode is used as the counter electrode. For the 12-K arrays used in this thesis, the Pt-counter electrode has been sputtered onto the cap (known as hyb-cap, **Figure 4.3**) that fits over the array and provides the space for the reaction medium. Depending on the reaction of interest (oxidation or reduction), the working electrode in the array is either an anode or cathode by setting the potential of the electrode in the array either positive or negative relative to the cap. All of this is accomplished with the use of an

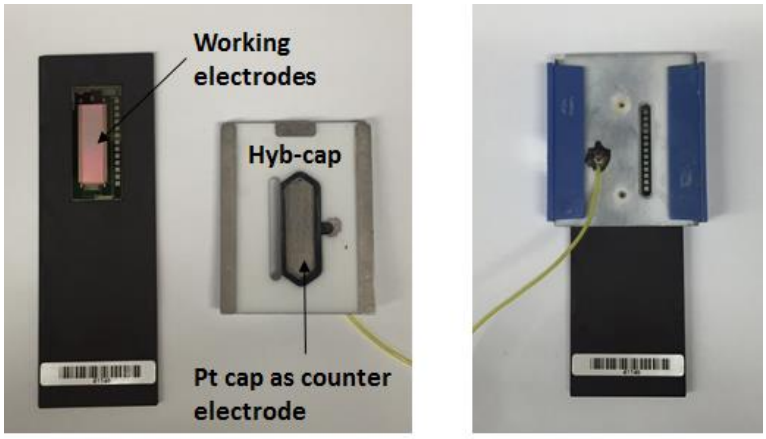

Figure 4.3. Hyb-cap as counter electrode for 12-K arrays.

ElectraSense reader that is also available through CustomArray Inc. The ElectraSense reader contains a series of addressable pins that make contact with conductive pads on the array that are wired to the electrodes.

There are certain criteria that must be met before we can monitor biological interactions on the arrays. First, the placement of the molecules onto the array must be confined to specific electrodes in the array so that the electrodes can be used to monitor their behavior. Substantial developments have been made by our lab toward the synthesis, placement, and characterization of molecules on the surface of a microelectrode array.[16–22] In fact, careful synthesis and manipulation of electrodes in addition to complete characterization of those molecules in terms of quality control assessment of the libraries synthesized is what sets the microelectrode arrays apart from its alternative methods.

4.1.2 Placing small molecules on the arrays

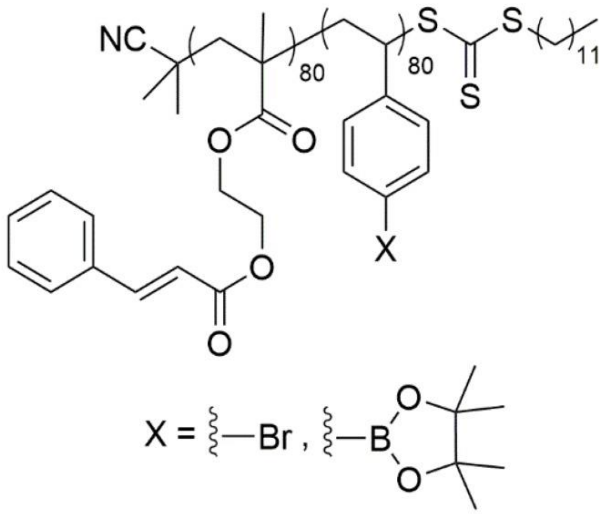

Figure 4.4. Diblock copolymers for coating arrays.

The placement of molecules onto the surface of an electrode in the arrays requires a stable, porous polymer coating on the electrode. This polymer provides the attachment points needed to fix molecules to the array proximal to the electrode, and insulates molecules on the surface from direct interactions with the electrode (an event that could interfere with a desired synthetic transformation).[23] The nature of the polymer is vital because it must be inert to the range of synthetic reagents used to build molecules on the array while porous enough to allow those reagents to reach the surface of the electrode below. In addition, the polymer must be stable over time so that the library on the array can be used multiple times, and it must be fully compatible with the analytical experiments to be conducted. To meet these needs, we have found diblock copolymers having the general structure described in **Figure 4.4** to be extremely effective. The polymers are comprised of one block of a cinnamate-functionalized methacrylate that is cross-linkable and used to impart stability to the surface, and one block of a functionalized polystyrene that is used as attachment points to fix molecules to the surface of the electrodes in the array. The resulting surfaces are stable and allow the use of nucleophiles, electrophiles, oxidants, reductants, acids, bases, and transition metal catalysts on the arrays. While the use of the diblock copolymer is ideal in many ways, it does force the use of an indirect method to detect binding events that occur on the surface of the array. Molecules bound to the surface of the polymer cannot be observed directly. Thus binding events on the array are monitored with the use of a solution phase redox couple.

4.1.3 Use of cyclic voltammetry (CV) to screen protein ligand interactions

Once molecules have been placed on the surface of the array, they can be analyzed for their affinity to a receptor of interest. This is done by taking advantage of cyclic voltammetry experiments on the array.[19,24] To this end, the functionalized array is treated with a solution

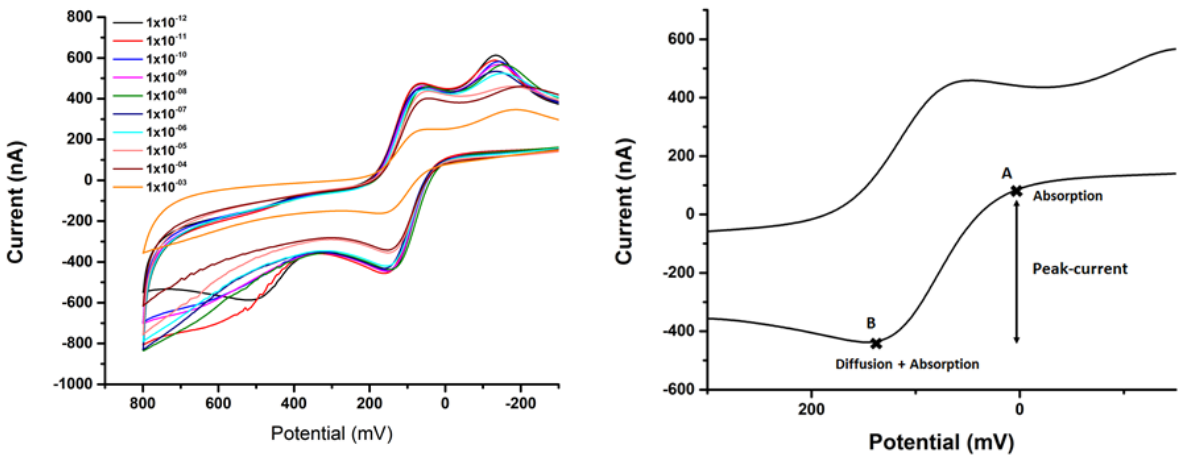

Figure 4.5. Overlapping CV scans with increasing concentration (legend in the figure, M) of protein depicting impedance of current (***left***); Anodic current for Fe^{2+} was measured by noting the difference between current at baseline (A) and the peak (B) (***right***).

phase redox couple (usually a Fe (II)/Fe (III) system). The functionalized electrodes on the array are then used as anode and the remote counter electrodes serve as cathode. The potential of the electrodes in the array is swept from low to high relative to the counter electrode and then back again. The current associated with the redox mediator is recorded at each potential. The height of the peak in the CV **(Figure 4.5**) is dependent on the amount of iron present based on adsorption to the surface and diffusion. The size of this current (known as a peak-current) is measured by noting the change in current between the baseline (**A** in **Figure 4.5)** and the peak (**B** in **Figure 4.5)**. A baseline peak-current is established for each experiment in the absence of the receptor. With the addition of the receptor to the solution above the array, a change in the peak-current (either a decrease due to impedance of the iron to the surface or an increase due to the improved conductance of the surface) indicates a binding event between the receptor and the surface of the electrode. The effect from impedance of current is often large and can be readily observed in the raw data collected. For example, the CV data for an impedance type experiment is shown in

Figure 4.5 (***left).*** Often in our binding experiments, we see impedance of current, and this type of behavior can be explained through a mechanism illustrated in **Figure 4.6**.[23,25,26]

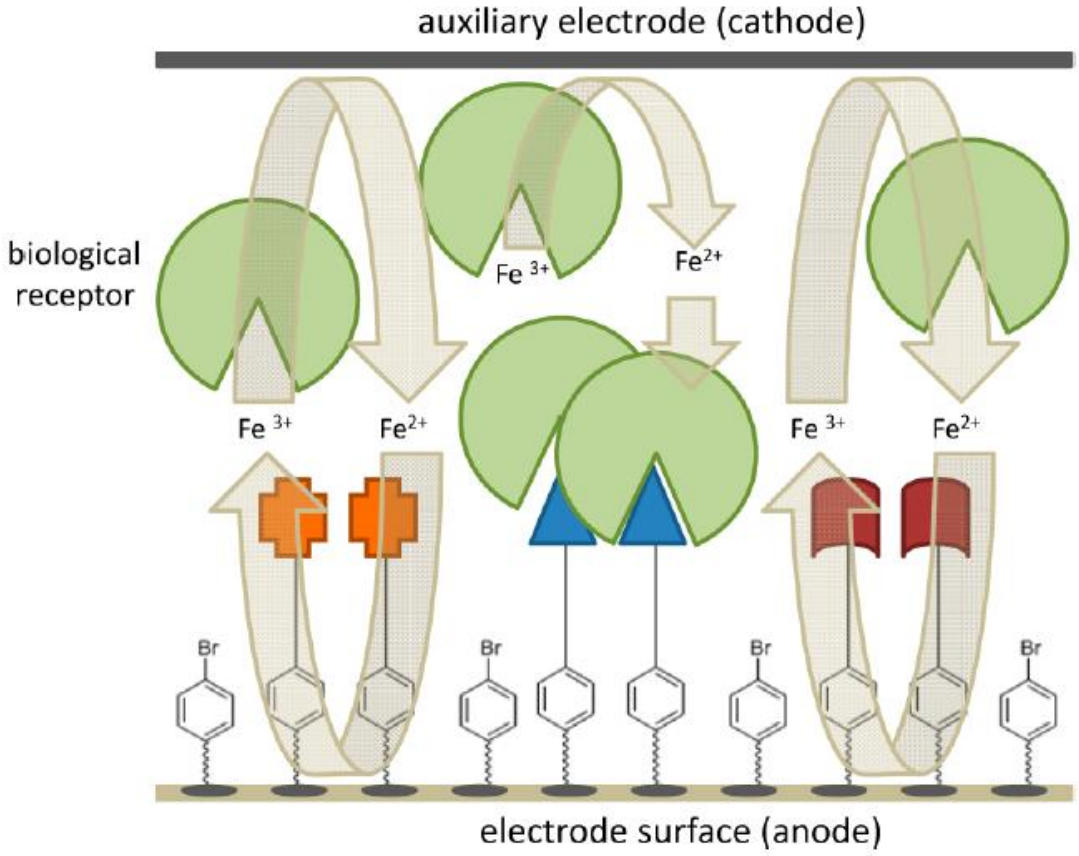

Figure 4.6. Impedance experiment on microelectrode array. Binding interaction between blue triangle representing the target molecule and the protein in solution denoted by green balls blocks the iron species from reaching the electrode surface. Figure obtained from Stuart-Fellet, M. *et al.* Site-selective chemistry and the attachment of peptides to the surface of a microelectrode array. *J. Am. Chem. Soc. 2012, 134, 16891–16898.*

4.1.4 Need for PEGylation of array surface

Our motivation for developing microelectrode arrays was envisioned to provide a rapid method for screening interactions between G proteins and their molecular binders. We intend to place simplified YM analogs onto the array surface and then monitor their binding interactions

with purified Gα subunits using cyclic voltammetry. But before we could start testing out these events, we needed to solve a challenge and that was the use of poly (ethylene glycol) (PEG)-polymer groups on the arrays. PEG-polymers are often suggested in connection with pacifying surfaces toward non-specific binding events with a variety of protein targets.[27-29] Many of our initial electrochemical studies looking at small molecule protein interactions on the arrays had shown significant background binding events,[25] so we hoped to utilize PEG-groups to at least mitigate this problem to an extent. In addition, the immobilization of small molecules directly onto the array surface can hinder its binding properties to the protein because of steric issues. Hence, in order to ensure that the immobilized molecule is in proper conformation, orientation and accessible to the protein, attachment of the molecule away from the surface via a linker or spacer arm is recommended.[27,28] PEG-based linkers are a popular choice because of their desirable physical and chemical properties (such as hydrophilic, non-toxic, low rate of degradation by biomolecules).[27–31] For this reason, we hoped to use them in connection with our small molecule-G protein binding studies as well.

However, Dr. Libo Hu in our group had found that modifying the surface of the diblock copolymer with the PEG-polymer groups led to problems with the subsequent cyclic voltammetry experiments. In those experiments, the peak-current for the iron redox mediator steadily increased over time. The PEG groups appeared to be binding the iron thereby steadily increase the amount of the mediator adsorbed onto the surface of the array. And as a result, a baseline peak-current could not be established, and the effort was initially abandoned.

But was the issue really a “lost-cause”, or was there a way to get around the problem and utilize groups on the arrays anyway? This chapter will focus on strategies that allow for the use of PEG-functionalized diblock copolymer coatings on microelectrode arrays. All experiments

described in this chapter were carried out using bovine serum albumin (BSA) as the protein with a relatively high affinity for diblock copolymer coated arrays.

4.2 Results and discussion

4.2.1 PEGylation of polymer coated array

In order to functionalize the polymer coated arrays with PEG groups, a microelectrode array was spin coated with PCEMA-b-pBSt (**Figure 4.4**, X = Bpin), photolyzed to crosslink the cinnamate esters and add stability to the surface, and then functionalized with a PEG-polymer having 16 repeating units and a methyl ether on one end (PEG-16). The chemistry took advantage of the Chan-Lam coupling method previously developed to place alcohols on the surface of the array above the electrodes.[32] In this reaction, a Cu(II)-PEG complex undergoes an electrophilic substitution on the aromatic ring that exchanges the borate ester for Cu(II)-PEG. A reductive elimination then couples the PEG to the aryl ring. The electrode is then used to regenerate the Cu(II)-catalyst.

The success of this reaction was demonstrated by showing that the addition of PEG-polymer groups decreased the water contact angle of the surface from 78.3^0 to 55.1^0 (sessile drop technique).[33,23] In this experiment, a drop of water is placed on a surface and then the contact angle between the surface and the water droplet is measured (Drop analysis, Image J software) to determine the hydrophobicity of the surface. The decrease in contact angle indicates that the functionalized surface is now more hydrophilic.

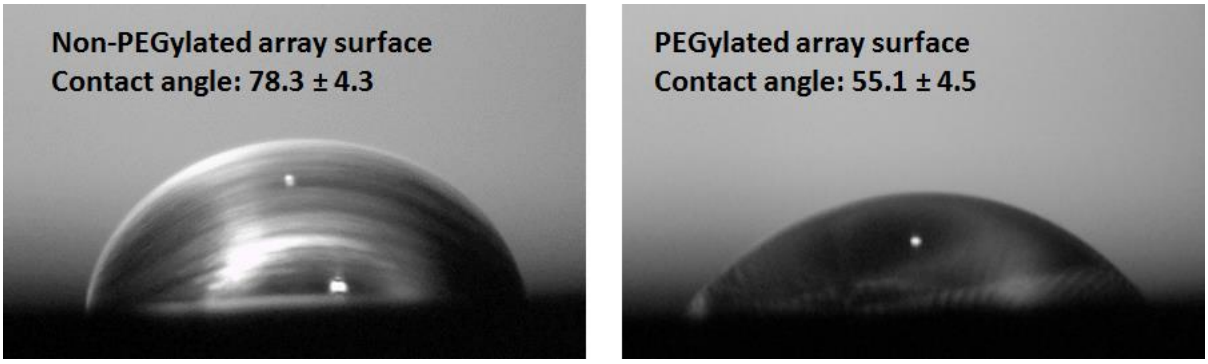

Figure 4.7. Sessile drop technique. Water droplet was placed on a non-PEGylated array surface (***left)*** and a PEG-functionalized array surface (***right)***. Contact angle measurements were made on three independent drops and data represents mean (±standard deviation).

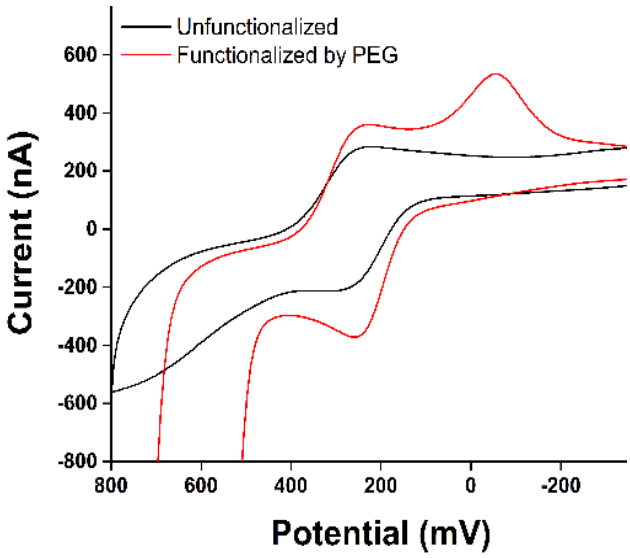

Figure 4.8. CV for ferrocene carboxylic acid (FCA) with the PEG-functionalized polymer (***red line***) and unfunctionalized polymer (***black line***).

In addition, functionalization of the diblock copolymer with PEG-16 led to an increase in the magnitude of the current measured for the redox mediator (ferrocene carboxylic acid, FCA) and

a change in the overall shape of the wave relative to that obtained with the non-PEG-functionalized surface (**Figure 4.8**). Both observations can be explained by the change in the nature of the polymer caused by the incorporation of the hydrophilic PEG-16 group. The more hydrophilic polymer swells better in water, a situation that allows higher adsorption of the iron species into the polymer leading to a higher peak-current. This increase in peak-current is beneficial for the subsequent binding experiments because it makes it easier to detect changes in the current when binding events occur on the surface of the electrode.

4.2.2 Ferrocene carboxylic acid (FCA), a new redox mediator for CV studies on PEG-functionalized arrays

Most of our early work with block copolymers utilized a bromine substituted polystyrene block (**Figure 4.4, X = Br**) to attach molecules to the array. Dr. Libo Hu had modified this polymer with PEG-groups to perform studies described in the introduction. The ferricyanide/ferrrocyanide couple has been used most frequently in connection with this polymer.[19,23,25] While the use of the bromostyrene based polymer was effective, a desire to build tunable surfaces on the arrays led to the development of a diblock copolymer that contained a borate ester substituted polystyrene block (**Figure 4.4, X = Bpin**). While this new polymer offered numerous synthetic advantageous, the use of the borate ester on the array initially led to the same issues during subsequent cyclic voltammetry studies that we had seen in the original PEG-functionalized surface studies. Namely, the surface appeared to adsorb iron during the CV experiment, and the current measured for a ferricyanide redox mediator on an array coated with the borate ester polymer was not stable.[23] Fortunately, it was discovered that this drift on the borate ester surface stabilized with time. Would this also be true for a PEGylated surface?

As part of the effort to address this question, we decided to study the use of a second redox mediator on the arrays in addition to the ferricyanide/ferrocyanide used in most of our previous studies. We hoped that switching the redox mediator to one based on the highly reversible and stable ferrocene/ferrocenium redox couple, FCA would reduce the adsorption of iron by the surface. The use of the carboxylic acid-functionalized version of ferrocene (**Figure 4.9**) was due to its increased water solubility, a major factor in FCA being selected for use in numerous other electrochemical biosensors.[34,35]

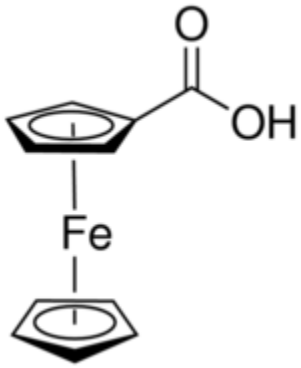

Figure 4.9. Ferrocene carboxylic acid (FCA).

Before discussing the specific experiments, it is essential to note that a CV obtained using the arrays is not a "normal" CV with a reference electrode. Instead, the CV registers the relative potential drop across the cell that leads to the current flow and thus, the potentials measured on an array cannot be compared to literature potentials measured with reference electrodes. In fact, the potential at which the signal is observed can drift from experiment to experiment depending on the overall resistance of the cell. Hence, it is essential not to 'read' into changes along the X-axis of the CVs recorded.

The first experiment attempted examined whether the currents measured on the PEG-functionalized surface would stabilize over time, and if so, which mediator would serve best in this capacity. To test this, two microelectrode arrays were coated with the borate ester diblock copolymer and then functionalized by every electrode with PEG-16. The functionalized array was then covered with a buffer solution containing either ferricyanide or FCA with potassium nitrate as the electrolyte. The current measured for a series of 50 CV experiments using either the ferrocyanide based or FCA based mediator (**Figure 4.10**). The data quickly showed that the use

of the FCA mediator did lead to a stabilization of the current at a much faster rate than was observed with the ferrocyanide mediator. The peak-current for both experiments did eventually stabilize.

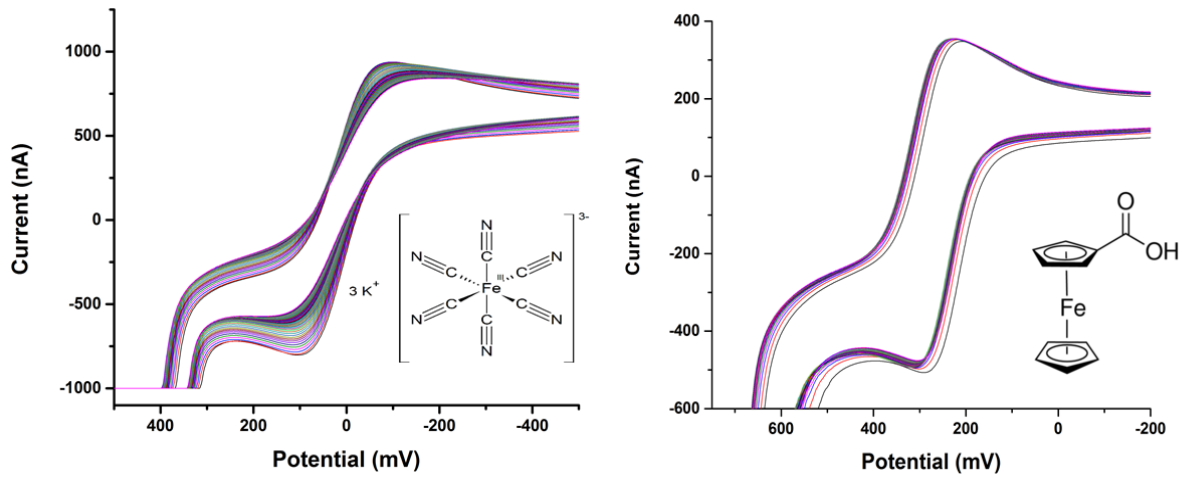

Figure 4.10. CV scans (1-50) obtained from PEG-functionalized array surface. Ferricyanide (***left)*** and FCA ***(right)*** used as a redox mediator.

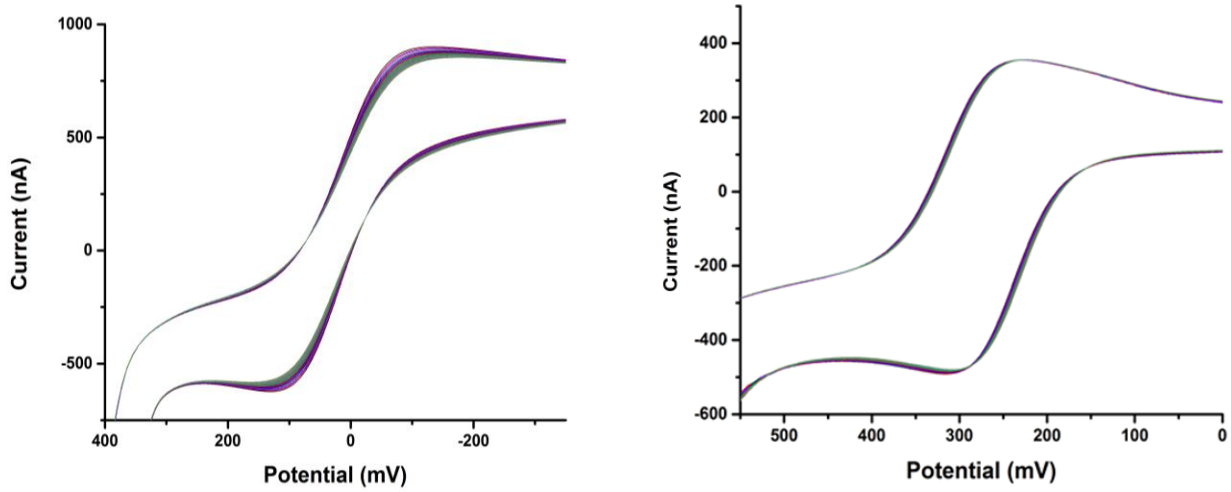

Figure 4.11. CV scans (20-40) obtained from PEG-functionalized array surface. Ferricyanide (***left)*** and FCA ***(right)*** used as a redox mediator.

With the use of FCA, the peak-current stabilized after approximately 20 CV scans. The superiority of the FCA experiment can be further seen by examining scans 20-40 for a pair of CV experiments that were run out to 64 scans (**Figure 4.11**). Again, the true reproducibility of the data obtained with FCA can be clearly seen. Based on this finding, all of the studies discussed below were conducted with FCA as the redox mediator.

4.2.3 BSA non-specific binding study on the PEG-functionalized array surface

Once a baseline peak-current was established, the PEG-functionalized array and the CV strategy forwarded above was examined for its compatibility with CV-based binding studies. For this experiment, non-specific binding of BSA to the polymer coating on the array was studied. Hence an array coated with PEG-16 modified diblock copolymer was incubated in a 1 picomolar (pM) solution of BSA in HEPES buffer containing FCA and potassium nitrate as an electrolyte. A block of twelve electrodes on the array was used to collect CV data for FCA. In the first trial, 30 CVs were run in order to make sure that the anodic current for the oxidation of iron (Fe^{2+}) was stabilized. This procedure was repeated using two additional blocks of twelve electrodes. The current obtained from each of the three blocks of electrodes was then averaged and recorded with the spread in the data determining the error bars used for the point. Following the experiment with 1 pM BSA, the array was washed three times with an electrolyte solution that contained 10 pM BSA. The CV experiment was then repeated in triplicate using a new concentration of BSA. Again, the peak-current was measured after 30 CV scans. This procedure was then repeated each time increasing the concentration of the protein in solution by a factor of ten. The experiment was stopped at 1 mM BSA. The data obtained was then plotted on a chart that compared the relative current change to the concentration of BSA in solution (**Figure 4.12**). The data in the chart was normalized by assigning the highest peak-current measured on the

array a value of zero (drops in the current are all relative numbers) and the lowest peak-current on the array a value of one. In this way, larger percent changes in the graph relate to greater binding of BSA to the surface. As indicated above, the error bars shown in **Figure 4.12** show the spread in the data recorded at three separate sites on the array for each concentration of BSA. This variance in the data was small relative to the total drop in current. Hence, we concluded that the surface of the array did have the uniformity necessary for the analytical experiment.

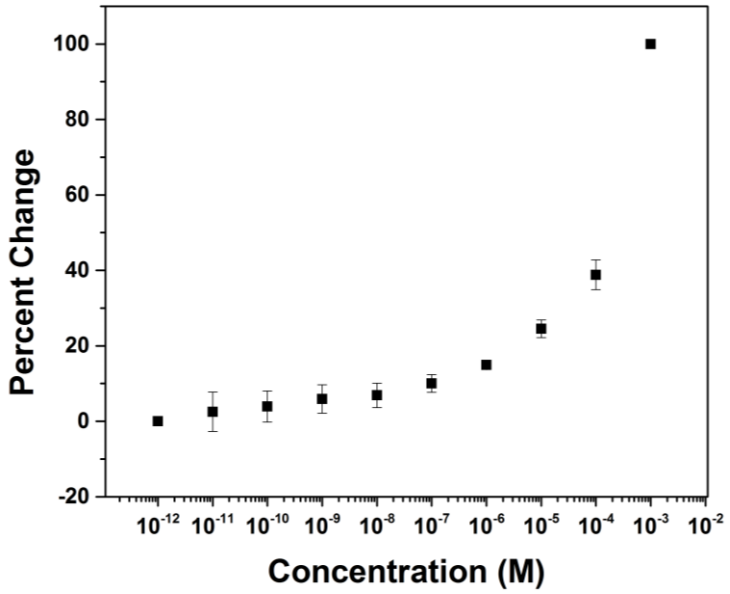

Figure 4.12. Curve for the non-specific binding of BSA to an array coated with a PEG-functionalized array using 30th CV scan. The curve represents normalized data (mean ± SD, n=3).

The evidence showing the PEG-16-functionalized polymer to be compatible with the CV experiments led to two immediate questions. First, do we need to collect 30 CV scans in order to get a binding profile for the non-specific binding? In other words is the rate of change initially associated with the adsorption of iron equal to the rate of change after stabilization? If so, then the experiment can be conducted without waiting for the 30 CV scans as long as each experiment

is run at the same time point. Second, did the presence of the PEG pacify the surface at all, and if so would a longer PEG polymer be better or worse?

4.2.4 Comparison of binding profiles before and after current stabilization

As mentioned, the binding profile described in **Figure 4.12** was obtained using the 30th CV scan after the current had stabilized. This is potentially problematic because waiting for the current to stabilize increases the overall time of the experiment. The can be an issue with protein stability. So did we have to wait, or would the rate of change be consistent enough for us to conduct experiments prior to complete stabilization? The answer to latter question was yes. The experiment illustrated in **Figure 4.13** compared the non-specific binding of BSA to the PEGylated surface for three different experiments. In one (a repeat of **Figure 4.12**), the peak-current used to generate the graph was taken from the 30th CV scan at each concentration of BSA. Again, this was to make sure that the system would be fully equilibrated and current was stable. In the second, the peak current for the 10th CV scan at each concentration of BSA was used to generate the binding profile. In the third, the current for the 1st CV scan at each concentration of BSA was used. The goal of this experiment was to determine if the drift in current could be completely ignored. While the raw CV data in the three experiments did vary significantly, the change in that data relative to the amount of BSA present did not. All three experiments generated the same binding curve for non-specific binding of BSA to the PEGylated surface. Since the initial change in current occurs at a consistent rate, the same overall binding data can be obtained at any time point as long as the same time point is used. However, this generalization might not be applicable to all protein studies. Hence, for future studies, a similar experiment would be repeated to check if it is necessary to conduct 30 CV scans for each concentration before recording the data.

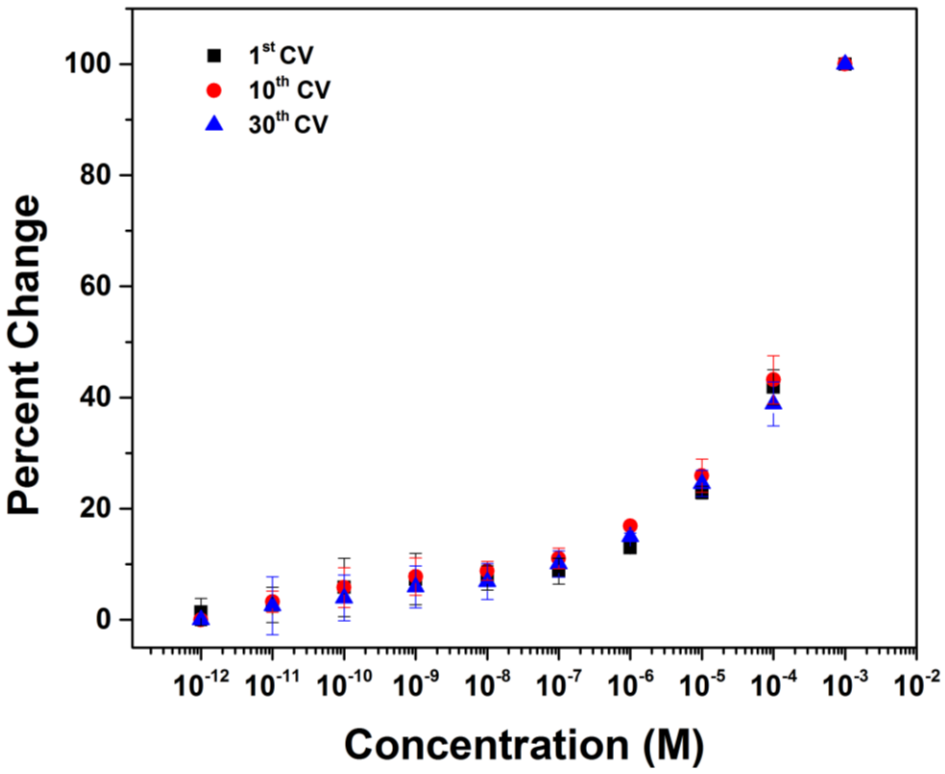

Figure 4.13. BSA non-specific binding experiment. Binding curves generated at different time points.

4.2.5 PEG-functionalized array surface reduces non-specific binding of BSA

The second question about pacification of the surface and the use of longer PEG-polymers was asked because longer PEG polymers are often superior in terms of pacifying a surface toward non-specific binding events.[29] To test the idea, an array coated with the borate ester diblock copolymer was functionalized with a PEG mono methyl ether that was made of 40 repeat units (PEG-40). The experiment to measure non-specific binding events on the surface was repeated using the exact same protocol used for the PEG-16 modified surface. The data was plotted along with the data obtained with the PEG-16 surface and the data obtained for a non-

PEGylated surface (**Figure 4.14)**. The binding experiment with the PEG-40-modified polymer-coated array worked very well. The shape of the curve for the non-specific binding of BSA to this surface (red dots) was nearly identical to the curve obtained with either the PEG-16-modified polymer (green squares) or the unmodified system (blue triangles). However, the surface functionalized with the PEG-40-modified polymer showed lower non-specific binding than did the other alternatives. Note how at each concentration of BSA greater than 10^{-7} M, the relative change for the PEG-40 modified problem was significantly smaller than the other two curves. In this way, the use of the longer PEG was not only compatible with the experiment, but also more successful in pacifying the surface to non-specific interactions with BSA.

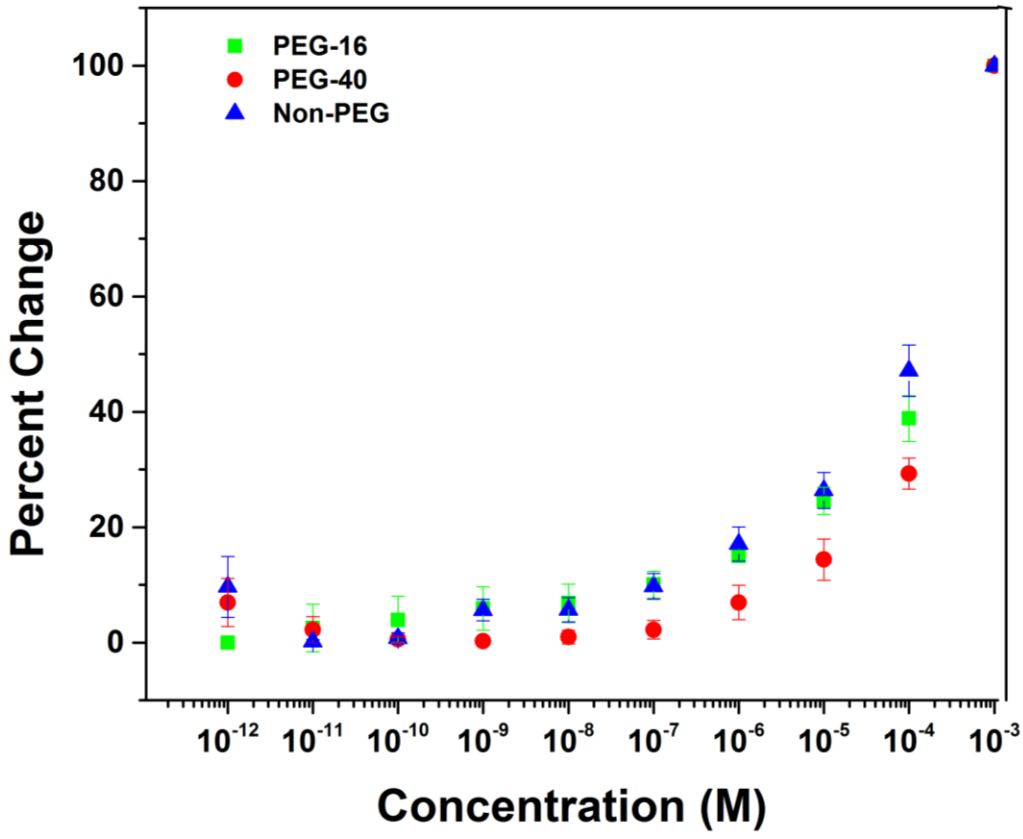

Figure 4.14. Comparison of polymer-coated array surface functionalized with different lengths of PEG.

At this time, the exact origin of the difference between the PEG-16 and the PEG-40 is not known. It might be that the greater pacification of the surface with PEG-40 is simply due to its larger size. Alternatively, the greater suppression of background binding may be due to better surface coverage of the electrode. Currently, we do not have an accurate assessment of surface coverage for the two polymers. In principle, this can be done by placing the PEG-oligomers on the surface of the array and then using the same chemistry to place small fluorescent probes on the surface. The extent of fluorescence would give an approximation of how much surface area the PEG-oligomer covered.

4.3 Conclusions

PEG-modified diblock copolymer coated microelectrode arrays can be used in analytical experiments that monitor the current associated with an iron redox couple as long as the experiments are conducted at a consistent point in time. That point in time can be the first CV scan taken, a scenario that minimizes the overall time required for conducting an analysis. These findings open the door for the use of PEG-polymers on microelectrode arrays for reduction of non-specific binding of proteins and as linkers. **Chapter 5** of this dissertation will focus on binding studies carried out by purified Gα subunits.

4.4 Experimental section

Unless noted otherwise, all chemicals were ordered from Sigma Aldrich (St. Louis, MO). All other vendor information is noted in the experimental section. The ElectraSense® reader and 12-K microelectrode arrays can be purchased from CustomArray,Inc. (Bothell, WA). The microelectrode arrays (containing 12,544 electrodes/cm^2) were spin-coated using a MODEL

WS-400B-6NPP/LITE spin-coater (Laurell Technologies Corporation, North Wales, PA). For voltammetric measurements, the reader is used to activate selected electrodes on the array and an external BAS 100B/W potentiostat controls the potential sweep and records the currents measured.

4.4.1 Procedure for coating arrays with block copolymer

The diblock copolymer Polycinnamoyloxy ethyl methacrylate-b-poly-4-pinacolatoborylstyrene (PCEMA-b-pBSt, **Figure 4.4, X = Bpin**) was prepared by Matthew Graaf as previously reported.[23] Three drops of 0.03 g/mL block copolymer solution (PCEMA-b-pBSt in 4:1.5 DMF/THF) were placed on the array making sure that the entire electrode area of the array was covered. The array was then spun at 800 rpm for 40 secs. The block copolymer coating was allowed to dry for 15 min and then cross-linked using a 100 W mercury lamp for 15 min before use.

4.4.2 PEGylation of PCEMA-b-pBSt polymer using Chan-Lam coupling on arrays

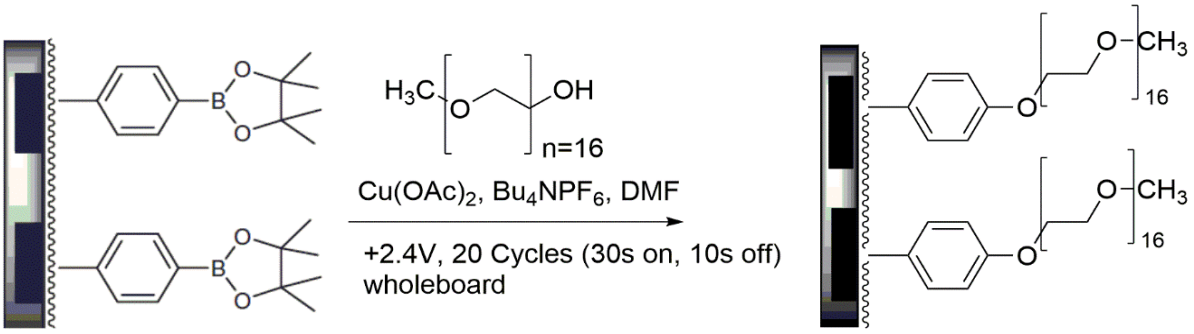

Scheme 4.1. Chan-Lam type coupling reaction on a microelectrode array.

The following procedure was adapted from the known Chan-Lam coupling.[23,32] Poly (ethylene glycol) methyl ether-750 (10.0 mg) and 50.0 mg of tetrabutylammonium hexafluorophosphate were dissolved in 1.0 mL of DMF. To this solution, 50.0 µL of a 25 mM copper(II) acetate in water solution was added. The contents were mixed, and then 120 µL of this solution was added to the array. The array was placed into an ElectraSense reader and all 12,544 electrodes selected and used as anodes. A potential of +2.4 V relative to the auxiliary electrode was used to pulse the electrodes for 20 cycles of 30 s on and 10 s off. After completion of reaction, the array was washed extensively (~5-7 mL) with 95% ethanol.

4.4.3 Contact angle measurements

Contact angles were measured with the sessile drop technique.[33] Pictures were taken from a Nikon camera equipped with a microlens (Dr. Joshua Maurer). Contact angles measurements were made using drop analysis (Image J software, Bethesda, MD).

4.4.4 General procedure for conducting CV experiments on a 12-K array

CV was carried out on a BAS 100B Electrochemical Analyzer potentiostat (BAS 100W version 2.31 control software). A 12-K microelectrode array was cleaned with Nano-strip (Cyantek Corporation, Fremont, CA) and spin coated with the block copolymer solution as described in **Section 4.4.1**. The cross-linked polymer was then functionalized next to the electrodes as described previously.[24] An iron solution (120 µL/ either 5 mM ferrocene carboxylic acid or 8 mM ferrocyanide and 8 mM ferricyanide) in 20 mM HEPES, pH 8.0 with 0.1 M potassium nitrate that contained a predetermined concentration of BSA was added onto the PEG-functionalized array. The array was then placed in an ElectraSense reader and one block of 12 electrodes was activated. CV measurements were made by sweeping the potential at selected

electrodes on an array from −800 to 800 mV at a scan rate of 400 mV/s. The potential in these experiments refers to the difference in potential of the working electrode relative to the counter electrode; a platinum plate of area 0.75 cm^2 located approximately 650–800 μm away from the array with an O-ring. Each experiment was conducted at three independent blocks of 12 electrodes each chosen randomly from different areas of the array. After the measurement was made for a concentration of BSA in solution, the array was washed with the next concentration of BSA by injecting and withdrawing the solution three times. Detailed protocols on operating the microelectrode arrays have been published.[25]

4.5 References

(1) Sullivan, M. G.; Utomo, H.; Fagan, P. J.; Ward, M. D. *Anal. Chem.* **1999**, *71*, 4369–4375.

(2) Zhang, S.; Zhao, H.; John, R. *Anal. Chim. Acta* **2000**, *421*, 175–187.

(3) Hintsche, R.; Albers, J.; Bernt, H.; Eder, A. *Electroanalysis* **2000**, *12*, 660–665.

(4) Gardner, R. D.; Zhou, A.; Zufelt, N. A. *Sensors Actuators, B Chem.* **2009**, *136*, 177–185.

(5) Beyer, M.; Nesterov, A.; Block, I.; König, K.; Felgenhauer, T.; Fernandez, S.; Leibe, K.; Torralba, G.; Hausmann, M.; Trunk, U.; Lindenstruth, V.; Bischoff, F. R.; Stadler, V.; Breitling, F. *Science* **2007**, *318*, 1888.

(6) Devaraj, N. K.; Dinolfo, P. H.; Chidsey, C. E. D.; Collman, J. P. *J. Am. Chem. Soc.* **2006**, *128*, 1794–1795.

(7) Wassum, K. M.; Tolosa, V. M.; Wang, J.; Walker, E.; Monbouquette, H. G.; Maidment, N. T. *Sensors* **2008**, *8*, 5023–5036.

(8) Zhang, Y.; Wang, H.; Nie, J.; Zhang, Y.; Shen, G.; Yu, R. *Biosens. Bioelectron.* **2009**, *25*, 34–40.

(9) Maurer, K.; Yazvenko, N.; Wilmoth, J.; Cooper, J.; Lyon, W.; Danley, D. *Sensors* **2010**, *10*, 7371–7385.

(10) Cooper, C. S. *Breast Cancer Res.* **2001**, *3*, 158–175.

(11) Koch, M.; Wiese, M. *Curr. Pharm. Des.* **2013**, *19*, 790–805.

(12) Miller, M. B.; Tang, Y.-W. *Clin. Microbiol. Rev.* **2009**, *22*, 611–633.

(13) McWilliam, I.; Kwan, M. C.; Hall, D. *Methods Mol. Biol.* **2011**, *785*, 345–361.

(14) Beier, M.; Hoheisel, J. D. *Nucleic Acids Res.* **2000**, *28*, E11.

(15) Wang, J.; Bai, Y.; Li, T.; Lu, Z. *J. Biochem. Biophys. Methods* **2003**, *55*, 215–232.

(16) Tanabe, T.; Bi, B.; Hu, L.; Maurer, K.; Moeller, K. D. *Langmuir* **2012**, *28*, 1689–1693.

(17) Tian, J.; Maurer, K.; Tesfu, E.; Moeller, K. D. *J. Am. Chem. Soc.* **2005**, *127*, 1392–1393.

(18) Tesfu, E.; Maurer, K.; Ragsdale, S. R.; Moeller, K. D. *J. Am. Chem. Soc.* **2004**, *126*, 6212–6213.

(19) Bartels, J. L.; Lu, P.; Maurer, K.; Walker, A.; Moeller, K. D. *Langmuir* **2011**, *27*, 11199–11205.

(20) Bi, B.; Huang, R. Y. C.; Maurer, K.; Chen, C.; Moeller, K. D. *J. Org. Chem.* **2011**, *76*, 9053–9059.

(21) Hu, L.; Stuart, M.; Tian, J.; Maurer, K.; Moeller, K. D. *J. Am. Chem. Soc.* **2010**, *132*, 16610–16616.

(22) Bi, B.; Maurer, K.; Moeller, K. D. *J. Am. Chem. Soc.* **2010**, *132*, 17405–17407.

(23) Hu, L.; Graaf, M. D.; Moeller, K. D. *J. Electrochem. Soc.* **2013**, *160*, G3020–G3029.

(24) Moeller, K. D. *Organometallics* **2014**, *33*, 4607–4616.

(25) Fellet, M. S.; Bartels, J. L.; Bi, B.; Moeller, K. D. *J. Am. Chem. Soc.* **2012**, *134*, 16891–16898.

(26) Uppal, S.; Graaf, M.; Moeller, K. *Biosensors* **2014**, *4*, 318–328.

(27) Sato, S. ichi; Murata, A.; Shirakawa, T.; Uesugi, M. *Chemistry and Biology*, **2010**, *17*, 616–623.

(28) Chen, H.; Chen, Y.; Sheardown, H.; Brook, M. A. *Biomaterials* **2005**, *26*, 7418–7424.

(29) Michel, R.; Pasche, S.; Textor, M.; Castner, D. G. *Langmuir* **2005**, *21*, 12327–12332.

(30) Piehler, J.; Brecht, a; Valiokas, R.; Liedberg, B.; Gauglitz, G. *Biosens. Bioelectron.* **2000**, *15*, 473–481.

(31) VandeVondele, S.; Vörös, J.; Hubbell, J. A. *Biotechnol. Bioeng.* **2003**, *82*, 784–790.

(32) Sanjeeva Rao, K.; Wu, T.-S. *Tetrahedron* **2012**, *68*, 7735–7754.

(33) Dimitrov, A. .; Kralchevsky, P. .; Nikolov, A. .; Noshi, H.; Matsumoto, M. *Journal of Colloid and Interface Science*, **1991**, *145*, 279–282.

(34) Boztas, A. O.; Guiseppi-Elie, A. *Biomacromolecules* **2009**, *10*, 2135–2143.

(35) Bartlett, P. N.; Pratt, K. F. E. *Journal of Electroanalytical Chemistry*, **1995**, *397*, 53–60.

Chapter 5: Testing G protein Compatibility Towards Microelectrode Arrays

5.1 Introduction

In **Chapter 4**, the PEGylation of microelectrode array surface was discussed as an approach to reduce non-specific binding between proteins and the array. In addition, the compatibility of PEG groups with the analytical studies on the arrays provides an opportunity for the utilization of PEG-based linkers. Prior to screening small molecules for their binding interactions with purified Gα subunits, it is essential to examine whether the electroanalytical approach is compatible with the G proteins. Does binding of the protein to the surface of the array alter the capacitance of the surface? Is the protein inert to the iron species used as the mediator in the reactions? In order to answer these questions and further develop the analytical capabilities of the arrays so they can be used to study G protein interactions, the work described in this chapter was dedicated towards determining the non-specific binding of G proteins to the surfaces used on the arrays, and demonstrating that we can see a known interaction between a short peptide and a G protein above the background signal using the arrays. To this end, we have shown the capabilities of the arrays for detecting in real-time the binding of the peptide R6A to $G\alpha_{i1}$.

5.1.1 Use of purified $G\alpha_{i1}$ for background experiments

As mentioned in **Chapter 2**, both $G\alpha_{i1}$ and $G\alpha_o$ can be easily expressed and purified from *E.coli* (in comparison to insect cells) in large quantities. Therefore, we wanted to perform the background control experiments using one of these two, much more readily available proteins. Using CLUSTALW2 sequence alignment software (The European Bioinformatics Institute

(EMBL-EBI), Cambridge, UK), we found that $G\alpha_{i1}$ exhibits ~55% homology to $G\alpha_q$ making this protein a desirable candidate to perform optimization studies on the arrays (**Table 5.1** shows homology results from sequence alignment). For our future studies, we hope to use the arrays to evaluate the selectivity of YM analogs for a series of G proteins, one of which will be $G\alpha_{i1}$. Hence, this protein was selected for our initial study. The effort began with an assessment of the non-specific binding of $G\alpha_{i1}$ to the PCEMA-b-pBSt-polymer-coated array, and the influence coating the surface with PEG might have.

Table 5.1. CLUSTAL 2.1 sequence alignment summary.

Seq A	Name	Length	Seq B	Name	Length	Score
1	$G\alpha_o$	354	2	$G\alpha_{i1}$	354	72.32
1	$G\alpha_o$	354	3	$G\alpha_q$	353	52.69
2	$G\alpha_{i1}$	354	3	$G\alpha_q$	353	55.52

5.1.2 Testing specific binding of $G\alpha_{i1}$ to small molecules

In order to test the capability of the arrays to monitor small molecule-G protein interactions, we needed to pair $G\alpha_{i1}$ with a small molecule that it is known to bind with. In general, short peptides have been used extensively to either activate or antagonize G proteins.[1–4] A polypeptide found at the C-terminus of the AGS3 protein is known to specifically bind to the $G\alpha_i$ class of G proteins and slow its ability to spontaneously exchange nucleotides. We have already introduced this 28 amino acid long peptide in **Chapter 3** so we knew that it binds to our purified $G\alpha_{i1}$. This AGS3-derived peptide is known to bind $G\alpha_{i1}$ with micromolar affinity (K_D = ~1μM)[5] and inhibit GDP-GTP exchange in a manner similar to that of YM blocking the interdomain movement in

$G\alpha_q$.[5,6] In addition, another peptide known as R6A was identified that exhibits high affinity (K_D = 60 nM) towards $G\alpha_{i1}$.[7] Based on this data, we selected AGS3 and R6A as peptide ligands for $G\alpha_{i1}$ in our array based studies.

5.2 Results and discussion

5.2.1 $G\alpha_{i1}$ non-specifically binds to the PCEMA-b-pBSt polymer-coated array

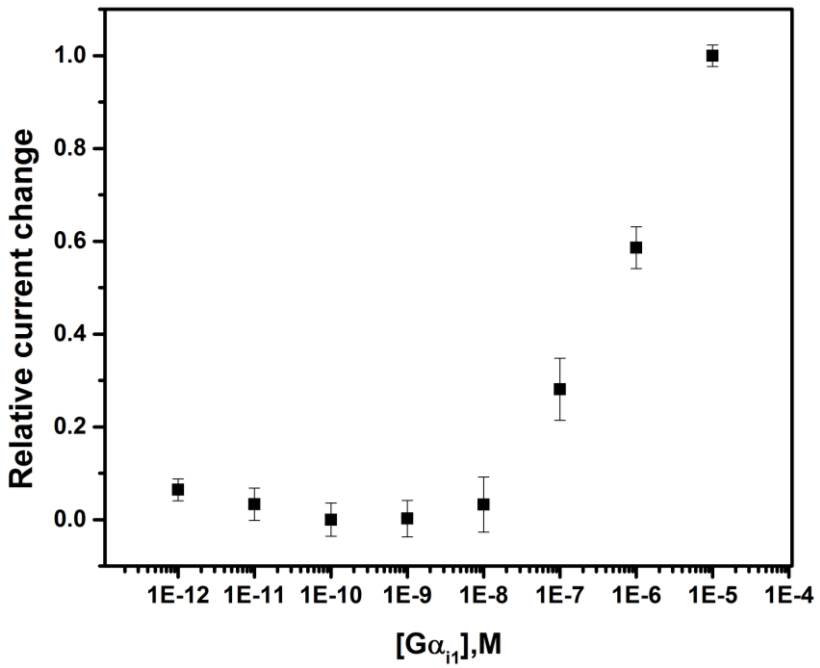

Figure 5.1. Non-specific binding of $G\alpha_{i1}$ on PCEMA-b-pBSt polymer-coated array.

In order to examine the behavior of $G\alpha_{i1}$ towards the polymer-coated microelectrode arrays, an electroanalytical signaling experiment was conducted. To this end, a microelectrode array was spin coated with the PCEMA-b-pBSt polymer and a set of CV experiments were conducted using increasing concentrations of $G\alpha_{i1}$. These experiments were similar to the ones carried out in connection with the non-specific binding of BSA to the arrays discussed in **Chapter 4**. Data

from 3rd CV taken at each concentration was analyzed to obtain a peak-current that was in turn plotted with respect to the concentration of $G\alpha_{i1}$ in the solution above the array. The data in **Figure 5.1** represents the average of the peak-current measured at three different sites on the array. The average peak-current was plotted as a percent change based on a normalized curve with the highest current being measured given a value of zero and the lowest current measured a value of one. The standard deviation of the relative change for the three sites on the array at each protein concentration provides the error bars shown in the figure. As visible from the data in **Figure 5.1**, a non-specific binding interaction between the protein and the surface of the array did occur starting with a protein concentration of around 10^{-8} M. In other words, $G\alpha_{i1}$ starts adsorbing on the polymer surface after 10^{-8} M (~30 % binding based on the data provided). This is a significant amount of non-specific binding that we hoped to reduce by the addition of PEG groups to the polymer.

5.2.2 PEG-modification of polymer did not reduce non-specific binding of $G\alpha_{i1}$

The attempt to minimize the non-specific binding event shown in **Figure 5.1** utilized the PEG-40 group that had proven effective in connection with the previous BSA binding studies. In the experiment, half of the electrodes (top half of array) on a PCEMA-b-pBSt polymer-coated array were functionalized with the PEG-40 polymer. The lower half was left unfunctionalized. The array was then incubated with varying concentrations of $G\alpha_{i1}$ and then in each case CVs were obtained for each concentration at selected blocks (four blocks each for the PEG-40 functionalized surface and for a set of unfunctionalized control blocks). The peak-current was assessed after three CV scans at each concentration of the receptor. The raw CV data is shown in **Figure 5.2**.

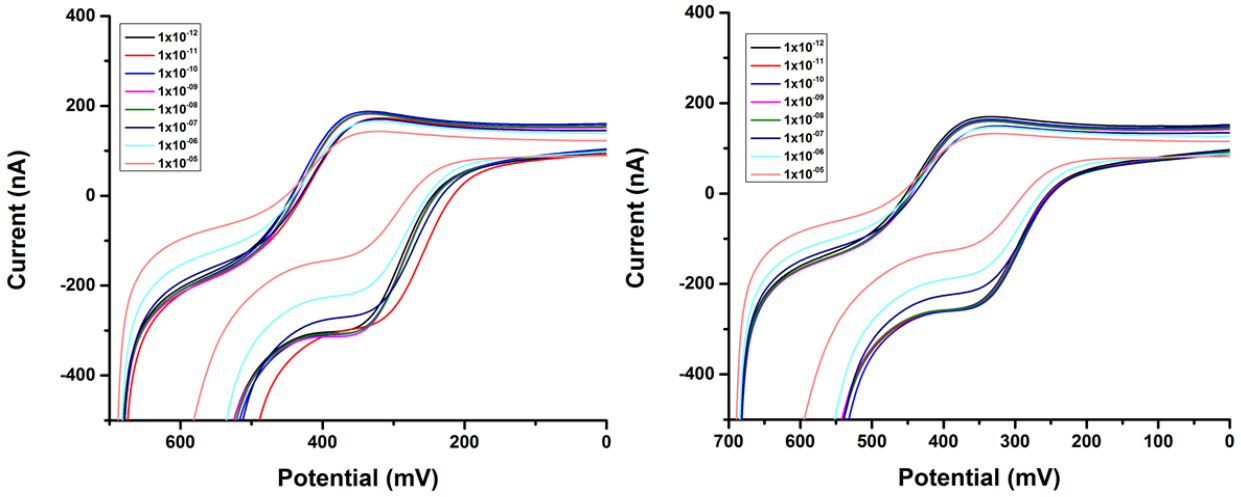

Figure 5.2. $G\alpha_{i1}$ non-specific binding on unfunctionalized surface (***left***) and PEG-40 functionalized surface (***right***). Conditions: 5 mM FCA dissolved in 20 mM HEPES, pH 8.0 with 0.1 M potassium nitrate. $G\alpha_{i1}$ concentration varied from 10^{-12} to 10^{-5} M.

The first thing that we noticed was that CV scans obtained from unfunctionalized surface (***left***) drifted on horizontal scale more than the CV scans obtained from PEG-40-functionalized surface. This is an example of why we measured peak-current by noting the change in current between the baseline and the peak and did not simply record the current at a given potential. The second observation that we made was that the relative current change at each concentration was similar for both surfaces except for the very last concentration. At 10^{-5} M, there was a sudden change in current associated with the unfunctionalized surface. But no concrete conclusions are made from raw CV scans and therefore we normalized the data as explained before. **Figure 5.3** summarizes the binding curve generated for $G\alpha_{i1}$ non-specific binding to the unfunctionalized (black dots) and PEG-40-functionalized surface (red square). Clearly, $G\alpha_{i1}$ binds to both surfaces in a similar fashion. The non-specific binding starts after 10^{-8} M and if we were monitoring weak binding interactions, PEG-40 is not the answer to reducing non-specific binding interactions between the surface and $G\alpha_{i1}$.

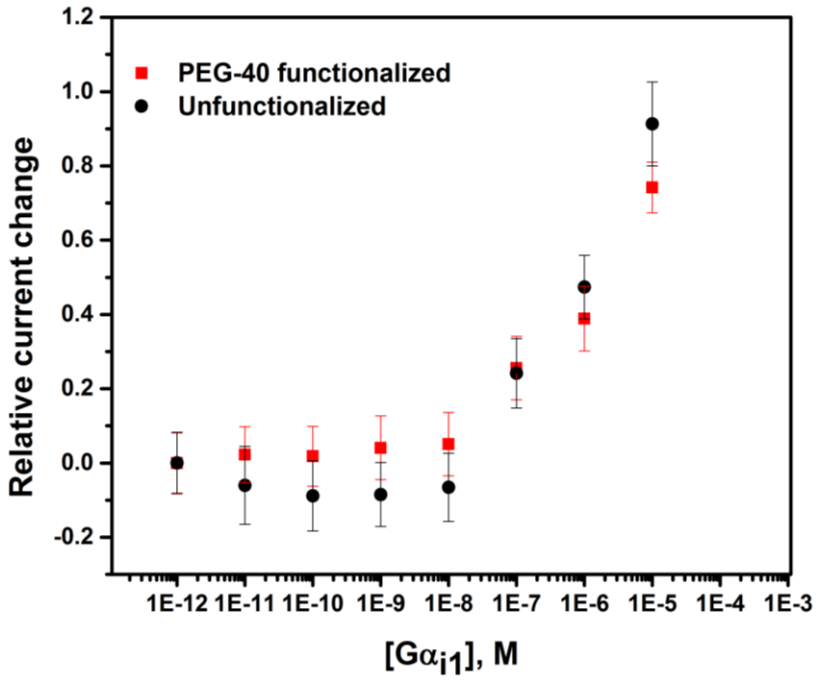

Figure 5.3. Binding curve generated for $G\alpha_{i1}$ non-specific binding to unfunctionalized surface (***black dots***) and PEG-40-functionalized surface (***red squares***). The curve represents normalized data (mean ± SD, n=3).

While the PEG-groups did not solve the non-specific binding issue encountered, it was becoming clear that the studies were a success. One of the biggest motivations for the project was to determine whether G proteins were compatible with the analytical experiments on the microelectrode arrays and the use of the iron mediators employed to date for such studies. In this regard, the preliminary results shown above did demonstrate the viability of the experiments.

While the level of background binding was disconcerting, we had previously shown that the detection of specific binding event can be amplified by the use of an array. For example, the nanomolar binding of an RGD peptide to its integrin receptor was observed with picomolar concentrations of receptor in solution.[8] If a similar amplification was seen in the case of G proteins, then we might be able to see a specific interaction between AGS3 and $G\alpha_{i1}$ before or on top of the non-specific binding event.

5.2.3 Binding of AGS3 peptide to $G\alpha_{i1}$

AGS3 peptide has been expressed in *E.coli* cells with a N-terminal His_6 tag without affecting its binding to $G\alpha_{i1}$.[6] Hence, it would appear that the protein tolerates steric bulk at the N-terminal side of the peptide, an observation consistent with using that location for attaching the peptide to the array. For that purpose, the AGS3 peptide was ordered with a cysteine on the N-terminus. The peptide was then placed onto our PCEMA-b-pBSt polymer-coated array utilizing the Chan-Lam coupling via the cysteine.[9–11] As a control that provides a measure of non-specific binding to the polymer coating, we added a random tetra-peptide (CYAL) to blocks of electrodes on the array in addition to the AGS3 peptide. We used the peptide instead of analyzing blocks of electrodes with an unfunctionalized surface because the presence of the short peptide tends to swell the polymer upon incubation with aqueous buffer. This increases the conductance of the surface and leads to peak-currents of a magnitude that can be more readily compared with those obtain for the electrodes coated with the AGS3-functionalized polymer. Hence, the top part of PCEMA-b-pBSt polymer-coated array was functionalized with AGS3 and the bottom part of the array was functionalized with CYAL. The middle of the array was left unfunctionalized. The functionalized array was then incubated with solution containing the redox mediator and $G\alpha_{i1}$. Five CV scans were then taken at each block of electrodes selected for the study for each concentration of the protein employed.

Figure 5.4 illustrates the binding curves generated from three different types of electrodes in the array. Once again, non-specific binding of the protein to the surface of the array started at a concentration of protein around 10^{-7} M. This was true for both the unfunctionalized and functionalized surface with the CYAL peptide. Unfortunately, the data generated from the electrodes functionalized with the AGS3 peptide was not statistically different from the

background data. No additional binding due to a specific interaction could be observed. Either the background level was simply too high or the surface bound peptide did not bind to the protein. There was a concern over the ability of the surface bound AGS3 to bind the receptor because the peptide was placed directly onto the polymer-coated array without a linker. Hence, sterics may have made the peptide inaccessible to the protein. With that in mind, we decided to repeat the experiment with a linker and with a peptide known to have better affinity for $G\alpha_{i1}$.

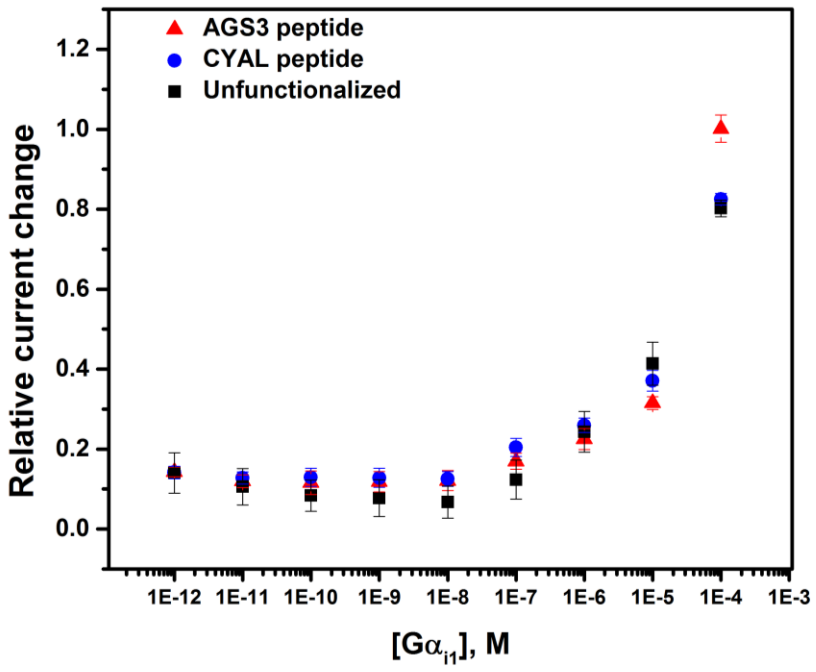

Figure 5.4. Binding curve generated for $G\alpha_{i1}$ binding to AGS3-functionalized (***red triangle***); CYAL-functionalized (***blue dots***) and unfunctionalized surface (***black squares***)**.** The curve represents normalized data (mean ± SD, n=3).

5.2.4 Binding of R6A peptide to $G\alpha_{i1}$

In vitro selection using mRNA display libraries based on the AGS3 motif has revealed a set of novel peptide sequences with conserved residues that are known to bind $G\alpha_{i1}$ with higher

affinity.[7] The dominant peptide from this selection, R6A, was shown to bind $G\alpha_{i1}$ with a binding constant, K_D = 60 nM as measured by surface plasmon resonance (SPR).[7] Since this peptide is a stronger binder of $G\alpha_{i1}$, it made for an ideal candidate for assessing the capabilities for the arrays to monitor small molecule-G protein interactions. In a preliminary experiment, the R6A peptide was placed on an array without a linker. To this end, half of a PCEMA-b-pBSt polymer-coated array was functionalized with the R6A peptide. This array was then incubated with a solution containing the redox mediator and $G\alpha_{i1}$. Since R6A specifically binds to GDP bound $G\alpha_{i1}$, the solution above the array contained 25 µM GDP to ensure GDP-bound state of $G\alpha_{i1}$. CV scans were then collected for the electrodes increasing concentrations of the protein as in the previous experiments. The data was normalized as before to obtain a binding curve depicted in **Figure 5.5**.

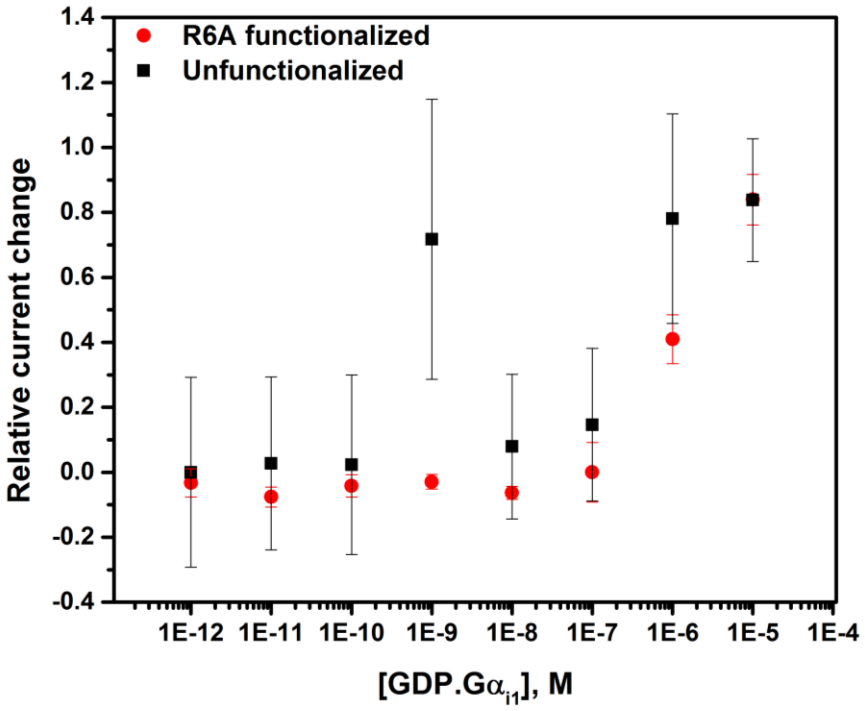

Figure 5.5. Binding curve generated for $G\alpha_{i1}$ binding to R6A-functionalized (***red dots***); and unfunctionalized surface (***black squares***)**.** The curve represents normalized data (mean ± SD, n=3).

The large error bars associated with the data obtained for the unfunctionalized surface indicate a significant problem with the experiment. Typically we use small error bars relative to the total change of current on the array to characterize a polymer coating as having uniform electrochemical properties. Clearly, that was not the case in this experiment and a problem with the polymer coating was suspected. Nevertheless, it was clear from the data obtained using R6A-functionalized electrodes that a binding event with the protein did not happen at the expected protein concentration. Instead, the data appeared similar to the one obtained for the non-specific binding of $G\alpha_{i1}$ to the surface. Clearly something was amiss. Two changes were needed for a definitive experiment. First, a linker had to be placed between the peptide and the surface in order to move the ligand away from the array. This was needed in order to make the peptide more accessible to the protein. Second, a scrambled version of the R6A peptide had to be placed on the array using the same linker employed for the R6A peptide. This was needed in order to establish a more accurate baseline for non-specific binding in the experiment. What is the exact non-specific binding curve generated for the functionalized surface and with the linker in place could we see the known specific binding between R6A and $G\alpha_{i1}$?

5.2.5 Binding of R6A peptide conjugated with a PEG linker to $G\alpha_{i1}$

With respect to the linker, we decided to place a PEG group at the C-terminus of R6A. The R6A peptide has been expressed in *E.coli* with a maltose-binding protein (MBP) tag on the C-terminus without a loss of binding affinity.[7] In the same paper, authors had immobilized R6A for the SPR experiments via its C-terminus. Therefore, we knew modification at the C-terminus will not affect its ability to bind $G\alpha_{i1}$. As for the length of the linker, we decided to place a PEG-6 linker (length ~32 Å) at the C-terminus of the peptide followed by a cysteine. This length of linker was decided because of its commercial availability. The thiol of the cysteine was used to

attach the molecule to the array in order to capitalize on the same array chemistry employed earlier.

Next we needed a scrambled version of R6A. Consequently, the peptide sequence of R6A was inserted into a scrambled peptide generator (mimotopes, the peptide company). This generator provides multiple permutations of the original sequence and the first generated sequence was used as the scrambled R6A peptide for our binding study. The scrambled version of the R6A peptide was then modified in the same way with PEG-6 conjugated at the C-terminus followed by a cysteine so it could be placed on the array in a manner identical to R6A.

The experiment was initiated with the functionalization of the array using R6A-PEG-6, an LRSC tetra-peptide (to make sure the polymer coating was behaving properly from an electrochemical standpoint) and scrambled R6A- PEG-6. Unlike our other signaling experiments where we use a block of 12 electrodes to run CV, we decided to use blocks of 65 electrodes each. Blocks with a greater number of electrodes generate 'nicer' CVs because of the larger currents that are involved. The larger current makes it easier to detect changes in peak-current. In addition, our range for the concentration of $G\alpha_{i1}$ started with 10^{-15} M. The iron solution containing varying amounts of $G\alpha_{i1}$ was incubated onto the functionalized array for 3 min before generating CV scans (3 min incubation time was decided based on the previously reported SPR study[7]). **Figure 5.6** summarizes the results from this binding experiment.

As seen from the figure, there is a minimal relative change in current associated with LRSC-functionalized electrodes throughout the experiment. It seems like the presence of the tetra-peptide did suppress the non-specific binding to the surface. The same could not be said for the surface functionalized with the scrambled R6A peptide. In this case, a strong non-specific interaction was seen right from the start of the experiment. It seems that $G\alpha_{i1}$ sits down well on

the peptide surface and quickly interferes (impedes) the iron mediator from reaching the electrode below. Interestingly, the specific binding interaction known to occur with R6A affects the experiment in the opposite fashion. The binding of $G\alpha_{i1}$ to the surface causes an increase in current (why the opposite direction for the "curve"). This is not uncommon. Binding of the peptide to a molecule at the end of a tether attached to the surface does little to sterically block the surface of the electrode. However, it can nicely improve the swelling of the polymer and in so doing increase both the amount of iron that absorbs into the polymer and the rate of diffusion to the surface of the electrode. Both of these effects increase the conductivity of the surface. Hence, while $G\alpha_{i1}$ interacts with both the surfaces, one functionalized with the scrambled R6A and the other functionalized with R6A, at roughly the same concentration, it does so with a different mechanism leading to opposite changes in the conductivity of the surface. The result is that the interaction with the R6A peptide can be clearly seen "over" the background signal. In fact, the observation that the binding curve "drops" in spite of the background impedance due to non-specific binding suggests a stronger interaction with the R6A peptide at the lower concentrations.

One method for examining the interaction between R6A and $G\alpha_{i1}$ more clearly is to subtract the non-specific background peak-current from the peak-current measured for R6A. After all, this was the reason that the scrambled peptide was placed on the array so that the most accurate non-specific binding current could be obtained. The result of subtracting the background peak-current from the R6A data is shown in **Figure 5.7**. The data shows the clear increase in conductance associated with the binding event, and then saturation of that signal at a higher protein concentration where the current stabilizes.

It does appear that the use of array to measure the binding event has amplified the signal to the point where we are only seeing the final portion of a binding curve. According to the literature, R6A is a nanomolar binder for $G\alpha_{i1}$.[7] As mentioned earlier we have seen similar amplifications of binding events on the array when examining RGD-peptide/integrin interactions (another nanomolar binder). The literature suggests that the increase in binding is associated with an exchange of the protein between peptide ligands on the surface of the electrode that does not allow the protein to escape from the electrode surface even when it is not bound.[12] This amplification can in principle be reduced by decreasing the surface coverage of the peptide ligand on the electrode (discussed in **Section 6.2**). Future work will take advantage of this chemistry in order to "move" the binding curve generated for the R6A-$G\alpha_{i1}$ interaction back toward the nanomolar range where it can be properly observed and analyzed.

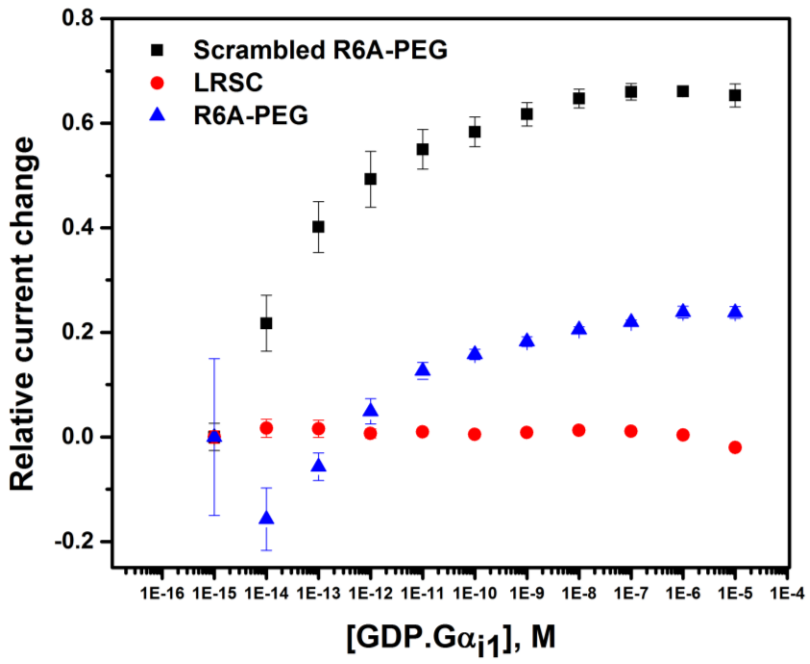

Figure 5.6. Binding curve generated for $G\alpha_{i1}$ binding to scrambled R6A-PEG-6-functionalized (***black squares***); LRSC-functionalized (***red dots)*** and R6A-PEG-6 functionalized surface (***blue triangles*****).** The curve represents normalized data (mean ± SD, n=3).

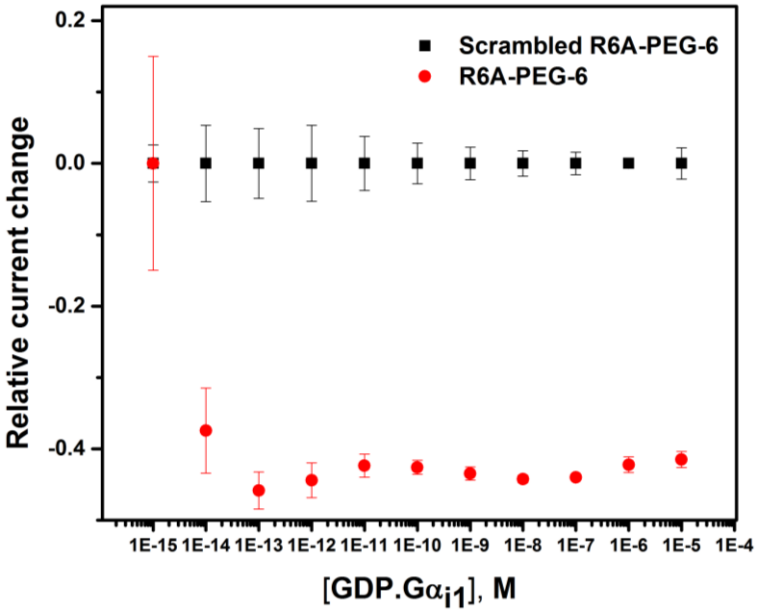

Figure 5.7. Binding curve generated for $G\alpha_{i1}$ binding to scrambled R6A-PEG-6-functionalized (***black squares***); and R6A-PEG-6 functionalized (***red dots***)**.** Average peak-current from 3 data groups was normalized to the peak-current obtained from scrambled R6A-PEG-6 functionalized surface; error bars represent standard deviation.

5.3 Conclusions

In conclusion, we have shown the compatibility of G proteins with the electroanalytical methods employed on microelectrode arrays. In addition, our preliminary results depict a known binding interaction between a short peptide, R6A and $G\alpha_{i1}$ using arrays. The signal for the binding event was seen above the non-specific background signal associated with a scrambled R6A peptide. While the overall technique was successful, additional experiments will be performed because the desired interaction is amplified by the array to a point where it is partially obscured by the detection limits of the technique. Moreover, this binding study showed that the random tetra-peptide, LRSC can be used to reduce non-specific binding of $G\alpha_{i1}$ to the polymer-coated array.

5.4 Experimental section

Unless noted otherwise, all chemicals were ordered from Sigma Aldrich (St. Louis, MO). All other vendor information is noted in the experimental section. Basic procedure for conducting electrochemical experiments and cyclic voltammetry has been discussed in detail in **Chapter 4**.

5.4.1 $G\alpha_{i1}$ non-specific binding to PEGylated PCEMA-b-pBSt polymer-coated array

The following procedure was adapted from the known Chan-Lam coupling.[9,10] Poly (ethylene glycol) methyl ether (n=40), MW= ~2,000 (10.0 mg) and 50.0 mg of tetrabutylammonium hexafluorophosphate were dissolved in 1.0 mL of DMF. To this solution, 50.0 µL of 25 mM copper (II) acetate solution was added. Contents were mixed, and then 120 µL of this solution was added to the array. The array was placed into an ElectraSense reader and half of 12,544 electrodes were selected and used as anode. A potential of +2.4 V relative to the auxiliary electrode was used to pulse the electrodes for 20 cycles of 30 s on and 10 s off. After reaction completed, the array was washed extensively (~5-7 mL) with 95 % ethanol.

Upon functionalization of half of the electrodes on the array with PEG-40, non-specific binding experiment was initiated. Accordingly, general procedure for conducting CV experiments on a 12-K array as mentioned in **Section 4.4.4** was followed except instead of BSA, array was incubated with $G\alpha_{i1}$ (concentration range 1 pM to 10 µM). 4 blocks (12 electrodes each) were selected from functionalized and unfunctionalized part of the array to conduct CV experiments. The data was analyzed and graphed using MS excel and Origin 9.0 respectively.

5.4.2 Binding of AGS3 peptide to $G\alpha_{i1}$ on a microelectrode array

AGS3 peptide (CTMGEEDFFDLLAKSQSKRMDDQRVDLAG, purity > 90 %) and a tetra-peptide (CYAL, purity > 90 %) were purchased from Genscript (Piscataway, NJ). The C terminus of both peptides was blocked by amidation and the N terminus by acetylation. Peptides were delivered as white lyophilized powder and were used without further purification.

AGS3 peptide (3.0 mg) and 15.0 mg of tetrabutylammonium hexafluorophosphate were dissolved in 300 µL of DMF. To this solution, 15.0 µL of 25 mM copper(II) acetate solution was added. Contents were mixed, and then 120 µL of this solution was added to the array. The array was placed into an ElectraSense reader and 1000 electrodes were selected and used as anode. A potential of +2.4 V relative to the auxiliary electrode was used to pulse the electrodes for 20 cycles of 30 s on and 10 s off. After completion of reaction, the solution was replaced with fresh solution and the reaction was run again (20 cycles of 30 s on and 10 s off). Upon completion of reaction, the array was washed extensively with 95 % ethanol. In order to functionalize array on new 1000 electrodes with tetra-peptide (CYAL), the same procedure was carried out.

Upon functionalization of array with both AGS3 and CYAL peptide, binding experiment was initiated. 125 µL of $G\alpha_{i1}$ (final concentration 100 µM) was added to 180 µL iron solution (18 mg FCA dissolved in 50 mM Tris-HCl pH 8.0, 1 mM EDTA, 10 mM $MgCl_2$ and 0.1 M potassium nitrate). From here serial dilutions starting from 100 µM to 1 pM (500 µL each) were prepared. All protein solutions were placed at 0 °C. General procedure for conducting CV experiments on a 12-K array has been mentioned in **Section 4.4.4**. The electrochemical analysis began with CV tests at each block of electrodes using blank iron solution (no protein added). This part was done to select 4 blocks (12 electrodes each) from AGS3-functionalized, CYAL-functionalized and unfunctionalized part of the array to conduct CV experiments. Binding experiment was initiated

by incubation of iron solution containing the lowest concentration of $G\alpha_{i1}$ onto the array for 3 min and then running three CV scans for every selected block (total 12 blocks). The conditions for the CV included a potential sweep from -700 mV to + 700 mV and back again at a scan rate of 400 mV/s. In these experiments, the potential refers to the potential of the electrodes on the array relative to the platinum-counter electrode located on the hyb-cap. Before moving on to higher concentrations, the array was washed once with the next concentration of protein. Data from CV scan # 2 from every block was analyzed and graphed using MS excel and Origin 9.0 respectively.

5.4.3 Binding of R6A peptide to $G\alpha_{i1}$ on a microelectrode array

R6A peptide (MSQTKRLDDQLYWWEYLC, purity >90 %) was purchased from Genscript (Piscataway, NJ). The C terminus of the peptide was blocked by amidation and the N terminus by acetylation. Peptide was delivered as a white lyophilized powder.

R6A peptide (3.0 mg) and 15.0 mg of tetrabutylammonium hexafluorophosphate were dissolved in 300 µL of DMF. To this solution, 15.0 µL of 25 mM copper(II) acetate in water solution was added. Contents were mixed, and then 120 µL of this solution was added to the array. The array was placed into an ElectraSense reader and 1000 electrodes were selected and used as anode. A potential of +2.4 V relative to the auxiliary electrode was used to pulse the electrodes for 20 cycles of 30 s on and 10 s off. After the reaction completed, the solution was replaced with fresh solution and the reaction was ran again (20 cycles of 30 s on and 10 s off). Upon completion of reaction, the array was washed extensively (~5-7 mL) with 95 % ethanol.

Upon functionalization of array with R6A peptide, binding experiment was initiated. $G\alpha_{i1}$ (15 µL, final concentration 10 µM) was added to 300 µL iron solution (18 mg FCA dissolved in 10

mM HEPES pH 7.5, 150 mM NaCl, 3 mM EDTA, 8 mM $MgCl_2$, 25 µM GDP and 0.1 M potassium nitrate). From here serial dilutions starting from 10 µM to 1 pM (500 µL each) were prepared. All protein solutions were placed at 0 °C. General procedure for conducting CV experiments on a 12-K array has been mentioned in **Section 4.4.4**. The electrochemical analysis began with CV tests at each block of electrodes using blank iron solution (no protein added). This part was done to select 4 blocks (12 electrodes each) from R6A-functionalized and unfunctionalized part of the array to conduct CV experiments. Binding experiment was initiated by incubation of iron solution containing the lowest concentration of $G\alpha_{i1}$ onto the array for 3 min and then running three CV scans for every selected block (total 12 blocks). The conditions for the CV included a potential sweep from -700 mV to + 700 mV and back again at a scan rate of 400 mV/s. In these experiments, the potential refers to the potential of the electrodes on the array relative to the platinum-counter electrode located on the hyb-cap. Before moving on to higher concentrations, the array was washed once with the next concentration of protein. Data from CV scan # 2 from every block was analyzed and graphed using MS excel and Origin 9.0 respectively.

5.4.4 Binding of R6A-PEG-6 peptide to $G\alpha_{i1}$ on a microelectrode array

Both R6A peptide conjugated to PEG-6 linker (MSQTKRLDDQLYWWEYL-PEG6-C, purity > 90 %) and a scrambled version of R6A peptide also conjugated to PEG-6 linker (QLSEDTYLLMRWDYWQK-PEG6-C, purity > 90 %) were purchased from CPC Scientific, Inc. (Sunnyvale, CA). A tetra-peptide (LRSC, purity> 90 %) was purchased from Genscript (Piscataway, NJ). The C terminus of both peptides was blocked by amidation and the N terminus by acetylation. Peptides was delivered as a white lyophilized powder and were used without further purification.

The same procedure was carried out in order to functionalize array with R6A-PEG-6 (3.0 mg), scrambled R6A-PEG-6 (3.0 mg) and LRSC peptide (3.0 mg) as mentioned previously. However, the electrochemical analysis was done on 4 blocks with 65 electrodes each.

5.5 References

(1) Freissmuth, M.; Waldhoer, M.; Bofill-Cardona, E.; Nanoff, C. *Trends Pharmacol Sci*, **1999**, *20*, 237–245.

(2) Holler, C.; Freissmuth, M.; Nanoff, C. *Cell. Mol. Life Sci.* **1999**, *55*, 257–270.

(3) Taylor, J. M.; Neubig, R. R. *Cell. Signal.* **1994**, *6*, 841–849.

(4) Dower, W. J.; Mattheakis, L. C. *Curr. Opin. Chem. Biol.* **2002**, *6*, 390–398.

(5) Bernard, M. L.; Peterson, Y. K.; Chung, P.; Jourdan, J.; Lanier, S. M. *J. Biol. Chem.* **2001**, *276*, 1585–1593.

(6) Adhikari, A.; Sprang, S. R. *J. Biol. Chem.* **2003**, *278*, 51825–51832.

(7) Ja, W. W.; Roberts, R. W. *Biochemistry* **2004**, *43*, 9265–9275.

(8) Fellet, M. S.; Bartels, J. L.; Bi, B.; Moeller, K. D. *J. Am. Chem. Soc.* **2012**, *134*, 16891–16898.

(9) Sanjeeva Rao, K.; Wu, T.-S. *Tetrahedron* **2012**, *68*, 7735–7754.

(10) Hu, L.; Graaf, M. D.; Moeller, K. D. *J. Electrochem. Soc.* **2013**, *160*, G3020–G3029.

(11) Uppal, S.; Graaf, M.; Moeller, K. *Biosensors* **2014**, *4*, 318–328.

(12) Xiao, Y.; Li, C. M.; Liu, Y. *Biosens. Bioelectron.* **2007**, *22*, 3161–3166.

Chapter 6: Conclusions and Future Directions

6.1 Summarization of previous chapters

The motivation for this multidisciplinary project is the development of novel chemical probes that can directly target G proteins and help us learn about G protein mediated cell signaling. To this end, there are three crucial parts to this dissertation. First is synthesizing simplified analogs of a natural product YM-254890 known to inhibit signaling of G protein, $G\alpha_q$. Second, isolation of various G proteins to test the activity of simplified analogs and third, development of an electrochemical method to rapidly screen newly synthesized analogs. This dissertation is focused on the second and third part of the project. **Chapter 2** of this dissertation described details on how we isolated the necessary G proteins. We learned about Titerless Infected-cells Preservation and Scale up (TIPS) method and applied it for expression of $G\alpha_q$ (both wild-type and mutant forms). In addition, two other G proteins were expressed and purified from bacterial cells. Following the isolation of G proteins, we tested their biochemical activity using nucleotide exchange assays. During this period, we learned about $G\alpha_q$ in terms of its stability and its ability to undergo nucleotide exchange. A receptor-assisted nucleotide exchange assay was developed to test activity of $G\alpha_q$ and potency of the first simplified YM analog, WU-07047 (**Chapter 3**). We learned that the simplified YM analog retained its activity towards $G\alpha_q$, and preliminary data from fluorescent exchange assays depict that WU compound did not show any potency towards $G\alpha_{i1}$ and $G\alpha_o$. Having established a pathway for total synthesis of a YM analog, our efforts were directed towards development of a rapid screening method on microelectrode arrays. To this end, **Chapter 4** is focused on modification of polymer-coated array surface with PEG-polymer groups. We learned that with the use of another redox mediator, ferrocene carboxylic acid, we were able to generate

stable current with less time on a PEG-modified array surface. Moreover, use of longer PEG-polymer groups reduced non-specific binding of BSA to the modified array surface. **Chapter 5** investigates the compatibility of G proteins with microelectrode arrays. As a proof of principle, we examined a known binding interaction between a short peptide (R6A) and $G\alpha_{i1}$ using our electroanalytical methods. As discussed at the end of **Chapter 5**, we can clearly see the binding of the protein to R6A over the signal for background binding between the protein and a scramble R6A analog. The desired signal was amplified by the microelectrode arrays to a point where an accurate determination of a binding constant could not be made. Furthermore, the negative control showed large non-specific binding to the protein on the array.

In summary, this dissertation has laid the groundwork on both biochemical and analytical fronts of this project. Next, we propose future experiments that will continue to answer lingering questions and address the issues that were described above.

6.2 Optimization of ligand concentration

Recently, Matthew Graaf in the group has developed the synthetic strategy necessary to build arrays with peptide gradients. This experiment has shown that increase in reaction time can affect the coverage of ligand on array surface, and that the relationship between reaction time and coverage is linear. Hence, in order to decrease the peptide coverage on an electrode in a microelectrode array, the length of time for the reaction (less reaction cycles with the electrode turned on) should be performed. In our binding studies discussed in **Chapter 5**, all peptides were placed by conducting 60 reaction cycles (30 s on and 10 s off). Our first attempt to reduce the concentration of peptide on the array would be to run 10 reaction cycles for the Chan-Lam coupling used to place both the scrambled R6A and R6A onto the array. Upon functionalization of the array with these two peptides, we could ‘backfill’ with the tetra-peptide used in the final analytical

experiment shown in Chapter 5, since that peptide (LRSC) appeared to suppress the non-specific binding between $G\alpha_{i1}$ and the surface.

6.3 Expression of accessory proteins

The importance of the sepia rhodopsin receptor and the βγ dimer for assessing the activity of $G\alpha_q$ was discussed in **Chapter 3**. The receptor-assisted nucleotide exchange assays require these accessory proteins that were provided by the Tesmer lab at University of Michigan. Hartman *et al.* have isolated sepia rhodopsin from enucleated squid eyes.[1] His-tagged Gγ subunit has been co-expressed with Gβ subunit in sf9 cells.[2] One of our next goals should be to develop these methods in our labs. Once we have these reagents available, it would easier to perform nucleotide exchange assays.

Receptor-assisted nucleotide exchange assays for $G\alpha_q$ employs [^{35}S] GTPγS, but would this assay work with BODIPY®FL GTPγS? In theory, if slow GDP dissociation problem was resolved, the fluorescent ligand should work and added expense associated with radioactivity ligands could be avoided.

6.4 Testing mutant $G\alpha_q$

In **Chapter 2**, we discussed the isolation of a mutant form of $G\alpha_q$ (I190N) from insect cells. The YM compound loses its potency towards this mutant $G\alpha_q$.[3] However, this protein had not been expressed during the testing period of WU compound. But now we have the purified protein and we can examine the effect of WU and other simplified analogs on this protein. One can use this as a negative control in both the exchange assay and on the arrays. This protein might help us in learn additional information about the synthesized YM analogs. For instance, if the simplified compounds exhibit potency towards this protein, then we can assume a different mode of binding.

This mutation is present in an important region (switch I), which imparts specificity. Hence, the compounds showing potency towards this protein, might be able to bind other G proteins as well. In this way, we can prepare a collection of G protein subtype-selective modulators that would provide powerful tools for probing the functions of specific G proteins in diverse biological processes and diseases.

6.5 FRET studies to elucidate conformational dynamics

As mentioned previously in **Chapters 1 & 3**, YM inhibits release of GDP by preventing the interdomain movement. Would WU and related analogs inhibit the activity of G proteins in a similar manner? In order to study conformational dynamics, we intend to use site-directed fluorescence resonance energy transfer (FRET) measurements.[4–6] To this end, two cysteine residues (that can be conjugated to donor and acceptor fluorophores) can be introduced in the regions that need to move in order for GDP to release. If the two domains are in close proximity, a FRET signal is detected. However, movement of these domains will result in the loss of FRET signal. In this way, one can speculate the mechanism of action for the simplified analogs.

6.6 References

(1) Hartman IV, J. L.; Northup, J. K. *J. Biol. Chem.* **1996**, *271*, 22591–22597.

(2) Kozasa, T.; Gilman, A. G. *J. Biol. Chem.* **1995**, *270*, 1734–1741.

(3) Nishimura, A.; Kitano, K.; Takasaki, J.; Taniguchi, M.; Mizuno, N.; Tago, K.; Hakoshima, T.; Itoh, H. *Proc. Natl. Acad. Sci.* **2010**, *107*, 13666–13671.

(4) Ratner, V.; Kahana, E.; Eichler, M.; Haas, E. *Bioconjug. Chem.* **2002**, *13*, 1163–1170.

(5) Taraska, J. W.; Puljung, M. C.; Olivier, N. B.; Flynn, G. E.; Zagotta, W. N. *Nat. Methods* **2009**, *6*, 532–537.

(6) Winters, D. L.; Autry, J. M.; Svensson, B.; Thomas, D. D. *Biochemistry* **2008**, *47*, 4246–4256.